uOttawa

L'Université canadienne
Canada's university

FACULTÉ DES ÉTUDES SUPÉRIEURES ET POSTOCTORALES

u Ottawa

L'Université canadienne
Canada's university

FACULTY OF GRADUATE AND POSDOCTORAL STUDIES

Bojana Rakic
AUTEUR DE LA THÈSE / AUTHOR OF THESIS

Ph.D. (Chemistry)
GRADE / DEGREE

Department of Chemistry
FACULTÉ, ÉCOLE, DÉPARTEMENT / FACULTY, SCHOOL, DEPARTMENT

Small Molecule Effects on Hepatitis C Virus

TITRE DE LA THÈSE / TITLE OF THESIS

John Pezacki
DIRECTEUR (DIRECTRICE) DE LA THÈSE / THESIS SUPERVISOR

Natalie Goto
CO-DIRECTEUR (CO-DIRECTRICE) DE LA THÈSE / THESIS CO-SUPERVISOR

EXAMINATEURS (EXAMINATRICES) DE LA THÈSE / THESIS EXAMINERS

R. Ben

T. Scaiano

A. Ianoul

E. Meggers

Gary W. Slater
Le Doyen de la Faculté des études supérieures et postdoctorales / Dean of the Faculty of Graduate and Postdoctoral Studies

Small Molecule Effects on Hepatitis C Virus

by

Bojana Rakić

A Thesis submitted to the Faculty of Graduate and Postdoctoral Studies
In partial fulfillment of the requirements for the
PhD degree in chemistry

Candidate
Bojana Rakić

Supervisor
Dr. John Paul Pezacki

Ottawa-Carleton Chemistry Institute
Faculty of Science
University of Ottawa

Your file Votre référence
ISBN: 978-0-494-34142-1
Our file Notre référence
ISBN: 978-0-494-34142-1

Abstract

In this thesis, chemical biology approaches were used to study Hepatitis C Virus (HCV) in non-infectious, subgenomic HCV replicon model systems. Specifically, small molecules were used as probes for studying host-virus interactions. Compared to genetic techniques, small molecules are interesting potential therapeutics for HCV because they can diffuse relatively quickly to their targets and also act on proteins after they have been post-translationally modified. Small molecules are also much easier to deliver to cells.

In our first study we looked on the effects of using a small molecule agonists and antagonist of the host receptor, peroxisome proliferator activated receptor α (PPARα) on the HCV viral life cycle. We found that impaired function of PPARα perturbs lipid homeostasis within the cells, causing inhibition of HCV replication. We confirmed this effect by silencing the PPARα gene using small interfering (si)RNA molecules.

Our next project involved screening a library of abscisic acid (ABA) analogs for anti-HCV activity. ABA is a plant hormone, structurally similar to its counterpart in humans, retinoic acid. We found three ABA analogs that have anti-HCV activity comparable to known HCV inhibitors like lovastatin and 25-hydroxycholesterol. We identified the protein targets for one of the active ABA analogs by performing *in-vivo* experiments using an inhibitor-based profiling approach with a synthesized rhodamine fluorescent probe. Target identification allowed us to postulate a mechanism by which the ABA analog realizes its anti-HCV activity by interfering with the host protein responsible for both host and HCV protein folding.

Finally, we demonstrated anti-HCV activity of the antitumor drug bleomycin (BLM). BLM causes HCV inhibition by directly targeting and degrading the HCV RNA. Although toxic to the host cell due to DNA degradation, we showed that BLM acts much faster on viral RNA located in the cytoplasm than on host DNA located in the nucleus.

Acknowledgments

I must first express my sincere gratitude to Dr. John P. Pezacki for providing me the opportunity to work in his group. He has always been there for me regardless of the situation. His guidance, patience and support were greatly appreciated. John, thank you for inspiring me with your passion for research and helping me to develop scientifically. It was an enjoyable time for me.

My research at the NRC would not have been fun if I did not have a chance to work with brilliant colleagues. I would like to thank the whole Pezacki group for their help, in particular Jenny, Angela, Sylvie, Yanouchka and Tammy. I also want to thank Gianni, Selena, Matt, and Trevor for the scientific discussions I had with them and for their friendship. Thanks to Malgosia and Don for assisting me with instrumental techniques during my graduate studies and also for all the personal advice they gave me. Thank you to my collaborators Professors Sunney Xie and Sue Abrams. I would also like to thank Dr. Prabhat Arya for his mentorship at the beginning of my graduate studies.

I have been lucky to meet a lot of wonderful grad students and post-docs both at the NRC and at the university. Thank you Marius, Pat, Jessie, Sophie, Katya, Mike, Gregory and Rune for the great moments outside the lab! I am especially thankful for my friendship with Irina Denissova, my Canadian sister.

I take this opportunity to acknowledge and thank the University of Ottawa for giving me an international scholarship and the National Research Council for funding during my doctoral studies. Without this financial support I would not be able to come and study in Canada.

Finally I must acknowledge the love and patience of my husband Anthony. Thank you for reading my manuscripts, for discussing science with me, and for taking care of me always. And I would never have been able to make it this far without the support of my family back home. Thank you to my sisters Milijana and Ana and my brothers Bosko, Nemanja and Andrija for exchanging stories and pictures with me. I missed you all in Canada a lot. Thank you to my parents for sacrificing so much for educating all of us. This work goes to you. Volim Vas Puno!

Abbreviations

ABA	abscisic acid
ABPP	activity based protein profiling
ANOVA	ANalysis Of Variance
BA	2-chloro-5-nitro-N-(pyridyl) benzamide
Benzamide	2-chloro-5-nitro-N-(pyridyl) benzamide
BLM	bleomycin
cDNA	complementary deoxyribonucleic acid
Click reaction	Huisgen 2+3 cycloaddition
CPT1A	canitine palmitoyl transferase 1A
ELISA	Enzyme-Linked ImmunoSorbent Assay
EMCV	*encephalomyocarditis* virus
ER	endoplasmatic reticulum
HCV	Hepatitis C Virus
HMG-CoA	3-hydroxy-3-methylglutaryl-coenzyme A
Huh-7	Human Hepatoma Cell Line
IC_{50}	concentration of an inhibitor that is required for 50% inhibition of its target
IFN	interferon
IRES	internal ribosomal entry site
kDa	kilodalton
LC-MS	Liquid Chromatography – Mass Spectrometry
MS	Mass Spectrometry
NPT	neomycin phosphotransferase
NS	non-structural
ORF	open reading frame
PPAR	peroxisome proliferators activated receptor
PTP1D	protein-tyrosine phosphatase
RA	retinoic acid

Rh	rhodamine
RIG-I	retinoic-acid-inducible gene I
RNAi	RNA interference
SD	standard deviation
siRNA	short interfering RNA
SL	stem loops
SREBP	sterol response binding element
ss RNA	single stranded ribonucleic acid
TLR3	Toll-like receptor-3
U	uridine
UC	uridine cytidine
UTR	untranslated region

Table of Contents

List of Figures

List of Schemes

List of Tables

1

Introduction

This thesis describes research in which chemical biology approaches were used to study Hepatitis C Virus (HCV) in non-infectious HCV model systems. Chemical biology offers a wide range of small molecules, which are used as chemical probes for studying DNA, RNA, and proteins. Their scaffolds range from naturally occurring molecules containing carbohydrate and peptide moieties to molecules having incorporated unnatural amino acids. Small molecule probes are especially useful in understanding protein function, in living systems, as they allow fast and reversible modulation of individual protein domains without affecting the whole protein. Their effect can be controlled by varying probe concentration and treatment time. Small molecule probes have an advantage over using genetic approaches such as RNAi (RNA interference) because these silence the gene encoding protein and cause the loss of the whole proteins function. There are numerous examples of small molecules used for selectively modulating protein function. One such is the small molecule rapamycin, which specifically blocks one of TOR protein functions [1].

Small molecule probes can be used in several ways to inhibit the HCV viral life

cycle. Small molecules can: directly target the HCV proteins; affect the host proteins involved in HCV replication; modulate the host metabolic pathways; stimulate the immune system; or directly inhibit replicating RNA. Herein is reported an investigation using small molecules in two types of approaches. In the first approach, we develop probes to investigate the influence of host pathways on viral replication. We first studied the effects of modulating Peroxisome Proliferator-Activated Receptor α (PPARα) activity by small molecule inhibitors and activators by perturbing lipid homeostasis within the liver cells. In another project we screened a library of abscisic acid (ABA) analogs for their activity on HCV. Target identification was an essential step that enabled us to postulate a mechanism by which an active ABA analog realized inhibitory properties in HCV cellular replicons via a pathway that has never before been directly implicated in the HCV lifecycle. In our second approach, we studied the effects of small molecules on viral RNA directly. Using antitumor antibiotic bleomycin we were able to inhibit the HCV viral cycle in a model system by damaging the structure of replicating HCV RNA. In the long term, by exploring small molecule interactions with HCV in detail, we hope to offer new insights into the mechanism of HCV propagation that may lead to the development of new therapeutic treatments.

Although discovered 15 years ago, Hepatitis C Virus still threatens around 170 million people worldwide (3% of world population) [2]. The virus is classified into six genotypes according to geographical regions and risk groups [3]. The genotypes differ in nucleotide sequence of the genome, primarily in their envelope proteins. There has been little success in finding vaccines or drugs that are clinically effective in all patients. Currently, the only treatment is pegylated interferon-α (IFN-α) with ribavirin [4, 5]. However, sustained response rates to the drug are ~55% [6]. Thus, it is not surprising that

significant effort is being made to try to understand every aspect of HCV, including viral entry, viral replication, host-viral interactions, and response to drug treatments. Therefore, before explaining our contributions toward inhibiting HCV, we first summarize what is known so far about HCV genomic organization and key interactions.

Hepatitis C Virus

HCV belongs to the Flaviviridae family, which includes genus *Flavivirus* (yellow fever virus and West Nile virus), and genus *Pestivirus* (bovine diarrhea virus and hog cholera virus). The HCV genome was first cloned in 1989 from a complementary DNA (cDNA) library obtained from the plasma of persistently infected chimpanzees [7]. It is an enveloped, positive, single stranded (ss)RNA genome with a length of 9.6 kb, including a 5' untranslated region (UTR), a long open reading frame (ORF), and a 3' UTR. The 5' UTR contains a highly structured RNA sequence known as the internal ribosomal entry site (IRES). The HCV IRES binds the 40S ribosomal subunit allowing the initiation of polyprotein translation [8, 9]. The HCV 3' UTR can be divided into three segments: an approximately 40 nucleotide (nt) long variable region; a poly (U/UC) long sequence; and a 98-nt conserved end, which forms stem loop structures and is involved in the initiation of negative strand RNA formation. These interesting 3-dimensional stem loop structures in the HCV RNA represent a potential small molecule target. This subject is explored in one of the projects described in this thesis.

Upon translation, the polyprotein is co- and post-translationally processed by cellular endoplasmatic reticulum (ER) peptidase and two viral proteases (NS2 and NS3) into 10 mature viral proteins, classified as structural and nonstructural proteins. The structural

proteins are the core (C), and envelope proteins (E1 and E2). They are located in the amino terminal (N-terminal) region of the polyprotein. The nonstructural proteins are p7, NS2, NS3, NS4A, NS4B, NS5A, and NS5B and are located at the carboxylic (C-terminal) end of the polyprotein (Scheme 1.1). Some HCV proteins undergo posttranslational modifications upon cleavage from the polyprotein to become mature HCV proteins. These reactions are catalyzed by host enzymes. Many of them are still not identified and are subject of proteomics research. Small molecule probes are ideal tools for looking into the activity of HCV proteins but also for target identification of the host proteins that interact with HCV proteins. The main characteristics of all HCV proteins are summarized below.

HCV proteins

Core is a highly basic, hydrophobic protein. Its amino acid sequence is conserved amongst all six genotypes [10]. The primary role of Core is to form the capsid shell of the virus particle. Electron microscopy and confocal images have shown that Core is mostly found on the cytoplasmic surface of the ER [11]; and at the surface of lipid droplets [12], where it co-localizes with cellular apolipoprotein AII, a component of high-density lipid proteins [13]. Core protein binds to many cellular proteins and modulates cell processes such as cell signaling, apoptosis, carcinogenesis, and lipid metabolism [14]. Core also has an effect on the production of interferon stimulated gene factors by activation of several host cell protein kinases [15]. E1 and E2 structural proteins form the envelope of the viral capsid. Upon release from the polyprotein by host peptidase, E1 and E2 undergo post-translational modification, known as glycosylation by attaching sugar molecules to amino acid residues [16]. There are at least 6 sites on E1 and 11 sites on E2 that can be

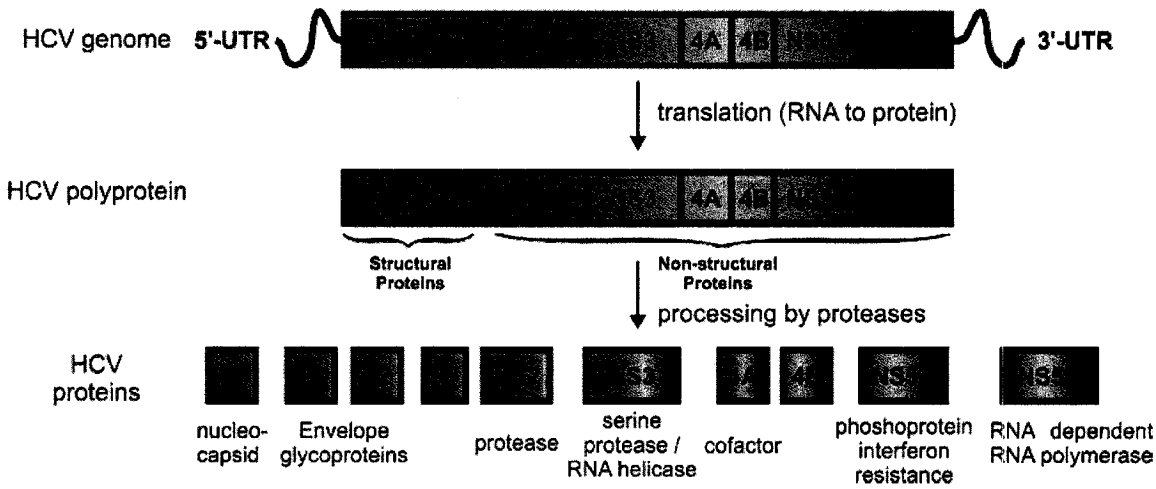

Scheme 1.1: HCV genome, HCV polyprotein and HCV proteins. HCV RNA genome (9.6 kb) translates into a long polyprotein (~3000 amino acids), which is further processed by host and viral proteases into 10 smaller HCV proteins. C, E1 and E2 are structural HCV proteins. P7, NS2, NS3, 4A, 4B, NS5A and NS5B are non-structural HCV proteins.

glycosylated by either N-linkage, in which sugars are attached to asparagine residues, or O-linkage, in which sugars are attached to serine or threonine residues. Glycosylation is catalyzed by the host enzymes, however, the mechanism and identities of these enzymes are still unknown. Development of small molecule probes that can target these glycosidases is highly important, because glycosylation of the envelope proteins is necessary for virus-host cell recognition, interaction, and therefore HCV virion entry and proliferation. E1 and E2 glycoproteins interact with other cellular proteins in the ER known as ER chaperons, which are involved in E1 and E2 productive, and nonproductive folding [17]. In addition the E2 HCV protein has a 12 amino acid sequence identical to the phosphorylation domains of interferon induced PKR protein kinase, and eukaryotic translation Initiation Factor 2alpha (eIF-2alpha). By binding to it, E2 modulates interferon function and prevents its antiviral activity [18]. *In vitro* studies have shown that E2 also binds to human tetraspanin CD81 protein expressed at the cell surface, which can explain a possible viral entry route [19]. The p7 protein is a small hydrophobic 63-amino acid polypeptide. p7 is not essential for viral replication, however, its deletion leads to production of non-infectious virus [20]. Although little is known about this protein, recent studies have shown that p7 possesses ion channel activity [21]. NS2 is a 23 kDa membrane protein. Together with a third of the N-terminal end of NS3, they constitute NS2/NS3 autoprotease, which cleaves the junction between these two proteins in the polyprotein [16]. NS3 is a 70 kDa hydrophilic protein that localizes in the cytoplasm. It forms a complex with NS4A, a 54 amino acid integral membrane polypeptide. NS3/4A is a serine protease responsible for releasing non-structural proteins from the polyprotein. It cleaves the junction between NS3 and 4A, 4A/4B, 4B/5A, and 5A/5B. NS3 also contains a NTPase/RNA helicase domain, which catalyzes unwinding

of the secondary structures in the genomic, or double stranded HCV RNA formed in the replication complex [16]. NS4B is a small, 27 kDa integral membrane protein. It induces changes in the host cellular membrane, forming a membranous web on which viral replication occurs [22]. NS5A is cytosolic HCV non-structural protein, which upon release from the polyprotein undergoes phosphorylation predominately at multiple serine residues, and to a lesser extent at threonine residues. NS5A can be found in a hypophosphorylated form, weighing 56 kDa, or hyperphosphorylated form, weighing 58 kDa. The degree of phosporylation can modulate the function of NS5A protein. Human kinases involved in NS5A phosphorylation are discovered by performing high-throughput screens on yeast kinases and comparing their sequence homology with the human one [23]. Unfortunately, it is unknown which kinases are responsible for phosphorylation of which form of HCV NS5A, nor which phosphorylation sites are functionally important. Since cellular processes such as signal transduction, transcription, protein synthesis, and cell growth and differentiation are regulated by phosphorylation-dependent mechanisms [24], phosphorylation of HCV NS5A protein can possibly interfere with any of these host processes. The HCV NS5A protein also plays an important role in virus replication, because perturbation of multiple intracellular signaling pathways leads to interferon resistance [25, 26]. NS5B is a 68 kDa cytoplasmic and integral membrane protein. It has the function of viral RNA-dependent RNA polymerase (RdRp) that catalyzes replication of the HCV RNA genome. It is prone to mutating and is one of the major therapeutic targets for viral inhibition [25].

Viral life cycle and evasion of the intracellular host defense system

The HCV life cycle takes place in the host cell cytoplasm. It starts with the entry of a

virion particle into a host hepatocyte. Viral entry is presumably induced by receptor mediated endocytosis. This is followed by release of the positive-sense, ssRNA HCV genome into the cytoplasm of the infected cell. The RNA genome has three functions during the viral cycle. It serves as messenger RNA (mRNA) for translation of the structural and nonstructural proteins, also as a template for RNA replication through double-stranded (ds)RNA, and finally it forms a new viral particle. Virions are most likely formed by budding into the endoplasmic reticulum (ER), and then released from the cell through the secretory pathway. The viral life cycle is summarized in Scheme 1.2.

Two host proteins were identified as binding receptors for ss HCV RNA and ds HCV RNA with specific secondary structures. One is Retinoic-Acid-Inducible gene I (RIG-I) receptor [27] and the other is Toll-like receptor-3 (TLR3) [28, 29]. Binding of HCV RNA to these receptors triggers the host cell innate immune response, which starts with phosphorylation and activation of Interferon Regulatory Factor 3 (IRF-3) in the cytoplasm. IRF-3 activation is followed by production of IFNβ cytokine in the nucleus. Unfortunately the HCV virus typically evades host cell immune response, presumably due to the HCV NS3/4A protease, which blocks phosphorylation and activity of IRF-3 in interferon production by cleaving one or more cellular proteins in the RIG-I signaling pathway [30]. Since IRF-3 has antitumor functions, its prolonged blocking may also promote chronic HCV and hepatocellular carcinoma [31]. However, if NS3/4A function is disrupted by small molecule inhibitors or by mutations in the NS3/4A gene, the function of IRF-3, as well as the innate immune system, is restored [32]. NS3/4A also stops the TLR3 signaling pathway by cleaving its cofactor, TRIF protein [33]. Both of these processes lead to attenuation of IFN production and inefficient activation of cytolytic T cells (Scheme 1.3).

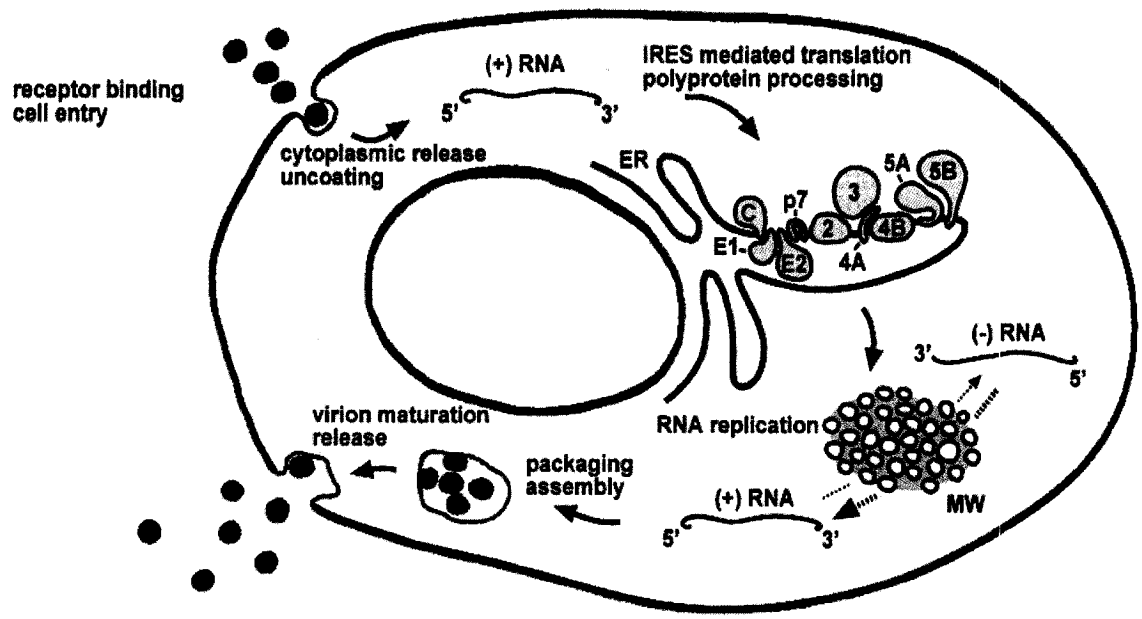

Scheme 1.2: HCV viral life cycle. HCV viral particle is shown by the black dots. ER represents the endoplasmatic reticulum. MW represents the membranous web, derived from the ER, where the replication complex resides. This scheme is copied from: Brass, V., Moradpour, D.,Blum, H. E.., Molecular Virology of Hepatitis C Virus (HCV): 2006 Update. *Int. J. Med. Sci.*, **2006**, *3*, 29-34.

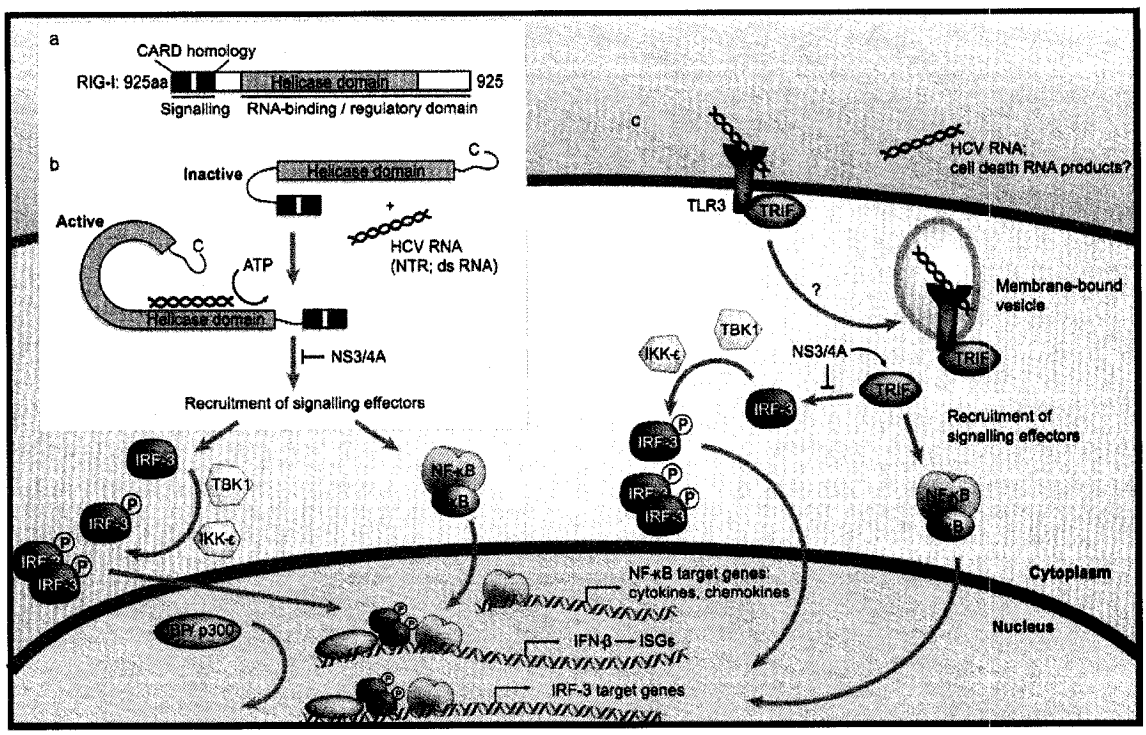

Scheme 1.3: Triggering IRF-3 activation by HCV through Rig-I or TLR-3, and signaling control by NS3/4A. a) RIG-I caspase activation and recruitment domain (CARD) and HCV RNA binding helicase domain. b) In the absence of HCV RNA, RIG-I is in an inactivated conformation. Binding of HCV RNA results in an open conformation and allows CARD signaling and recruitment of signaling effectors. Phosphorilation and activation of IRF-3 results in IFNβ production. The NS3/4A protease disrupts the RIG-I signaling pathway. c) HCV RNA also binds to TLR-3, which signals the phosphorilation and activation of IRF-3 and expression of genes that have antiviral action. NS3/4A protease cleaves TRIF between 372 and 373 amino acids preventing the antiviral signaling through the TLR-3 pathway. This scheme is copied from: Michael. G. and Foy, M. E., Evasion of intracellular host defence by hepatitic C virus. *Nature*, **2005**, *436*, 939-945.

HCV Model Systems

In order to study HCV viral replication, HCV proteins, virus interactions with host proteins, and HCV-specific drug development, appropriate model systems are required. Chimpanzees [34], transgenic and Severe Combined Immunodeficiency Disease (SCID) mice were used as animal models for studies [35]. However, the most widely used models for studying HCV are subgenomic, and full HCV replicons [20, 36]. Replicons represent a genetic element (DNA plasmid, or RNA) that can replicate under their own control in cells. Subgenomic replicons differ from the full replicons in that they do not include genes for all of the HCV proteins. The first subgenomic replicon was developed from genotype 1b by Bartenschlager's research group in 1999 [20]. This replicon had genes that encode for non-structural proteins only (NS2-NS5B). Genes encoding structural proteins were replaced by the selectable marker, *neo* gene, encoding the enzyme neomycin phosphotransferase (NPT). NPT enzyme inactivates the cytotoxic geneticin® antibiotic (G418). In cell media containing G418, only colonies of cells expressing the *neo* gene were generated. These selected transfected cells supported high levels of replication of HCV RNA. However, the number of colonies that were generated was small. A year later, a similar subgenomic replicon based on genotype 1a was developed by the Rice research group [37]. This replicon had mutations introduced within NS3, NS5A and NS5B proteins, which helped cell culture adaptation and produced a larger number of cell colonies. The cell culture adaptation was presumably due to altered interactions between viral proteins in the replication complex, or between viral proteins and host cell [38].

To allow high-throughput screening for developing anti-HCV agents, different

replicons have been designed. In one case, transcriptional trans-activator (Tat protein gene from human immunodeficiency virus) was introduced into the HCV genome [39]. Upon proteolytic cleavage of the polyprotein, the Tat protein would trans-activate nuclear transcription of the reporter gene, placental alkaline phosphatase, incorporated into the genome of host cell. Thus, levels of HCV RNA replication were indirectly measured by quantifying secretion of the reporter enzyme into the cell medium by performing a phospha-light chemiluminescent reporter assay. This approach was unique as the information about HCV replication was obtained without lysing the cells.

The research group of Moradpour has successfully generated a replicon containing the gene for green fluorescent protein (GFP) fused into the HCV NS5A region [40]. By using standard imaging techniques, such as confocal microscopy and electron microscopy, they were able to see the localization of the NS5A-GFP protein with other nonstructural HCV proteins and nascent viral RNA in a membranous web. This technique proved to be a good chemical biology tool for studying the formation of the HCV replication complex, its localization, and its turnover in cell culture.

Other replicons contain reporter genes such as firefly luciferase in their HCV genome. As the firefly luciferase enzyme does not require post-translational modification for its function, it can be used as a genetic reporter immediately after translation. Luciferase catalyzes an oxidative decarboxylation of Beetle luciferin substrate into oxyluciferin in the presence of adenosine triphosphate (ATP), oxygen and Mg(II) at basic pH. Light produced in this reaction at a wavelength of 562 nm can be quantified to indicate the amount of translated proteins. Another commonly used reporter gene is *Renilla* luciferase, which has similar function to the firefly luciferase enzyme. Luciferase-HCV replicons have been used

to study inhibition of HCV by small molecules [41-43], HCV inhibition by RNA interference (RNAi) [44-46], and serum levels of HCV during treatment [47]. Two subgenomic replicons are used throughout this thesis: the pFK-I389neo/NS3-3'/5.1 (bicistronic subgenomic replicon) and the pFK-I389neo/luc/NS3-3'/5.1 (tricistronic subgenomic replicon). They are non-infectious systems and contain HCV genomic sequences from NS3 protein to the 3' end of the HCV genome. The tricistronic subgenomic replicon contains the firefly luciferase gene promoter, which allows us to screen small molecules and siRNA against HCV activity.

Although a few full-length HCV replicons have been created, they were unable to produce infectious systems [36, 48]. The breakthrough in HCV research occurred with the discovery of infectious culture systems simultaneously by Chisari, Rice, and Wakita research groups in 2005 [49-51]. They were able to construct the full infectious replicon using the same nonstructural region from the JFH1 HCV genome, taken from a Japanese patient with fulminant hepatitis. Although the infectious *in vitro* HCV system exists for only one HCV genotype, it still provides the best model so far in which to study the complete viral life cycle, including cell entry, replication, and formation of new virus particles.

Replication complex, HCV protein interactions, and host-virus interactions

HCV forms a replication complex on the host ER membrane consisting of HCV proteins, the replicated HCV RNA, and altered cellular membrane proteins [52]. Expression of the whole polyprotein shows formation of the so-called membranous web on the ER, which consists of small vesicles embedded in a membranous matrix [40, 53, 54]. Experiments with replicons that express individual proteins have shown that the Core protein induces formation of lipid droplets, that NS4B can cause the membranous webs by itself, and

that NS3/4A protein induces formation of vesicles in the ER [52, 55]. Electron microscopy has shown that NS5A and NS5B do not contribute to membrane changes, but rather associate with it afterwards [22]. NS5A also colocalizes with the core protein in lipid droplets [56]. Experiments using a yeast two hybrid assay showed that non-structural HCV proteins not only colocalize, but also form a network of interactions among each other in the replication complex [57]. Therefore, HCV replication can potentially be disrupted by altering the membranous structures where replication occurs. This involves perturbation of lipid and cholesterol metabolism. Several studies have implicated host proteins involved both in cholesterol metabolism and the isoprenoid biosynthesis pathway (Figure 1.1) in supporting viral replication [43, 58-60]. HCV replication depends on viral protein association with the intracellular membrane. Many prenylated proteins are localized at cell membranes. Prenylation involves the addition of isoprenoids, farnesyl (15 carbon atoms) or geranylgeranoyl (20 carbon atoms) groups via thioether linkage to cysteine residues at the carboxy terminus of proteins with a CAAX sequence. (C is cysteine, A is any aliphatic amino acid except alanine and X is the C-terminal amino acid). Although large number of steps in the biosynthesis of geranylgeranoyl pyrophosphate and cholesterol are catalyzed by the same enzymes, it has been shown that in particular, inhibition of geranylgeranoyl transferase with small molecules disrupts viral replication [60]. So far, one geranylgeranylated protein required for HCV RNA replication has been identified. It is a cellular protein FBL2, which is shown to form a complex with NS5A HCV protein in the replication complex [59]. The synthesis of geranylgeranoyl pyrophosphate, and ultimately lipidation of membrane proteins, can be stopped by blocking the function of proteins upstream of geranylgeranoyl in the cholesterol and isoprenoid biosynthetic pathway [61].

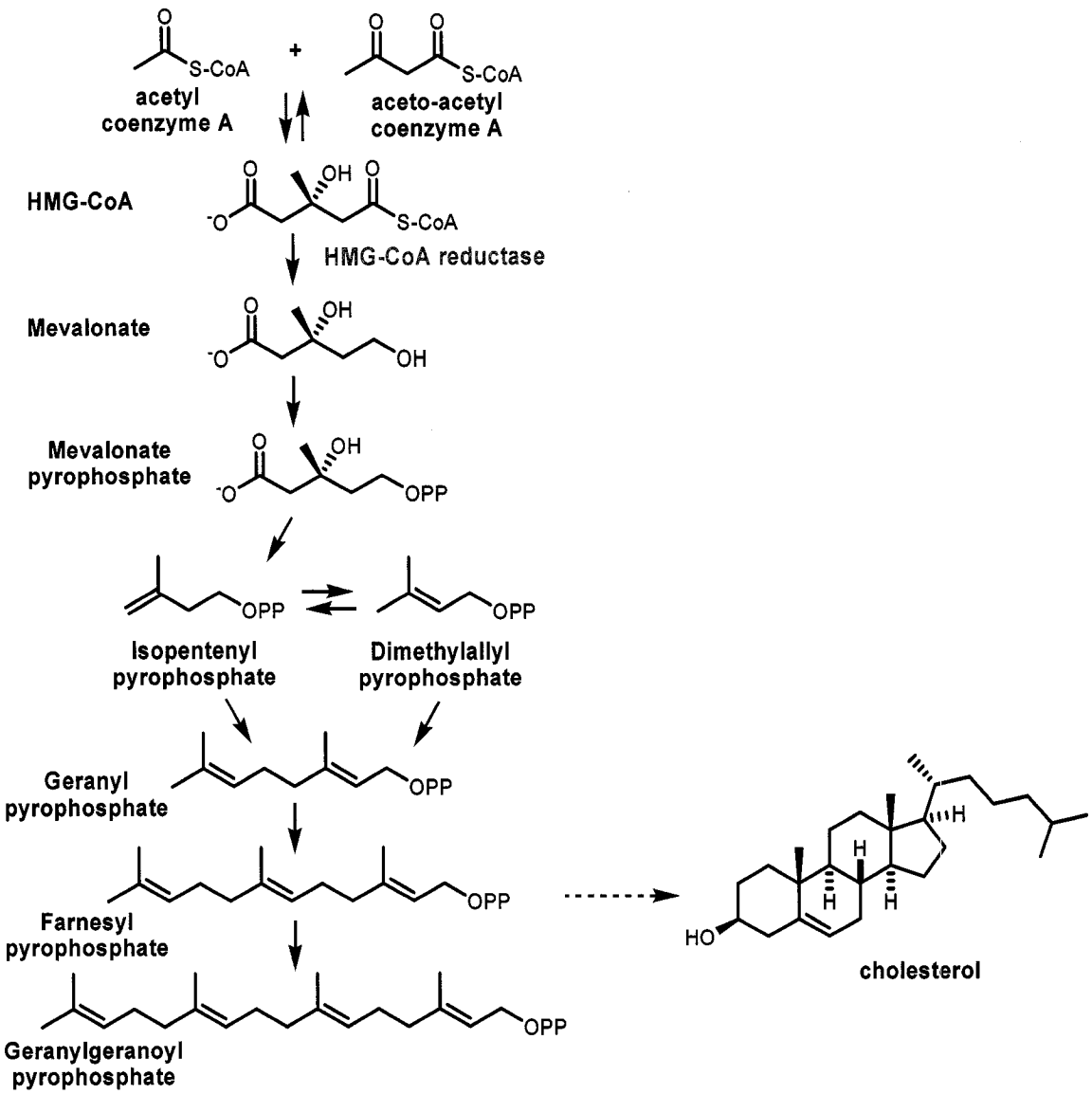

Figure 1.1: Mevalonate, isoprenoid and cholesterol biosynthetic pathways. Farnesyl pyrophosphate is a precursor of cholesterol as well as geranylgeranoyl pyrophosphate.

An example of a small molecule that inhibits HCV replication in cell culture is 25-hydroxycholesterol (Figure 1.2) [42, 43]. 25-hydroxycholesterol binds to sterol response-binding protein (SREBP), disabling its function to initiate transcription of genes associated with cholesterol and isoprenoid biosynthesis and fatty acid metabolism [62]. Two important genes that are under SREBP control encode 3-hydroxy-3-methylglutaryl-coenzyme A synthase (HMG CoA synthase) and HMG-CoA reductase enzymes, which catalyze important steps in the mevalonate pathway (Figure 1.1). Firefly luciferase experiments showed that after 24h treatment with 6.25 μM of 25-hydroxycholesterol, HCV replication was reduced by more than 90% in cell culture [43]. Another small molecule that shows the same effect in the HCV replicon cells is lovastatin, shown in Figure 1.2. Lovastatin blocks the activity of HMG-CoA (3-hydroxy-3-methylglutaryl-coenzyme A) reductase by binding to the enzyme near its active site, blocking access to HMG-CoA substrate [63, 64]. This prevents conversion of HMG-CoA into mevalonate and thereby inhibits formation of isoprenoids (Figure 1.1). Lovastatin was shown to inhibit HCV replication by more than 70% at 50 μM during 24h treatment in culture cells [43, 60]. HCV replication was restored by exogenous addition of geranylgeranoyl, thereby confirming the necessity of geranylgeranylated proteins in the replication complex [58]. The 25-hydroxycholesterol and lovastatin are not used for treating HCV-infected patients because the high concentrations of drugs are too toxic for the liver and other organs. Nevertheless, further studies on the precise mechanism of their antiviral actions and discovery of the host geranylgeranylated proteins involved in host-virus interactions are important for possibly developing new therapeutic agents against HCV disease. As all our research was performed in replicon systems, we used lovastatin and 25-xydroxycholestrol as positive controls for small molecule HCV inhibition in cell culture.

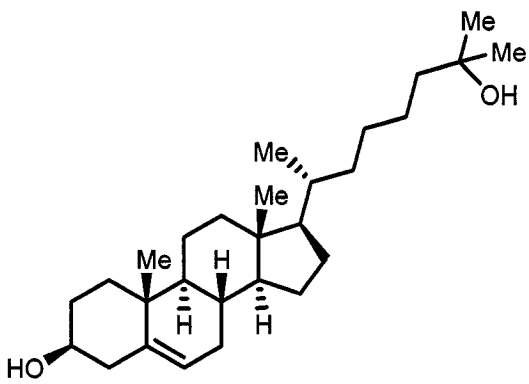

25-hydroxycholesterol

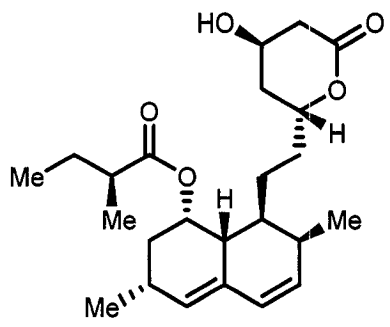

Lovastatin

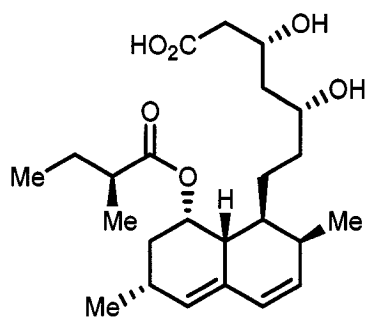

Activated Lovastatin

Figure 1.2: Chemical structures of lovastatin and 25-hydroxycholestrol. For use in cell culture lovastatin must be converted from its inactive lactone form into its active form. The β-hydroxy acid moiety of activated lovastatin mimics the HMG portion of the natural substrate HMG-CoA.

We studied the metabolic pathways involved in HCV replication by investigating the fatty acid catabolytic pathway. Results from this study using a small molecule PPARα antagonist highlighted the importance of this nuclear hormone receptor in the HCV life cycle.

Therapeutic agents in HCV

There are no other therapeutic agents for treating HCV currently in use besides pegylated interferon-α with ribavirin. However, it is not efficient in treating all HCV genotypes, which is one of biggest challenges in developing an HCV drug. Also, the HCV mutation rate is, on average one nucleotide change per replication cycle. This allows the virus to exist as a large number of viral variants (quasi-species), making it difficult to suppress. Current approaches include those based on the design of small molecules that can prevent functions of HCV enzymes, specifically NS3/4A and NS5B. These small molecules are usually discovered using library screening. Other therapeutic approaches use nucleic acids that can target viral RNA, or agents that increase the host immune responses. We summarize here only a few molecules that are currently in clinical trials (Figure 1.3). New approaches to establish novel interactions for therapeutic intervention are still desired.

The HCV NS3/4A enzyme is an interesting target because it catalyzes the release of four HCV proteins from the polyprotein and because it blocks the TLR3 and RIG I pathways of the innate immune response. NS3/4A is a chymotripsin-like enzyme with the catalytic active site consisting of the Ser-139, His-57 and Asp-81 catalytic triad [16]. However, the presence of a zinc atom and its heterodimeric structure distinguish this enzyme from the other host proteases. Unfortunately it is difficult to design a NS3/4A enzyme inhibitor for

two reasons; because it has a very flat and shallow binding pocket; and because it binds large peptide substrates, which do not have drug like properties [65]. The first HCV protease inhibitor that went into clinical trials was BILN 2061, synthesized by Boehringer Ingelheim (Figure 1.3) [66, 67]. Development of this peptide macrocyclic inhibitor was based on the structure of the N-terminal cleavage product (Asp-Asp-Ile-Val-Pro-Cys) derived from the NS5A/5B cleavage site, which inhibits the NS3-4A protease with (Ki=79 μM) [68]. BILN 2061 was active in patients infected with genotype 1-HCV and less active on genotype 2 and 3 viruses. Unfortunately, clinical trials were stopped in phase II as the compound showed cardiac toxicity in laboratory animals. Also, in replicon systems, BILN 2061 was inefficient in inhibiting viral replication if any of arginine 155, alanine 156, or aspartate 168 were substituted in the NS3 domain. This explained the lower efficacy of BILN 2061 in genotype 3, which has glutamine instead of aspartate at position 168. Currently peptidomimetic compound VX-950, developed by Vertex/Mitsubishi is in phase Ib clinical trials (Figure 1.3). The inhibitory mechanism is based on forming a reversible covalent bond between the α-ketoamide moiety in VX-950 and the serine residue in the NS3/4A catalytic active site. During two weeks treatment, VX-950 showed a fast decrease of the viral load in patients infected with genotype 1-HCV. However, the viral load returns after stopping therapy. *In vitro* resistance studies showed that there is only partial cross-resistance between VX-950 and BILN 2061 inhibitors, indicating differences in the interaction of the two inhibitors with NS3/4A protease [69].

NS5B RdRp catalyzes the synthesis of HCV RNA using its own RNA as a template. This enzyme is unique to the viral genome, making NS5B a very interesting target for therapeutics. The NS5B crystal structure shows that it resembles other RNA and DNA

polymerases with so called "right hand" structure, characterized by fingers, thumb and palm sub-domains. The palm domain contains the HCV NS5B active site while the fingers and thumb interact with the HCV RNA chain. Three aspartic acid residues form the active site which coordinates magnesium or manganese ions. NS5B can adopt either a "closed" conformation, in which the fingertips are in contact with the thumb, or an "open" conformation where the thumb-finger interactions are disrupted and the active site is more exposed [16]. There are more than 75 patents for NS5B inhibitors, which are grouped into nucleoside and non-nucleoside analogs [70]. Nucleoside analogs are converted into nucleotides by the host-cell machinery, where they play the role of competitive substrate analogs. They can either cause premature chain termination of the HCV genome, or can be incorporated into the genome but cause detrimental mutations. Ribavirin is the only nucleoside analog that is currently used in HCV therapy in combination with pegylated IFNα. It is a guanozin analog, and incorporates opposite to uracil or cytosine causing an RNA virus error catastrophe [71]. NM283 (Valopicitabine), developed by Idenix/Novartis is another nucleoside analog currently in phase II of clinical trials. It is a 3'-L-valine ester prodrug of 2'-C-methyl cytidine (Figure 1.3). In combination with pegylated IFNα, it causes a 10,000 fold reduction in viral load during 24 weeks treatment. Although 2'-C-methyl cytidines showed efficacy for all HCV genotypes, *in vitro* studies showed that the virus quickly becomes resistant by replacing Ser 282 in NS5B with Thr [72]. On the other hand, non-nucleoside molecules act as active site or allosteric binding site inhibitors. They are usually discovered by screening large, diverse libraries [73]. Examples of active site inhibitors are α,γ-diketo acids that inhibit the NS5B enzyme by chelating metal ions in its active site. The proposed mechanism of allosteric inhibition is through binding to the

NS5B protein far from the active site, disrupting thumb-finger interactions, thus causing an open enzyme conformation. This then prevents complex formation of NS5B polymerase with the positive template ssHCV RNA, stopping viral replication in the initial step. An example of a non-nucleoside analog is JTK-003, a compound developed by Japan Tobacco, which is currently in phase II clinical trials. JTK-003 and related potential inhibitors are derived from the benzimidazole scaffold and have a cyclohexyl ring at the N(1)- position and a carboxyl function at C(5) position. JTK-003 has a large lipophilic aromatic group. However, this moiety can be replaced with a small heterocycle ring without losing much potency. Furthermore, the activity can be improved almost 84 fold by further derivatization of the carboxyl group to produce a benzimidazole carboxamide [70]. Unfortunately, a single mutation replacing proline 495 in NS5B with alanine or leucine causes resistance to JTK-003 and related analogs (Figure 1.3) [74].

Besides small molecule drugs that are currently under development as HCV inhibitors, there are small interfering (si)RNA that are being explored as therapeutic agents [75, 76]. Also, small molecules that stimulate the host innate immune system are considered important inhibitors. So far there are three compounds in phase I clinical trial that inhibit HCV by acting as agonists of Toll receptors [77]. Their activation induces production of IFNα and IFNβ as well as natural killer cells. Actilon (CpG-10101), developed by Coley Pharmaceutical Group showed activity in reducing viral load even in patients who failed IFN-based therapy. ANA245 (7-thia-8-oxoguanosine), and its prodrug ANA975, developed by Anadys Pharmaceuticals are guanine nucleoside stimulators of TLR-7. A daily dose of ANA245 for a week showed a great reduction in HCV titer that did not depend on the viral genotype.

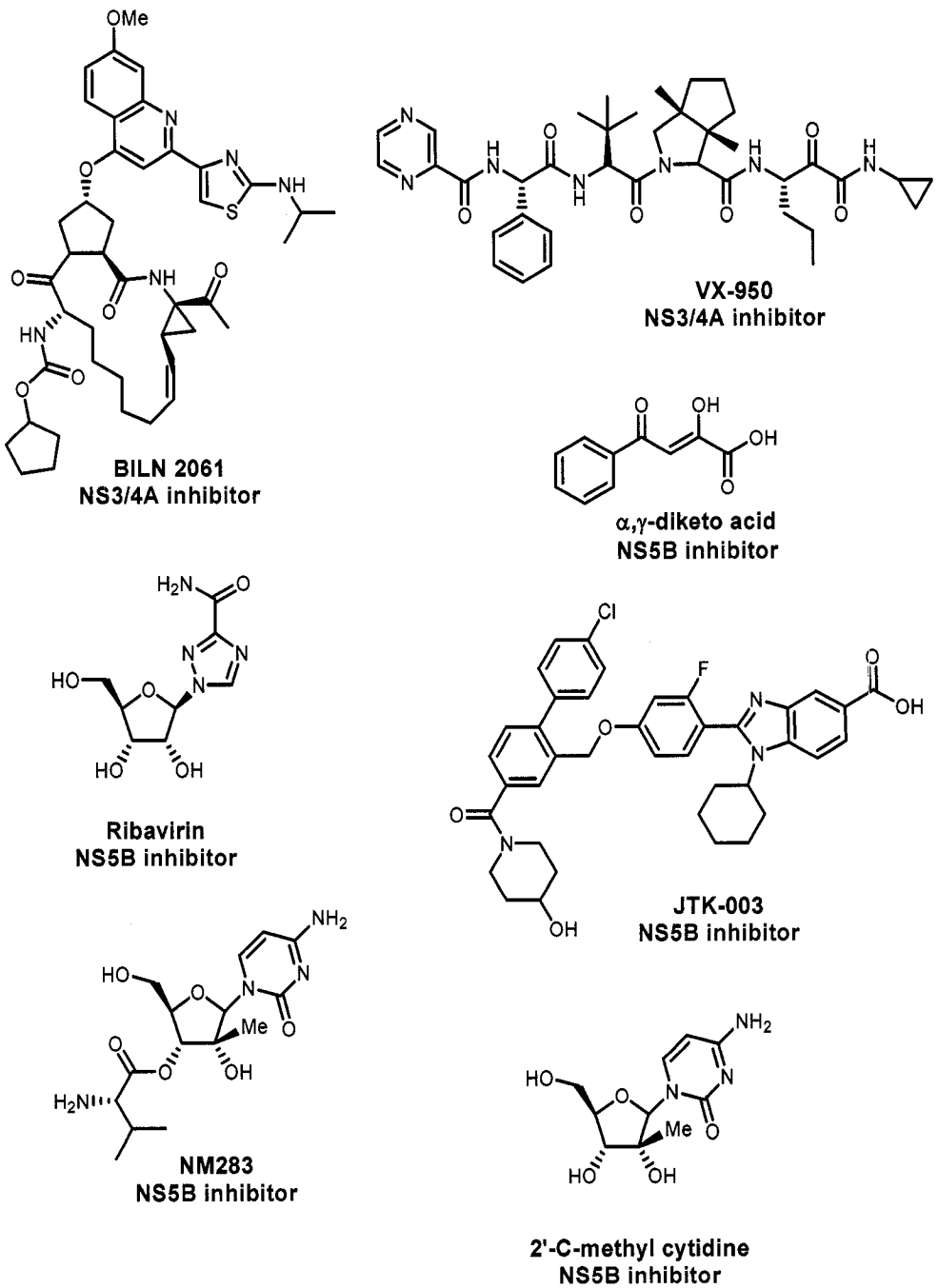

Figure 1.3: Chemical structures of small molecules developed as therapeutic agents for HCV. BILN 2061 and VX-950 are NS3/4A inhibitors; Ribavirin, NM283, α,γ- diketo acid, and JTK-003 are NS5B inhibitors.

References:

[1] Zheng, X.-F.; Fiorentino, D.; Chen, J., et al., TOR kinase domains are required for two distinct functions, only one of which is inhibited by rapamycin. *Cell* **1995**, *82*, 121-130.

[2] Wasley, A.; Alter, M. J., Epidemiology of hepatitis C: Geographic differences and temporal trends. *Semin. Liver Dis.* **2000**, *20*, 1-16.

[3] Simmonds, P., Genetic diversity and evolution of hepatitis C virus - 15 years on. *J. Gen. Virol.* **2004**, *85*, 3173-3188.

[4] Brassard, D. L.; Grace, M. J.; Bordens, R. W., Interferon-alpha as an immunotherapeutic protein. *J. Leukoc. Biol.* **2002**, *71*, 565-581.

[5] Lau, J. Y. N.; Tam, R. C.; Liang, T. J., et al., Mechanism of action of ribavirin in the combination treatment of chronic HCV infection. *Hepatology* **2002**, *35*, 1002-1009.

[6] Feld, J. J.; Hoofnagle, J. H., Mechanism of action of interferon and ribavirin in treatment of hepatitis C. *Nature* **2005**, *436*, 967-972.

[7] Choo, Q. L.; Kuo, G.; Weiner, A. J., et al., Isolation of a Cdna Clone Derived from a Blood-Borne Non-a, Non-B Viral-Hepatitis Genome. *Science* **1989**, *244*, 359-362.

[8] Spahn, C. M. T.; Kieft, J. S.; Grassucci, R. A., et al., Hepatitis C virus IRES RNA-induced changes in the conformation of the 40S ribosomal subunit. *Science* **2001**, *291*, 1959-1962.

[9] Rijnbrand, R. C. A.; Lemon, S. M., Internal ribosome entry site-mediated translation in hepatitis C virus replication. In *Hepatitis C Viruses*, ed.; 'Ed.'^'Eds.' SPRINGER-VERLAG BERLIN: Berlin, 2000; 'Vol.' 242, p^pp 85-116.

[10] Bukh, J.; Purcell, R. H.; Miller, R. H., Sequence-Analysis of the Core Gene of 14 Hepatitis-C Virus Genotypes. *Proc. Natl. Acad. Sci. U. S. A.* **1994**, *91*, 8239-8243.

[11] Moradpour, D.; Englert, C.; Wakita, T., et al., Characterization of cell lines allowing tightly regulated expression of hepatitis C virus core protein. *Virology* **1996**, *222*, 51-63.

[12] Hope, R. G.; McLauchlan, J., Sequence motifs required for lipid droplet association and protein stability are unique to the hepatitis C virus core protein. *J. Gen. Virol.* **2000**, *81*, 1913-1925.

[13] Barba, G.; Harper, F.; Harada, T., et al., Hepatitis C virus core protein shows a cytoplasmic localization and associates to cellular lipid storage droplets. *Proc. Natl. Acad. Sci. U. S. A.* **1997**, *94*, 1200-1205.

[14] McLauchlan, J., Properties of the hepatitis C virus core protein: a structural protein that modulates cellular processes. *J. Viral Hepatitis* **2000**, *7*, 2-14.

[15] Darling, J. M.; Wright, T. L., Immune responses in hepatitis C: is virus or host the problem? *Curr. Opin. Infect. Dis.* **2004**, *17*, 193-198.

[16] Reed, K. E.; Rice, C. M., Overview of hepatitis C virus genome structure, polyprotein processing, and protein properties. *Curr. Top. Microbiol. Immunol.* **2000**, *242*, 55-84.

[17] Choukhi, A.; Ung, S.; Wychowski, C., et al., Involvement of Endoplasmic Reticulum Chaperones in the Folding of Hepatitis C Virus Glycoproteins. *J. Virol.* **1998**, *72*, 3851-3858.

[18] Taylor, D. R.; Shi, S. T.; Romano, P. R., et al., Inhibition of the interferon-inducible protein kinase PKR by HCV E2 protein. *Science* **1999**, *285*, 107-110.

[19] Flint, M.; Maidens, C.; Loomis-Price, L. D., et al., Characterization of Hepatitis C Virus E2 Glycoprotein Interaction with a Putative Cellular Receptor, CD81. *J. Virol.* **1999**, *73*, 6235-6244.

[20] Lohmann, V.; Korner, F.; Koch, J. O., et al., Replication of subgenomic hepatitis C virus RNAs in a hepatoma cell line. *Science* **1999**, *285*, 110-113.

[21] Pavlovic', D.; Neville, D. C. A.; Argaud, O., et al., The hepatitis C virus p7 protein forms an ion channel that is inhibited by long-alkyl-chain iminosugar derivatives. *Proc. Natl. Acad. Sci. U. S. A.* **2003**, *100*, 6104-6108.

[22] Egger, D.; Wolk, B.; Gosert, R., et al., Expression of Hepatitis C Virus Proteins Induces Distinct Membrane Alterations Including a Candidate Viral Replication Complex. *J. Virol.* **2002**, *76*, 5974-5984.

[23] Coito, C.; Diamond, D. L.; Neddermann, P., et al., High-Throughput Screening of the Yeast Kinome: Identification of Human Serine/Threonine Protein Kinases That Phosphorylate the Hepatitis C Virus NS5A Protein. *J. Virol.* **2004**, *78*, 3502-3513.

[24] Manning, G.; Whyte, D. B.; Martinez, R., et al., The Protein Kinase Complement of the Human Genome. *Science* **2002**, *298*, 1912-1934.

[25] Lindenbach, B. D.; Rice, C. M., Unravelling hepatitis C virus replication from genome to function. *Nature* **2005**, *436*, 933-938.

[26] Reyes, G. R., The nonstructural NS5A protein of hepatitis C virus: An expanding, multifunctional role in enhancing hepatitis C virus pathogenesis. *J. Biomed. Sci.* **2002**, *9*, 187-197.

[27] Yoneyama, M.; Kikuchi, M.; Natsukawa, T., et al., The RNA helicase RIG-I has an essential function in double-stranded RNA-induced innate antiviral responses. *Nat. Immunol.* **2004**, *5*, 730-737.

[28] Iwasaki, A.; Medzhitov, R., Toll-like receptor control of the adaptive immune responses. *Nat. Immunol.* **2004**, *5*, 987-995.

[29] Gale, M.; Foy, E. M., Evasion of intracellular host defence by hepatitis C virus. *Nature* **2005**, *436*, 939-945.

[30] Foy, E.; Li, K.; Sumpter, R., et al., Control of antiviral defenses through hepatitis C virus disruption of retinoic acid-inducible gene-I signaling. *Proc. Natl. Acad. Sci. U. S. A.* **2005**, *102*, 2986-2991.

[31] Hoofnagle, J. H., Course and outcome of hepatitis C. *Hepatology* **2002**, *36*, S21-S29.

[32] Foy, E.; Li, K.; Wang, C., et al., Regulation of Interferon Regulatory Factor-3 by the Hepatitis C Virus Serine Protease. *Science* **2003**, *300*, 1145-1148.

[33] Li, K.; Foy, E.; Ferreon, J. C., et al., Immune evasion by hepatitis C virus NS3/4A protease-mediated cleavage of the Toll-like receptor 3 adaptor protein TRIF. *Proc. Natl. Acad. Sci. U. S. A.* **2005**, *102*, 2992-2997.

[34] Kolykhalov, A. A.; Agapov, E. V.; Blight, K. J., et al., Transmission of hepatitis C by intrahepatic inoculation with transcribed RNA. *Science* **1997**, *277*, 570-574.

[35] Mercer, D. F.; Schiller, D. E.; Elliott, J. F., et al., Hepatitis C virus replication in mice with chimeric human livers. *Nat. Med.* **2001**, *7*, 927-933.

[36] Ikeda, M.; Yi, M. K.; Li, K., et al., Selectable subgenomic and genome-length dicistronic RNAs derived from an infectious molecular clone of the HCV-N strain of hepatitis C virus replicate efficiently in cultured Huh7 cells. *J. Virol.* **2002**, *76*, 2997-3006.

[37] Blight, K. J.; Kolykhalov, A. A.; Rice, C. M., Efficient initiation of HCV RNA replication in cell culture. *Science* **2000**, *290*, 1972-1974.

[38] Lohmann, V.; Korner, F.; Dobierzewska, A., et al., Mutations in hepatitis C virus RNAs conferring cell culture adaptation. *J. Virol.* **2001**, *75*, 1437-1449.

[39] Yi, M. K.; Bodola, F.; Lemon, S. M., Subgenomic hepatitis C virus replicons inducing expression of a secreted enzymatic reporter protein. *Virology* **2002**, *304*, 197-210.

[40] Moradpour, D.; Evans, M. J.; Gosert, R., et al., Insertion of Green Fluorescent Protein into Nonstructural Protein 5A Allows Direct Visualization of Functional Hepatitis C Virus Replication Complexes. *J. Virol.* **2004**, *78*, 7400-7409.

[41] Rakic, B.; Sagan, S. M.; Noestheden, M., et al., Peroxisome proliferator-activated receptor alpha antagonism inhibits hepatitis C virus replication. *Chem. Biol.* **2006**, *13*, 23-30.

[42] Sagan, S. M.; Rouleau, Y.; Leggiadro, C., et al., The influence of cholesterol and lipid metabolism on host cell structure and hepatitis C virus replication. *Biochem. Cell Biol.* **2006**, *84*, 67-79.

[43] Su, A. I.; Pezacki, J. P.; Wodicka, L., et al., Genomic analysis of the host response to hepatitis C virus infection. *Proc. Natl. Acad. Sci. U. S. A.* **2002**, *99*, 15669-15674.

[44] Wakita, T.; Moradpour, D.; Tokushihge, K., et al., Antiviral effects of antisense RNA on hepatitis C virus RNA translation and expression. *J. Med. Virol.* **1999**, *57*, 217-222.

[45] Yokota, T.; Sakamoto, N.; Enomoto, N., et al., Inhibition of intracellular hepatitis C virus replication by synthetic and vector-derived small interferring RNAs. *EMBO Rep.* **2003**, *4*, 602-608.

[46] Nakagawa, M.; Sakamoto, N.; Tanabe, Y., et al., Suppression of hepatitis C virus replication by cyclosporin A is mediated by blockade of cyclophilins. *Gastroenterology* **2005**, *129*, 1031-1041.

[47] Vrolijk, J. M.; Kaul, A.; Hansen, B. E., et al., A replicon-based bioassay for the measurement of interferons in patients with chronic hepatitis C. *J. Virol. Methods* **2003**, *110*, 201-209.

[48] Pietschmann, T.; Lohmann, V.; Kaul, A., et al., Persistent and transient replication of full-length hepatitis C virus genomes in cell culture. *J. Virol.* **2002**, *76*, 4008-4021.

[49] Lindenbach, B. D.; Evans, M. J.; Syder, A. J., et al., Complete replication of hepatitis C virus in cell culture. *Science* **2005**, *309*, 623-626.

[50] Wakita, T.; Pietschmann, T.; Kato, T., et al., Production of infectious hepatitis C virus in tissue culture from a cloned viral genome. *Nat. Med.* **2005**, *11*, 791-796.

[51] Zhong, J.; Gastaminza, P.; Cheng, G. F., et al., Robust hepatitis C virus infection in vitro. *Proc. Natl. Acad. Sci. U. S. A.* **2005**, *102*, 9294-9299.

[52] Gosert, R.; Egger, D.; Lohmann, V., et al., Identification of the hepatitis C virus RNA replication complex in Huh-7 cells harboring subgenomic replicons. *J.Virol.* **2003**, *77*, 5487-5492.

[53] Moradpour, D.; Gosert, R.; Egger, D., et al., Membrane association of hepatitis C virus nonstructural proteins and identification of the membrane alteration that harbors the viral replication complex. *Antiviral Res.* **2003**, *60*, 103-109.

[54] Moradpour, D.; Brass, V.; Bieck, E., et al., Membrane association of the RNA-dependent RNA polymerase is essential for hepatitis C virus RNA replication. *J. Virol.* **2004**, *78*, 13278-13284.

[55] Gosert, R.; Kanjanahaluethai, A.; Egger, D., et al., RNA replication of mouse hepatitis virus takes place at double-membrane vesicles. *J. Virol.* **2002**, *76*, 3697-3708.

[56] Shi, S. T.; Lee, K. J.; Aizaki, H., et al., Hepatitis C virus RNA replication occurs on a detergent-resistant membrane that coffactionates with caveolin-2. *J. Virol.* **2003**, *77*, 4160-4168.

[57] Dimitrova, M.; Imbert, I.; Kieny, M. P., et al., Protein-protein interactions between hepatitis C virus nonstructural proteins. *J. Virol.* **2003**, *77*, 5401-5414.

[58] Kapadia, S. B.; Chisari, F. V., Hepatitis C virus RNA replication is regulated by host geranylgeranylation and fatty acids. *Proc. Natl. Acad. Sci. U. S. A.* **2005**, *102*, 2561-2566.

[59] Wang, C. F.; Gale, M.; Keller, B. C., et al., Identification of FBL2 as a geranylgeranylated required for hepatitis C cellular protein virus RNA replication. *Mol. Cell* **2005**, *18*, 425-434.

[60] Ye, J.; Wang, C. F.; Sumpter, R., et al., Disruption of hepatitis C virus RNA replication through inhibition of host protein geranylgeranylation. *Proc. Natl. Acad. Sci. U. S. A.* **2003**, *100*, 15865-15870.

[61] Goldstein, J. L.; Brown, M. S., Regulation of the Mevalonate Pathway. *Nature* **1990**, *343*, 425-430.

[62] Brown, M. S.; Goldstein, J. L., The SREBP pathway: Regulation of cholesterol metabolism by proteolysis of a membrane-bound transcription factor. *Cell* **1997**, *89*, 331-340.

[63] Tabernero, L.; Rodwell, V. W.; Stauffacher, C. V., Crystal structure of a statin bound to a class II hydroxymethylglutaryl-CoA reductase. *J. Biol. Chem.* **2003**, *278*, 19933-19938.

[64] Istvan, E. S.; Deisenhofer, J., Structural mechanism for statin inhibition of HMG-CoA reductase. *Science* **2001**, *292*, 1160-1164.

[65] Lipinski, C. A.; Lombardo, F.; Dominy, B. W., et al., Experimental and computational approaches to estimate solubility and permeability in drug discovery and development settings. *Adv. Drug Delivery Rev.* **1997**, *23*, 3-25.

[66] Faucher, A.-M.; Bailey, M. D.; Beaulieu, P. L., et al., Synthesis of BILN 2061, an HCV NS3 Protease Inhibitor with Proven Antiviral Effect in Humans. *Org. Lett.* **2004**, *6*, 2901-2904.

[67] Lamarre, D., An NS3 protease inhibitor with antiviral effects in humans infected with hepatitis C virus. *Nature* **2003**, *426*, 186-189.

[68] Llinas-Brunet, M., Peptide-based inhibitors of the hepatitis C virus serine protease. *Bioorg. Med. Chem. Lett.* **1998**, *8*, 1713-1718.

[69] Lin, C., In vitro resistance studies of hepatitis C virus serine protease inhibitors, VX-950 and BILN 2061: structural analysis indicates different resistance mechanisms. *J. Biol. Chem.* **2004**, *279*, 17508-17514.

[70] Beaulieu, P. L.; Tsantrizos, Y. S., Inhibitors of the HCV NS5B polymerase: new hope for the treatment of hepatitis C infections. *Curr. Opin. Investig. Drugs* **2004**, *5*, 838-850.

[71] Crotty, S.; Cameron, C. E.; Andino, R., RNA virus error catastrophe: Direct molecular test by using ribavirin. *Proc. Natl. Acad. Sci. U. S. A.* **2001**, *98*, 6895-6900.

[72] Migliaccio, G., Characterization of resistance to non-obligate chain-terminating ribonucleoside analogs that inhibit hepatitis C virus replication in vitro. *J. Biol. Chem.* **2003**, *278*, 49164-49170.

[73] LaPlante, S. R., Binding mode determination of benzimidazole inhibitors of the hepatitis C virus RNA polymerase by a structure and dynamics strategy. *Angew Chem. Int. Ed. Engl.* **2004**, *43*, 4306-4311.

[74] Tomei, L., Mechanism of action and antiviral activity of benzimidazole-based allosteric inhibitors of the hepatitis C virus RNA-dependent RNA polymerase. *J. Virol.* **2003**, *77*, 13225-13231.

[75] Kapadia, S. B.; Brideau-Andersen, A.; Chisari, F. V., Interference of hepatitis C virus RNA replication by short interfering RNAs. *Proc. Natl. Acad. Sci. U. S. A.* **2003**, *100*, 2014-2018.

[76] Wilson, J. A.; Jayasena, S.; Khvorova, A., et al., RNA interference blocks gene expression and RNA synthesis from hepatitis C replicons propagated in human liver cells. *Proc. Natl. Acad. Sci. U. S. A.* **2003**, *100*, 2783-2788.

[77] De Francesco, R.; Migliaccio, G., Challenges and successes in developing new therapies for hepatitis C. *Nature* **2005**, *436*, 953-960.

2

Peroxisome Proliferator-Activated Receptor α Antagonism Inhibition of Hepatitis C Virus Replication

Introduction

HCV is known to induce changes in lipid metabolism [1, 2], and initiate the formation of ER-derived membranous webs on which HCV replicates [3, 4]. HCV also causes steatosis, the accumulation of lipid droplets within liver cells. HCV structural proteins are known to reside on these lipid droplets [5-8]. The liver is the organ responsible for lipid homeostasis by balancing fatty acid β-oxidation and ketogenesis. Peroxisome Proliferator-Activated Receptors (PPARs) are key mediators in maintaining this balance [9-13]. Gene expression analysis in chimpanzees has shown that among others, genes regulated by PPARs are suppressed during HCV viral increase [1]. We decided to test the converse, if modulation of PPAR expression had effects on HCV replication. In this investigation, we utilized a predictive chemical genetics approach using a small molecule antagonist, and small interfering (si)RNA to modulate PPAR expression.

Peroxisomes [14] are organelles bound by a single membrane and are involved in various metabolic functions such as fatty acid oxidation, peroxide derived respiration, glycerolipid synthesis, and cholesterol metabolism within the cell [15]. Peroxisome proliferator-activated receptors (PPARs), named after their role in peroxisome synthesis, are the nuclear receptors responsible for the effects of ligands, collectively known as peroxisome proliferators that alter both the number and size of peroxisomes [13]. PPARs were first cloned from mouse liver in 1990 by Issemann and Green [13]. Three major PPAR isoforms have been identified in mammals, namely α, β/δ, and γ [9-12, 16-18]. Although the different PPAR isoforms have high amino acid homology and very similar structures, they are encoded by separate genes and differ in their localization, function, and ligand specificity. PPARα is primarily expressed in tissues with high lipid metabolism including brown adipose and liver tissue, as well as kidney, heart, and skeletal muscle tissue [12, 16, 17]. PPARβ/δ has highest expression in the gut, kidney, and heart, although it is expressed at low levels in almost every tissue [16]. PPARγ is highly expressed in adipose tissue and to a lesser extent in the colon, kidney, liver, spleen, immune system, and retina [16].

Like other nuclear hormone receptors, PPARs have several functional domains. These are: the ligand-independent transactivation domain (AF-1) located in the variable NH_2-terminal region; the highly conserved DNA binding domain (DBD), which recognizes specific DNA sequences; the linker region; the ligand binding (LBD) and dimerization domain; and the ligand-dependent transactivation domain (AF-2) in the CO_2H- terminal region (Scheme 2.1). Upon ligand binding, PPARs form heterodimers with the retinoid X receptor α (RXR-α). The heterodimer binds to specific DNA sequences known as PPAR response elements (PPRE) in the 5' promoter sequence of the target genes through the DNA-

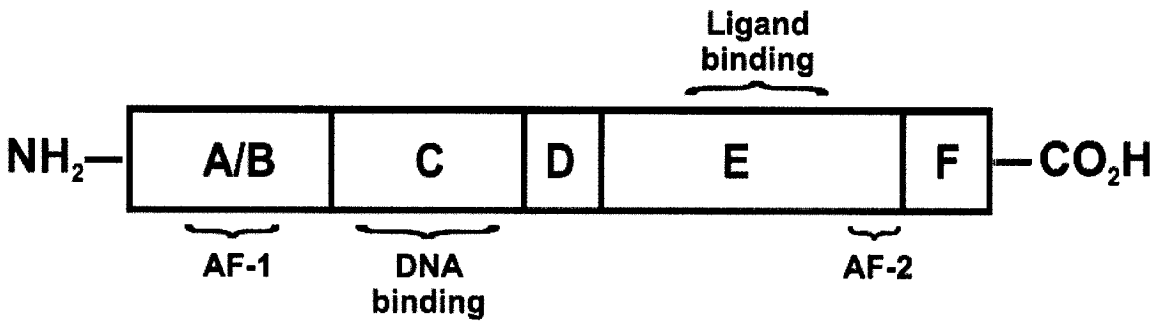

Scheme 2.1: Schematic representation of the nuclear hormone receptor. The nuclear hormone receptor contains several functional domains (A-F). The ligand independent transactivation domain (AF-1) is in the A/B region at the NH_2-terminal end. The DNA binding domain is in the C region. D is linking domain. The Ligand binding domain is in the E region. The Ligand-dependent transactivation domain (AF-2) is at the CO_2H terminal end.

binding domain of PPAR and RXR [9, 10, 19-21]. In this way, PPARs regulate and activate gene transcription (Scheme 2.2).

PPAR receptors are important pharmaceutical targets for the treatment of diseases that involve the misregulation of glucose, cholesterol, and fatty acid metabolism, such as diabetes [22]. PPAR receptors naturally bind to a number of fatty acids and metabolites as well as synthetic ligands including peroxisome proliferator, hypolipidemic, anti-inflamatory, and insulin-sensitizing compounds (Figure 2.1) [23-26]. Although different amino acid sequences in the LBD create ligand specificity, it is common that agonists or antagonists of PPAR show cross reactivity between isoforms [23-25]. Cross reactivity of ligands between PPARα and PPARγ is most common primarily because the ligand binding pockets are closest in size and shape to each other [24, 25]. The major factor in their selectivity is thought to be due to a substitution of Tyr-314 in PPARα for His-323 in PPARγ [24, 25]. In contrast, the PPARδ binding pocket is much smaller and shows little cross reactivity. ([4-Chloro-6-(2,3-xylidino)-2-pyrimidinylthio]acetic acid (Wy 14,643) and clofibrate, both activators of PPARα, have effects on lipid metabolism but at higher concentrations they also activate PPARγ [27]. Rosiglitazone and pioglitazone, two examples of thiazolidinediones (TZD) antidiabetic drugs, are effective in lowering glucose levels by targeting PPARγ, but also have a modest effect on lipid levels due to cross reactivity with the other isoforms [28, 29]. Farglitazar is an agonist of both PPARα and PPARγ and has robust effects on glucose, high density lipoprotein, and triglycerides in diabetic patients [22].

PPARα acts as a sensor for the level of free fatty acids and modulates the responses of fat-oxidizing tissues [23]. In the liver, PPARα regulates expression of genes encoding

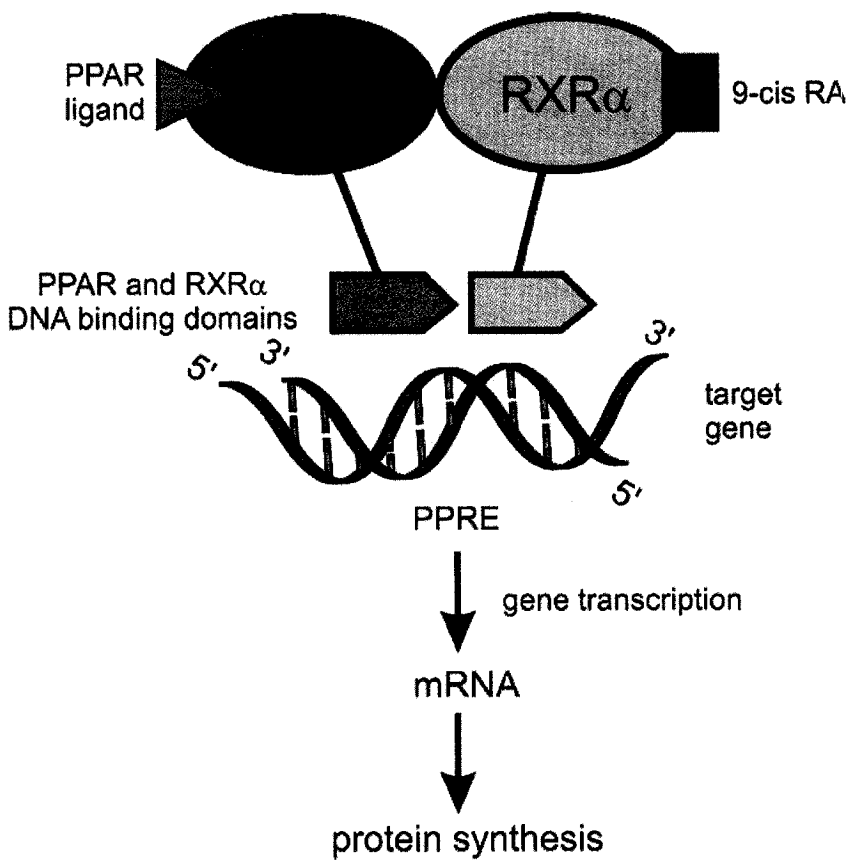

Scheme 2.2: Molecular mechanism of the action of PPAR. PPAR isoforms and RXR-α form a heterodimer in the presence of their ligands (PPAR ligand and 9-cis retinoic acid (RA) respectively). The heterodomain then binds to PPAR response elements (PPRE) of PPAR regulated genes via PPAR and RXR-α DNA-binding domains (orange and green). Coactivators and corepressors regulate transcription of PPAR target genes such as genes involved in adipogenesis, lipid metabolism, cell growth and differentiation.

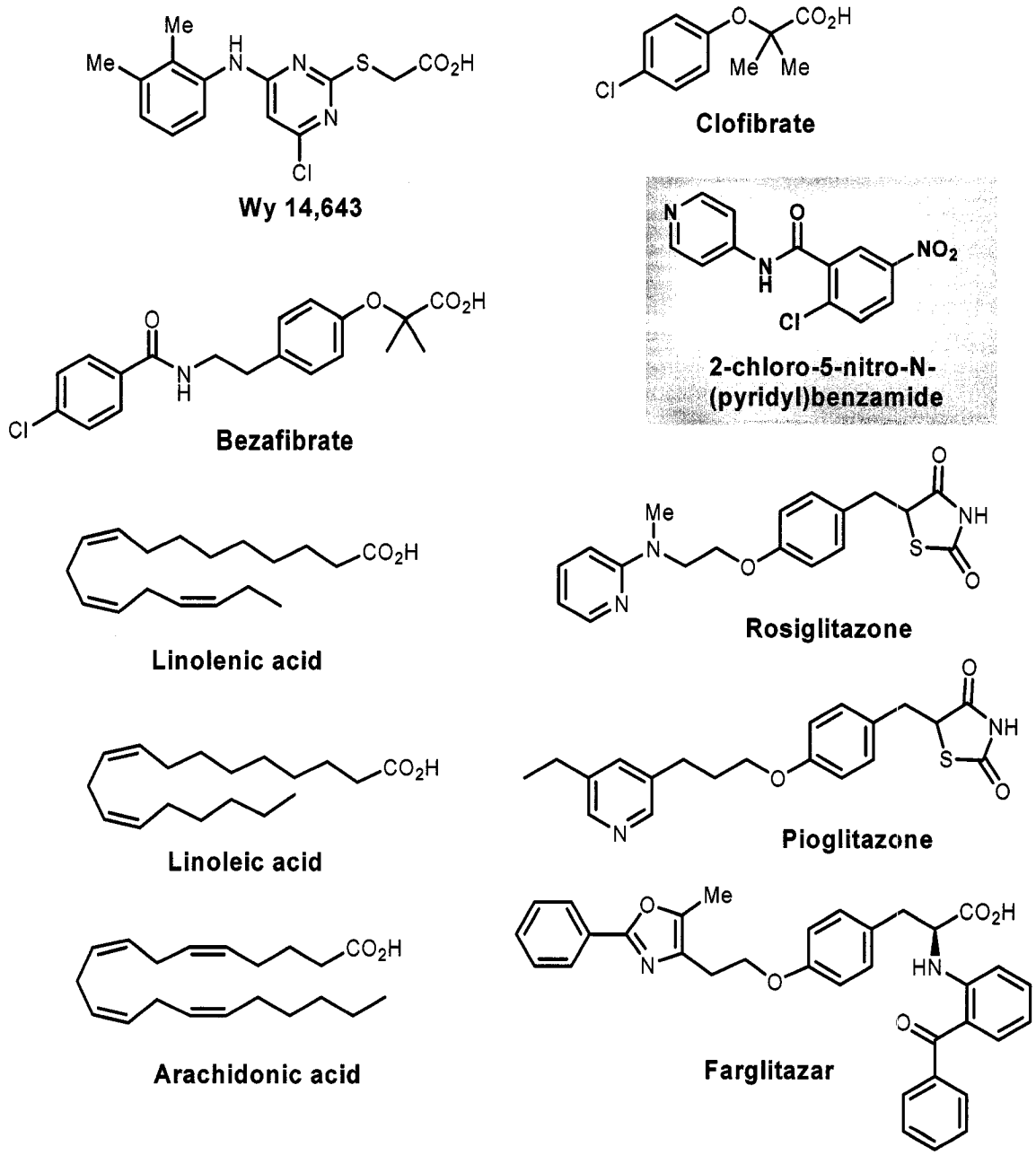

Figure 2.1: Natural and synthetic PPAR ligands. Natural PPAR ligands include polyunsaturated fatty acids and their metabolites. Synthetic PPAR ligands include peroxisome proliferators (Wy 14,643), fibrates (bezfibrate, clofibrate), thiazolidine diones (rosiglitazone, pioglitazone), and benzamide.

several enzymes that are involved in peroxisomal, microsomal and mitochondrial β-oxidation pathways. Three enzymes: acyl CoA synthase (acetyl-CoA synthase), carnitine palmitoyl transferase 1A (CPT1A), and 3-hydroxy-3-methylglutaryl-CoA synthase (HMG-CoA synthase), are very important for fatty acid β-oxidation and keto body formation because they catalyze the rate determining steps [30]. Fatty acid β-oxidation occurs in mitochondria and peroxisomes (for chains longer than 22 carbons) and produces fatty acids that are two carbon atoms shorter and acetyl coenzyme A (acetyl-CoA). This process is highly exothermic and complete oxidation leads to formation of many molecules of ATP and acetyl-CoA. In order for the reaction to occur, the fatty acids have to be activated. This is catalyzed by acyl CoA synthase, whose gene transcription is regulated by PPARα. Before oxidation occurs the activated fatty acids have to be transported from the cytosol into the mitochondria. This transfer is catalyzed by the second PPARα regulated enzyme, CPT1A. Finally, during fasting acetyl-CoA can be further oxidized into keto bodies (acetone, acetoacetate, and D-β-hydroxybutyrate), which is regulated by HMG-CoA synthase. Activated PPARα up-regulates transcription of the aforementioned genes which leads to increased breakdown of triglycerides and fatty acids, increased cellular fatty acid uptake, and reduced triglyceride and fatty acid synthesis. Deactivation of PPARα leads to the opposite effects and reduced uptake of fatty acids into mitochondria, which causes the accumulation of lipids in tissues that have fast fatty acid catabolism such as the heart and the liver.

Misregulation of PPARα or its downstream targets have been implicated in liver-specific disease states. For example, PPARα knock-out mice develop fatty livers and respond very poorly to fasting, resulting in hepatic lipid accumulation, hypoglycemia, and

impaired ketogenesis [9, 23, 31, 32]. On the other hand PPARα activation over prolonged periods is linked to tumorigenesis in rats [20], the development of steatosis, and delayed liver regeneration in knockout mice following partial hepatectomy [19, 33-35]. Hepatocellular levels of PPARα and its downstream target (CPT1A) have been shown to be depressed in untreated patients with HCV infections [36, 37], implying a role for PPARα in HCV infection and pathogenesis. A link between this disruption of PPARα gene expression at the mRNA level and HCV core protein expression in HepG2 cells, and thus a link between PPARα and HCV pathogenesis, has also been made [36]. Therefore, we wanted to study the influence of this misregulation on HCV replication in replicon systems.

Chemical genetics:

One of the approaches that we used in this thesis was based on studying of biological systems by using small molecule interrogators. This is known as chemical genetics. Small molecules are used to interact with transcribed proteins to modulate downstream genes and proteins. In this way, the hierarchical connections between genes and proteins can be elucidated. There are three approaches to chemical genetics that one can apply [38]. In forward chemical genetics, a particular phenotype of interest is first defined. High-throughput screening of a library is used to select molecules inducing the desired phenotype. This is followed by identification of the protein target. Reverse chemical genetics first selects the protein target of interest followed by screening of a library for molecules that perturb that protein's activity. Thirdly, in predictive chemical genetics, the protein of interest is chosen based on gene expression analysis. Parallels can be drawn between genetics, that uses genetic manipulation, and chemical genetics, that uses chemical

manipulation, to study genes. Forward genetics uses random mutagenesis to induce a desired phenotype and then identifies the gene. Likewise, reverse genetics starts with a target gene and then determines the phenotype.

One advantage of using small molecule modulators over genetic modulators is that they often induce biological effect reversibly where the level of activity is controlled by concentration. Furthermore, the biological effect of small molecules is usually fast, being diffusion controlled and provides information on the kinetics of the interaction. Additionally, small molecules can potentially be used to modulate individual functions of multifunctional proteins selectively and by doing so small molecules can identify novel biological targets that are not easily identified by genetic techniques.

Genetic knockout leads to permanent, steady state effects. Often, genetic manipulations use siRNA and intracellular ribozymes, which are highly specific modulators at the gene level. The expression of any gene can be blocked upon introduction of siRNA duplexes into the cell. The mechanism by which animals recognize and destroy exogenous RNA, such as dsRNA, is called RNA interference. Several steps define the dsRNA destruction pathway (Scheme 2.3). In the first, initiation step, the dsRNA gets processed into 20-25 nucleotide siRNAs by an RNase III-like enzyme called Dicer. In *in-vivo* experiments these short siRNA sequences can be introduced directly into cells. Once inside cells the siRNA duplex is assembled into an endoribonuclease-containing complex known as a RNA-induced silencing complex (RISC). RISC then unwinds the duplex, recognizes and binds to the complementary mRNA to be silenced, and catalyzes its cleavage. This is called the effector step, which results in gene silencing. Compared to small molecules, the effects of siRNA are not rapid and they are not cell permeable, which creates cell delivery problems.

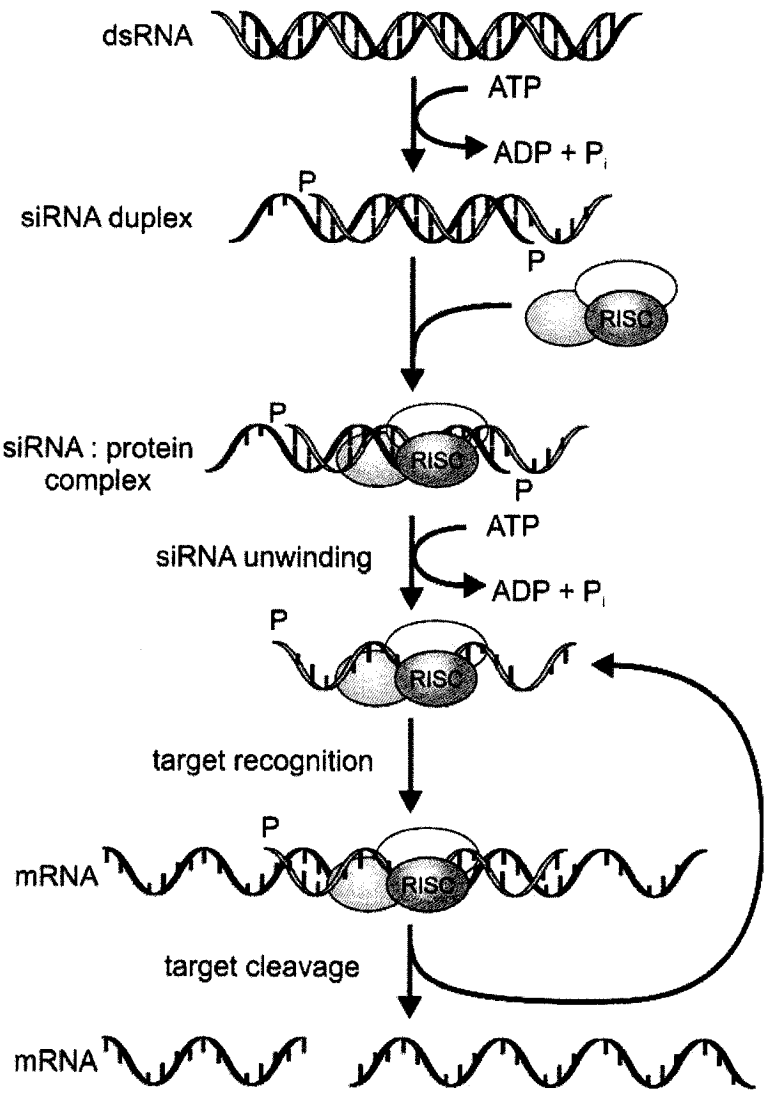

Scheme 2.3: RNAi mechanism. In the initiation step, dsRNA is processed into 21-23 nucleotide small interfering RNAs (siRNAs). In the effector step, the siRNA duplexes bind to a nuclease complex to form the RNA-induced silencing complex, or RISC. An ATP-dependent unwinding of the siRNA duplex is required for activation of the RISC. RISC then unwinds the duplex, recognizes and binds to the complementary mRNA to be silenced, and catalyzes its cleavage.

Most importantly, as they act at the gene level, they cannot affect post-translationally modified proteins, nor sub-domains of multifunctional proteins. Therefore gene modulation cannot confirm if a translated protein is a viable drug target.

Even though small molecules can give temporal/kinetic control, they can be inefficient in modulating protein function especially when dealing with highly homologous active sites within a protein family. On the other hand any gene can be manipulated using genetics in a specific manner but without temporal control. Therefore, the ultimate way to perform studies on genes and proteins specifically and temporally is to use both chemical genetics and genetics methodologies in parallel. This approach, applied here in this PPAR-HCV study, is called orthogonal chemical genetics. We showed, using Huh-7 cells harboring subgenomic HCV replicons, that PPARα antagonism mediated by 2-chloro-5-nitro-N-(pyridyl)benzamide (BA) (Figure 2.1) and siRNA individually, result in decreased HCV viral replication. BA is actually a PPARγ antagonist that covalently modifies cysteine 313 [18]. This antagonist also shows cross reactivity towards PPARα although with about ~800 times less selectivity compared to PPARγ [18]. We speculate that the viral inhibition is linked with an observed misregulation of lipid homeostasis that increases intracellular lipid content.

Results and Discussion

In order to study host-virus molecular interactions that result from perturbation of PPAR signaling, we utilized Huh-7 cells harboring a tricistronic subgenomic replicon which was constructed from HCV genomic RNA of genotype 1b, and derived from the clone pFK-I389neo/luc/NS3-3'/5.1; and a bicistronic replicon derived from the clone pFK-

I389neo/NS3-3'/5.1 (Figure 2.2) [39]. We first investigated the activity of a number of small molecules, PPAR metabolism modulators for their effect on inhibiting HCV replication in replicon cells utilizing the firefly genetic reporter. We found 2-chloro-5-nitro-N-(pyridyl)benzamide, BA to be the most active [18]. As mentioned previously, BA antagonizes PPARγ, and to a lesser extent PPARα [18]. When ligand activators bind to PPAR, they cause changes in the receptor conformation which allows recruitment of co-activator protein complexes necessary for transcriptional activation of the PPAR target genes. However, BA reacts with cysteine 313 in PPARγ affecting the overall conformation of the receptor, preventing the recruitment of co-activators and actually promoting the binding of co-repressor proteins [18]. In this way BA antagonizes PPARγ function. BA presumably affects the PPARα activity in a similar way. BA activity was measured by performing firefly luciferase assays after treatment of replicon cells with a range of BA concentrations over a 24h time course (Figure 2.3). We used 1% v/v methanol in cell medium as the negative control or mock treatment. The activity data is replotted in Figure 2.4 as percent of maximum response, where 100% corresponds to complete HCV inhibition, and 0% corresponds to the mock treated cells. We determined IC_{50} against the HCV replicon for BA to be 30 μM. The IC_{50} represents the concentration of drug that causes 50% inhibition of viral replication. We then performed a cell viability assay, measuring lactate dehydrogenase (LDH), a stable cytosolic enzyme that is released upon cell lysis to determine the toxicicity of BA to replicon cells. Cytotoxicity assays, following 24h treatments indicated that BA was detrimental to cell viability only at concentrations exceeding 100 μM (Figure 2.5).

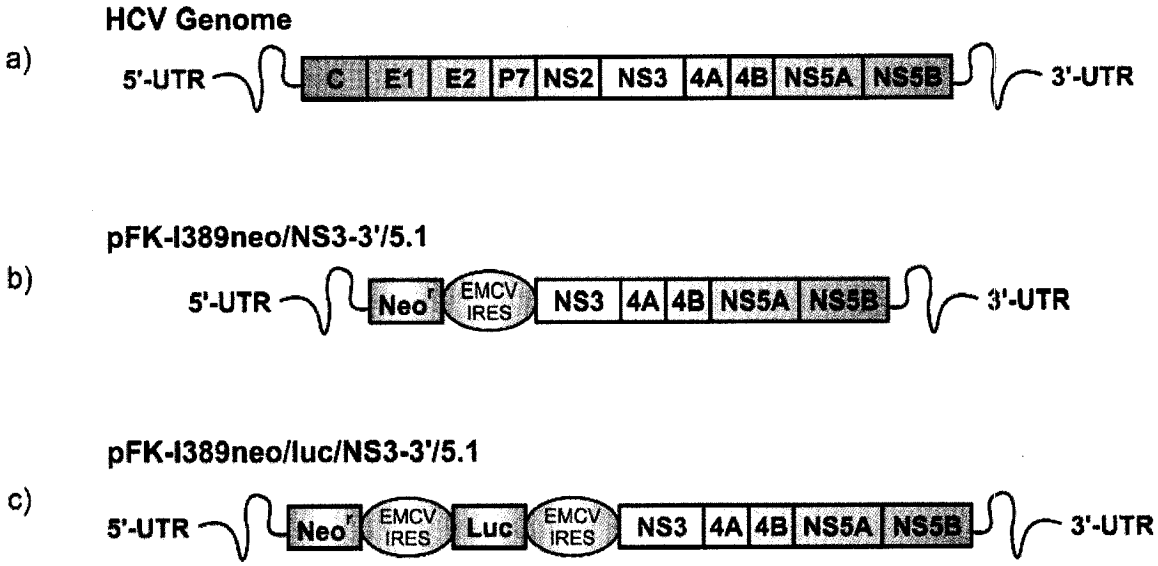

Figure 2.2: Schematic representation of the HCV genome and the subgenomic replicons used in the PPAR study. a) HCV genome with genes expressing structural and non-structural proteins. b) pFK-I389neo/NS3-3'/5.1 bicistronic sub-genomic replicon. c) pFK-I389neo/luc/NS3-3'/5.1 tricistronic sub-genomic replicon containing the firefly luciferase gene used in screening experiments.

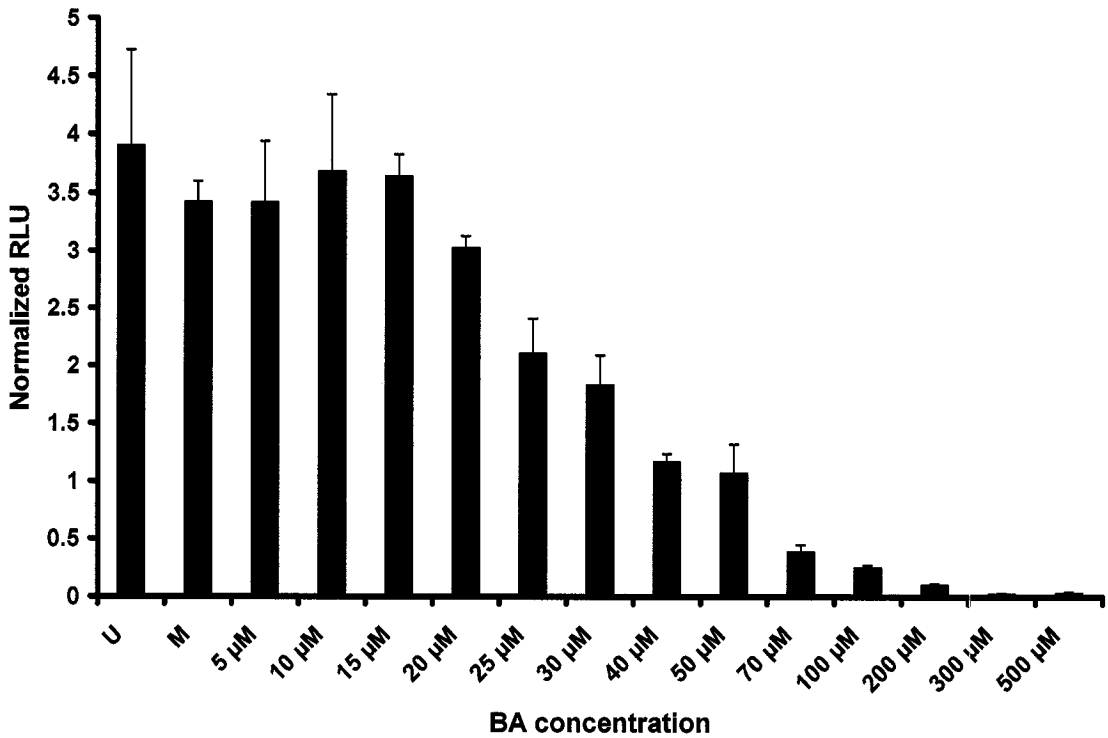

Figure 2.3: Normalized firefly luciferase data for Huh-7 replicon cells treated with 2-Chloro-5-nitro-N-(pyridyl)benzamide (BA). Activity was determined following 24h exposure to BA in concentrations ranging from 1 μM to 500 μM. Data has been normalized to total protein content. M is 1% v/v MeOH; U is untreated, replicon bearing Huh-7 cells. Error bars represent the mean ± SD.

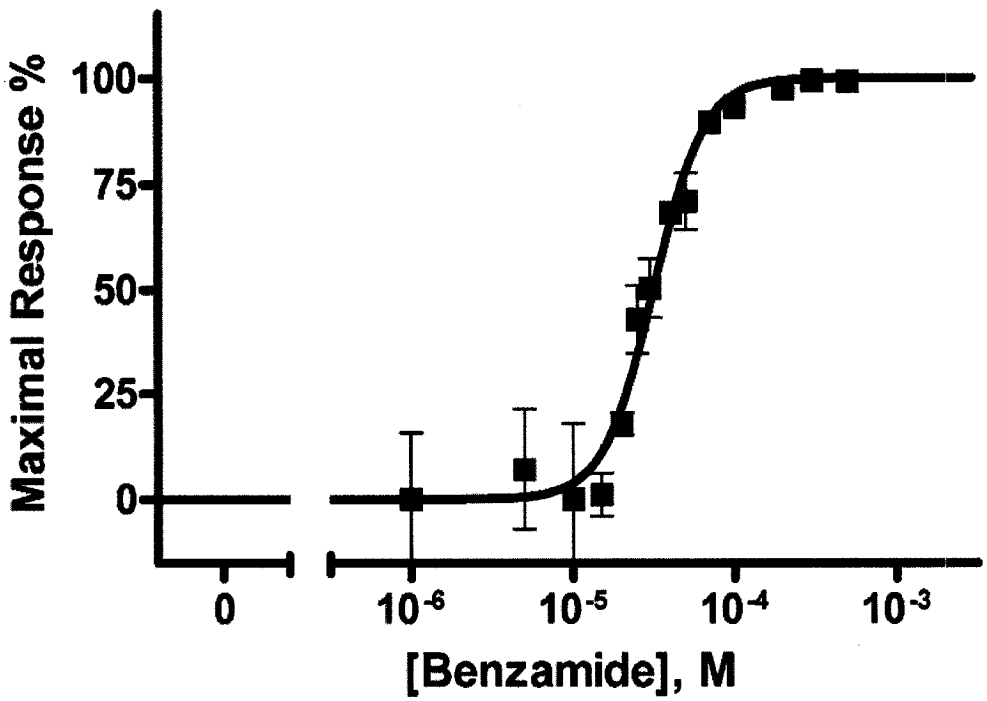

Figure 2.4: Benzamide activity data expressed as IC_{50}. Data shows concentration-dependent inhibition of HCV replication by BA in the sub genomic replicon system after 24h treatment. 0% and 100% response correspond to no effect on and complete inhibition of HCV replication respectively. The IC_{50} value of BA was determined to be 30 μM. Error bars represent the mean ± SD.

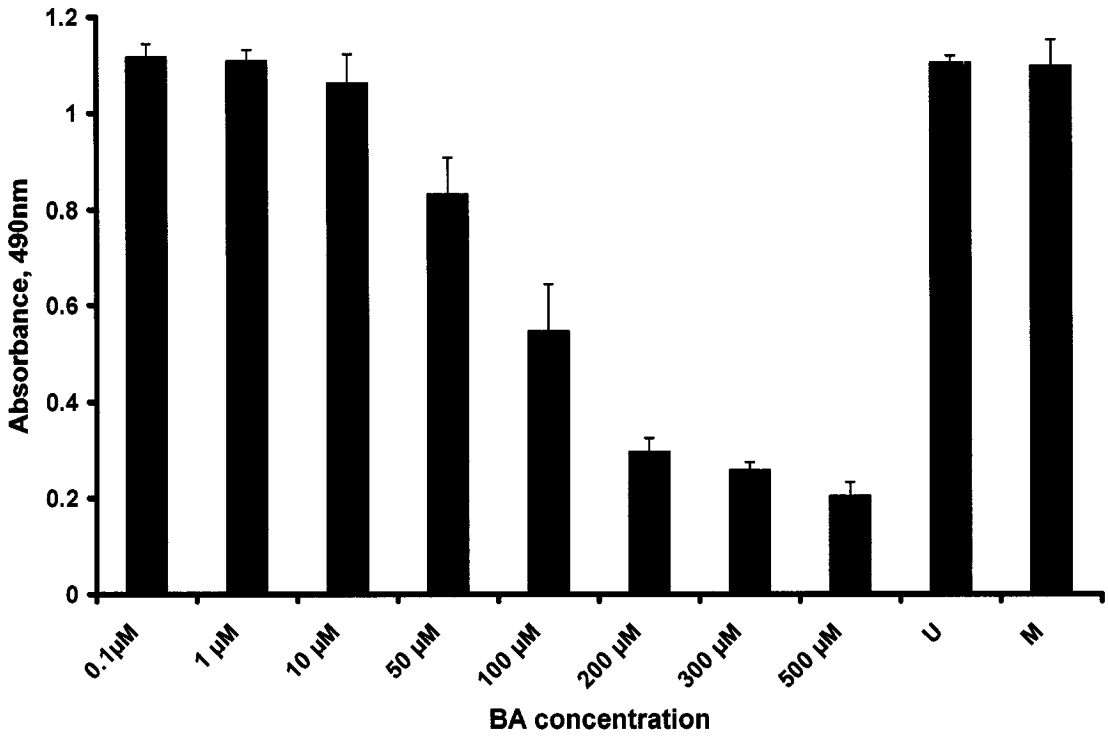

Figure 2.5: Cytotoxicity data for Huh-7 replicon cells treated with 2-Chloro-5-nitro-N-(pyridyl)benzamide (BA). Cytotoxicity was determined by LDH assay following 24h exposure to concentrations ranging from 0.1 µM to 500 µM of BA. M is 1% v/v MeOH; U is untreated, replicon bearing Huh-7 cells. Error bars represent the mean ± SD.

In order to determine the effect of BA on HCV protein expression levels, we performed Western blotting analysis of the HCV NS3 protein in the bicistronic replicon (Figure 2.2b). Western blotting (immunoblotting) is a method for detecting proteins in a protein extract. It separates negatively charged denatured proteins according to their mass using gel electrophoresis. The proteins are then transferred out of the gel onto a membrane (typically polyvinylidene difluoride or nitrocellulose), where they are "probed" using antibodies specific to the protein. In this experiment we used the effect of known inhibitors of HCV: interferon gamma (IFNγ), 25-hydroxycholesterol, and lovastatin [1, 2, 40], to compare against the effect of BA on HCV protein expression. We confirmed uniform gel loading using control antibodies against the protein-tyrosine phosphatase, PTP1D. PTP1D together with the rest of the PTP member proteins is involved in maintaining intracellular protein phosphatase homeostatis and cell cycle progression. Since none of small molecule inhibitors used in here affect cell cycle progression, expression level of PTP1D will not change and therefore is suitable for determining loading efficiency of protein samples. As expected, decreases in the HCV NS3 protein were observed for the positive controls. In addition, the BA treated cells also showed decreases in HCV NS3 protein, and hence, HCV replication at 75 μM and 50 μM at the 6h treatment point and at 25 μM at the 24h treatment point (Figure 2.6).

In order to determine whether the anti-HCV activity of BA was due to its effect on effecting PPARα or PPARγ protein, we examined the role of direct PPAR gene knockdown using standard RNA interference techniques (siRNA). We used the tricistronic HCV replicon (Figure 2.2c) to test the effects of siRNA's that target PPARα and PPARγ by performing firefly luciferase assays. Oligonucleotide duplexes that target luciferase GL2 and

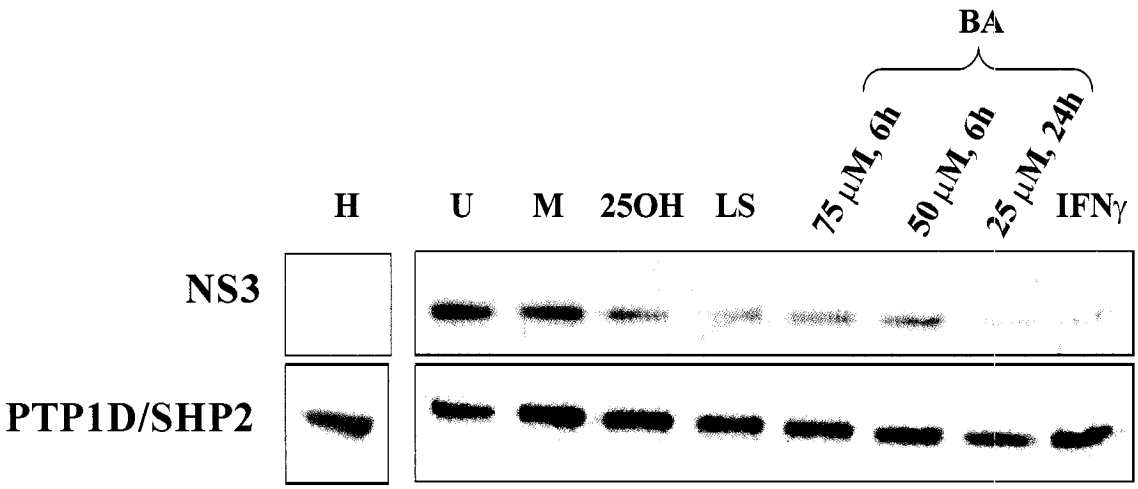

Figure 2.6: Western blot indicating the expression of HCV NS3 protein under various conditions. Lanes are: H – Huh-7 cells; U – untreated Huh-7 cells stably harboring an HCV subgenomic replicon derived from pFK-I389/neo/NS3-3'/5.1; M - 1% v/v MeOH; 25OH – 2 μM 25-hydroxycholesterol; LS - 50 μM lovastatin; BA – 2-Chloro-5-nitro-N-(pyridyl)benzamide (25, 50, 75 μM); IFNγ – 50 U interferon γ. The PTP1D/SHP2 housekeeping protein was used to confirm equal loading of all cells. The Western blot shows that expression levels of NS3 protein in cells treated with known inhibitors of HCV and with BA in replicon cells are similar. BA shows an effect upon 6h cells treatment and even greater effect on HCV inhibition after 24h cells treatment. 25OH and LS treatment times were 24h and IFNγ treatment time was 72h.

GL3 were used as positive and negative controls, respectively. The luciferase GL2 oligonucleotides target specifically the firefly luciferase gene contained within our tricistronic HCV replicon, whereas GL3 siRNA targets a different luciferase isoform not found in our replicon. Thus, HCV in our replicons will be inhibited by the GL2 siRNA, and conversely not affected by the GL3 siRNA. We treated cells with PPARα siRNA, PPARγ siRNA, known inhibitors of HCV such as IFN-γ and 25-hydroxycholesterol, mock species, and siRNA GL2 and GL3 control species over 72h time course. We observed inhibition of HCV replication with PPARα siRNA (Figure 2.7). Interestingly, knockdown of the PPARγ gene using siRNA had no effect on HCV replication (Figure 2.7). Examination of PPARγ mRNA levels in gene expression data suggests that this isoform is probably not abundantly expressed in Huh-7 cells. Furthermore, comparison of siRNA and BA activities reveals that the reduction in HCV replication with siRNA was not as significant as the reduction obtained with the benzamide ligand (Figure 2.3 and Figure 2.7). We also observed that the time required to reach similar HCV inhibition effect was significantly longer for the PPARα siRNA (72h) compared to BA (6-24h). This observation is not surprising keeping in mind the rapidity by which small molecules can diffuse to their target and the fact that they can act directly on the receptor post-translationally [18].

To confirm downregulation of the targeted PPARα, we performed Western blotting to look at the expression level of PPAR proteins in HCV replicons. Figure 2.8 shows the Western blot of PPARα and PPARγ expression in cells treated with PPARα siRNA and PPARγ siRNA, HeLa cells, 293T cells, untreated cells, and mock siRNA treatment cells. Due to high expression of PPARα HeLa (cervic carcinoma) cells were used as a positive control for PPARα but they also show expression of PPARγ. 293T cells (derivative of a

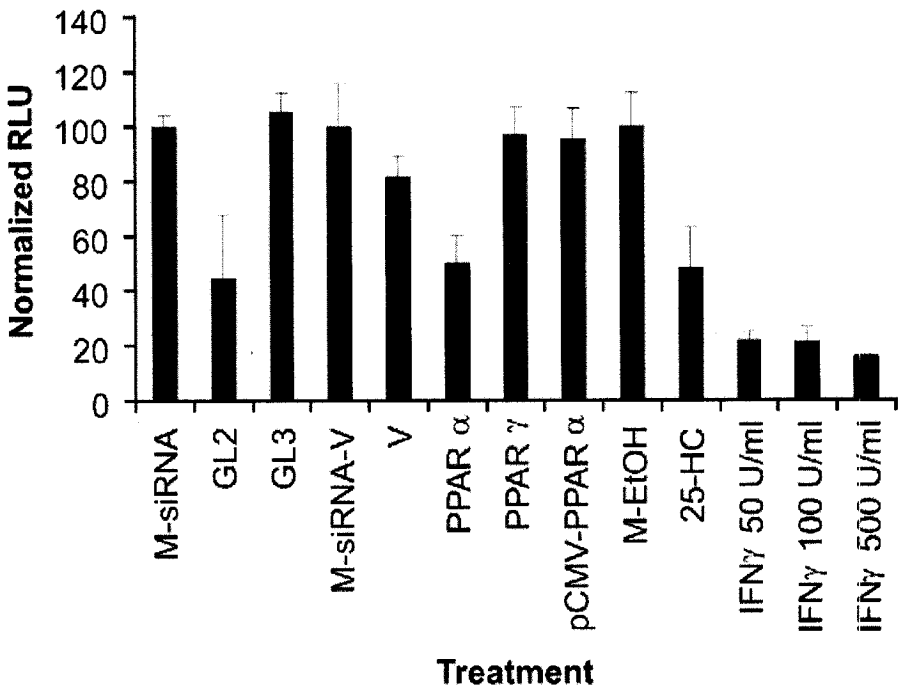

Figure 2.7: Normalized firefly luciferase data of Huh-7 replicon cells transfected with siRNAs 25-hydroxycholesterol and interferon γ. Activity was determined following 72h treatments: M-siRNA – mock siRNA treatment; GL2 – siRNA positive control molecule targeting the luciferase gene; GL3 – siRNA negative control molecule; M-siRNA-V – control for vectors expressing scrambled siRNA; PPARα and PPARγ siRNA vectors targeting PPARα and PPARγ; pCMV-PPARα overexpression vector for PPARα; M-EtOH – 1% v/v Ethanol; 25-HC – 2 μM 25-hydroxycholesterol; IFNγ – 50, 100, and 500 U treatments with interferon γ. Data has been normalized to total protein content. Data show that treatment with PPARα – siRNA inhibited HCV replication in replicon cells similarly to the positive control GL2-siRNA and small molecule 25-hydroxycholesterol. PPARα-siRNA had no effect on repicon cells with overexpression PPARa. Treatment with PPARγ – siRNA showed no effect on HCV inhibition. Error bars represent the mean ± SD.

human renal epithelial cell line) have lesser expression of PPARα and were used as a positive control for PPARγ. Upon 48h treatment with siRNA, PPARα protein levels were ~50% lower than the mock transfected cells. Furthermore, we overexpressed the PPARα gene in replicon cells. The PPARα siRNA had no effect on cells overexpressing PPARα protein, which was shown both by firefly luciferase assay (Figure 2.7) and by Western blotting (Figure 2.8). This confirmed our hypothesis that modulation of PPARα negatively affects HCV.

Although we showed by firefly luciferase and Western blotting experiments that the PPAR antagonist BA inhibits HCV replication, we had to confirm its specificity in PPARα signaling and lipid metabolism. In order to do so we performed two experiments. In the first experiment we looked at the activity of BA on HCV replicon cells with overexpressed PPARα. In the second experiment, we performed quantitative polymerase chain reaction (QPCR) analysis on genes regulated by PPARα. We overexpressed replicon Huh-7 cells with pCMV- PPARα vector for 72h, after which we treated cells for 24h with BA. We compared the activity of BA on PPARα overexpressed cells and on replicon Huh-7 cells using firefly luciferase assay. As expected, BA was less effective at inhibiting HCV replication in cells overexpressing PPARα and showed an effect on it only at the higher concentration of 75 μM. These observations provide further support that inhibition of HCV replication by BA results from antagonism of the PPARα protein in the Huh-7 and HCV replicon cell lines (Figure 2.9). Furthermore, HCV inhibition by IFNγ in replicon cells and overexpressed replicon cells did not change, which is in agreement with the mechanism of IFNγ action.

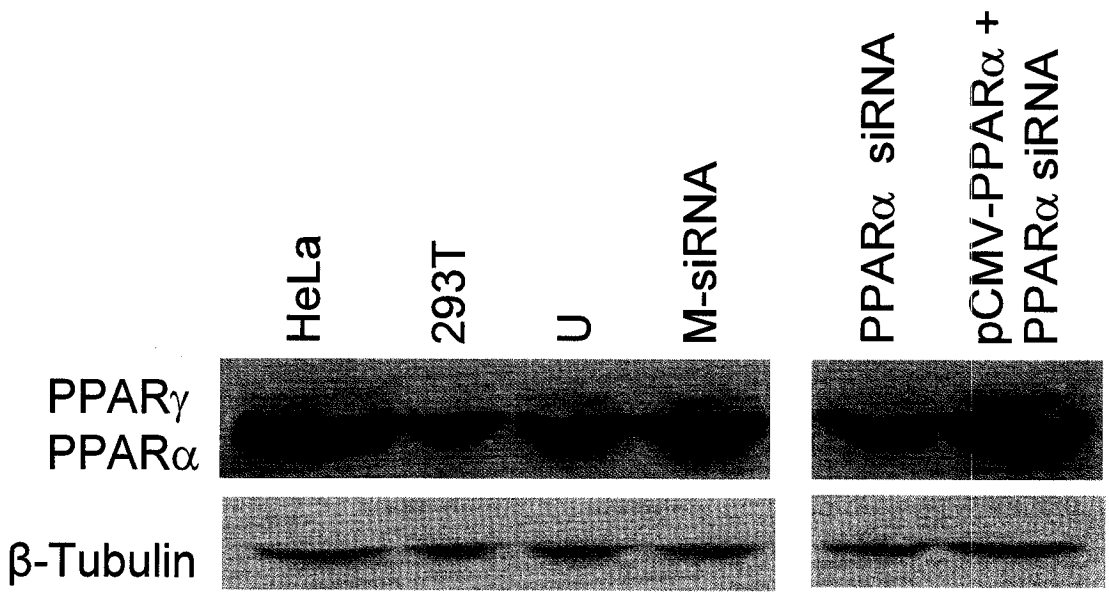

Figure 2.8: Western blots of Huh7 cells stably replicating a subgenomic HCV replicon under various conditions showing the expression of PPARα and PPARγ proteins. The upper panel shows Western Blots for PPARγ (52 kD) and PPARα (55 kD) performed using a primary antibody against human PPAR receptors. Lanes are : HeLa – HeLa cells; 293T – 293T cells; U – untreated Huh7 cells stably harboring an HCV subgenomic replicon derived from pFK-I389neo/luc/NS3-3'/5.1; M-siRNA – mock siRNA treatment; PPARα siRNA – siRNA vector targeting PPARα; pCMV-PPARα + PPARα siRNA – treatment with overexpression vector for PPARα and PPARα siRNA. HeLa cells are a control for PPARα but also show expression of PPARγ 293T cells are a positive control for PPARγ with lesser expression of PPARα. The lanes with HCV replicon lysates, mock transfected HCV replicon cells, and control transfected cells all displayed high levels of PPARα with lower levels of PPARγ. The lane containing lysates from PPARα siRNA treated cells shows downregulation of the PPARα gene (<50% relative to mock) after 48h treatment whereas the lane containing lysates from cells transfected with pCMV-PPARα followed by treatment with PPARα siRNA display larger amounts of PPARα protein relative to mock transfected cells.

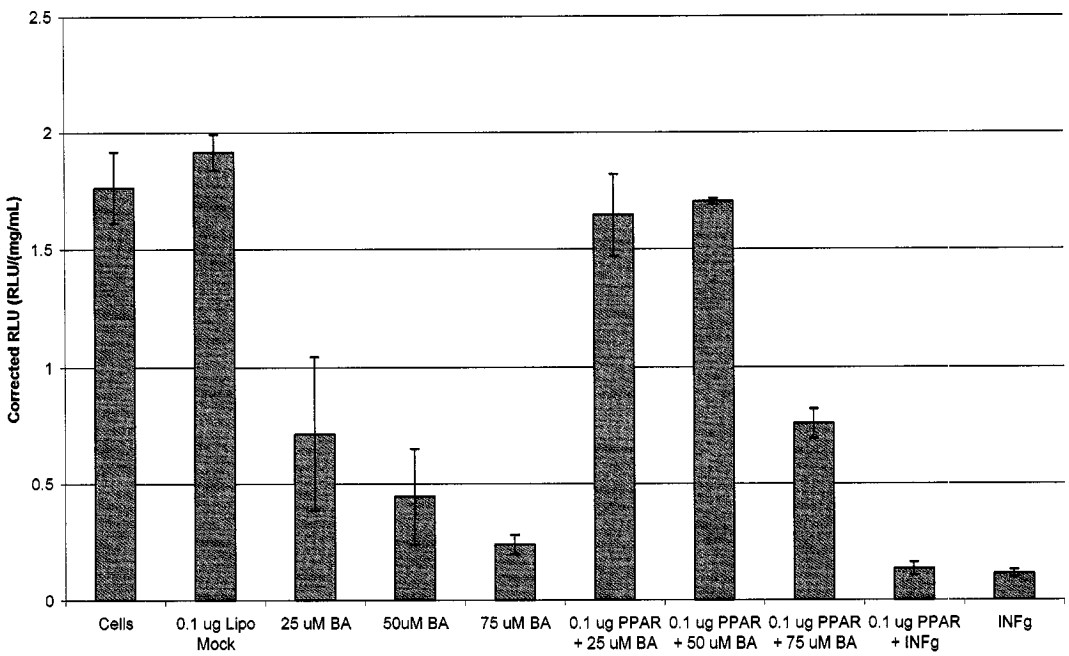

Figure 2.9: Normalized firefly luciferase data of Huh-7 replicon overexpressed with PPARα under various conditions. Data shows that overexpression of PPARα reverses the effects of 2-chloro-5-nitro-N-(pyridyl)benzamide, BA. The bar graph of corrected relative light units (RLU) vs treatment shows that overexpression of PPARα has no effect of HCV replication whereas it does reverse the anti-HCV effects of BA. The first 5 bars show the difference in luciferase signal between cells, mock transfected cells, and exposure of HCV replicons to increasing concentrations of BA per 24h treatment. Bars 6-8 show the influence of overexpressing PPARα (72h transient overexpression) using the pCMV-PPARα plasmid construct. Specifically, ~50% recovery of luciferase signal at the highest dose of BA was observed. The last two lanes show that overexpressing PPARα using the pCMV-PPARα plasmid (72h) has no effect on interferon gamma treatment. Error bars represent the mean ± SD.

PPARα regulates transcription and protein levels of many enzymes involved in fatty acid oxidation. Therefore, antagonists of PPARα will have a downregulation effect on transcription of downstream targets, including HMG-CoA synthase and CPT1A [30, 36]. The effects of BA on PPARα signaling and lipid metabolism were confirmed by Quantitative PCR (QPCR) analysis of mitochondrial HMG-CoA synthase mRNA levels and CPT1A levels relative to expression levels of house keeping genes, 18S ribosomal RNA (rRNA) and Glyceraldehyde-3-phosphate dehydrogenase GAPDH mRNA, which were not affected, and therefore used as a control. QPCR or Real–time PCR is a technique that allows quantification of levels of specific DNA and RNA sequences. QPCR is based on the detection of a fluorescent signal during amplification of a PCR product via intercalation of fluorescent reporter molecules such as SYBR Green I dye into the double-stranded DNA product [41]. The amount of fluorescent product is proportional to the amount of desired DNA sequence and corresponds to the mRNA expression levels. Treatment of Huh-7 cells bearing HCV replicons with BA for 24h resulted in decreases in HMG-CoA synthase levels from 3 to <180 fold for BA concentrations ranging between 25 μM and 50 μM BA. Under these conditions we did not observe any changes in CPT1A levels. These results are listed fully in Table 2.1.

In contrast with the action of agonists, antagonists of PPARα induce hyperlipidemia [9, 11, 21]. To determine the morphological effects of cells treated with BA, we used fluorescence microscopy. Huh-7 cells were treated with 25 μM and 50 μM concentrations of BA for 24 h. These cells were then fixed and stained for lipids with oil red O dye and counterstained with DAPI to reveal the nuclei. Representative images are shown in Figure 2.10. We observed a noticeable increase in lipid droplet accumulation (red) in the cells

cDNA	Gene	Mean Ct	Delta Ct	DD Ct	2^{-DDCt}	Fold Change
replicon	18S rRNA	15	14	5.9	0.01674646	
replicon	HMG CoAs	29				
30μM BA	18S rRNA	14.9	19.9			
30μM BA	HMG CoAs	34.8				-59.7
replicon	18S rRNA	15	14	7.533333	0.005398097	
replicon	HMG CoAs	29				
50μM BA	18S rRNA	14.76667	21.533333			
50μM BA	HMG CoAs	36.3				-185.3
replicon	18S rRNA	15.43333	N/A	N/A	N/A	0
replicon	CPTI	26.4				
25μM BA	18S rRNA	15.46667	9.8			
25μM BA	CPTI	26.26667				
replicon	GAPDH	15.83333	11.566667	1.7	0.307786103	
replicon	HMG CoAs	27.4				
25μM BA	GAPDH	15.83333	13.266667			
25μM BA	HMG CoAs	29.1				-3.25
replicon	GAPDH	15.83333	11.566667	4.433333		
replicon	HMG CoAs	27.4				
50μM BA	GAPDH	16.63333	16			
50μM BA	HMG CoAs	32.63333				-21.61

Table 2.1: Quantitative PCR Data for the Effects of BA on PPARα Regulated Genes. QPCR results on hydroxymethylglutaryl-CoA synthase (HMG-CoAs) mRNA levels using 18S rRNA and GAPDH mRNA levels as controls.

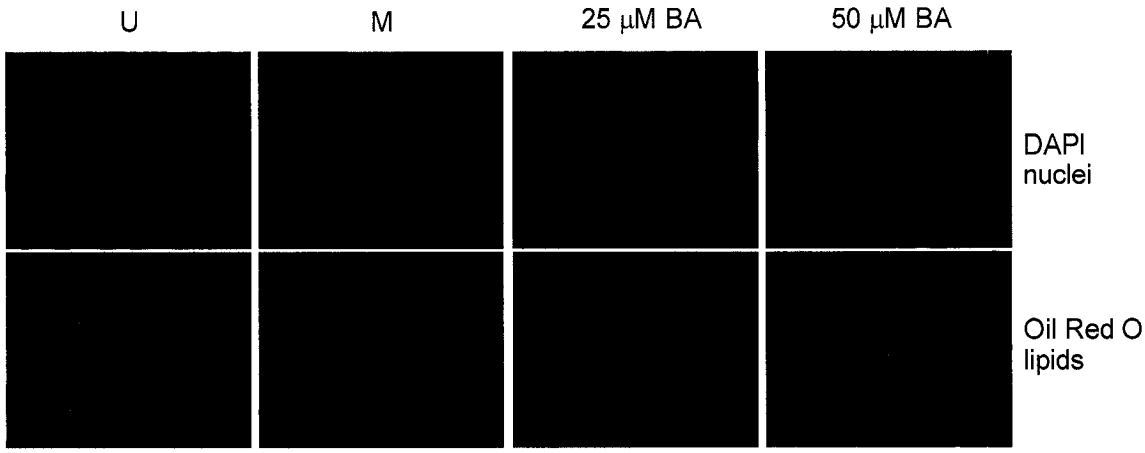

Figure 2.10: Fluorescent images of Huh-7 replicon cells treated with 2-choloro-5-nitro-N-(pyridyl)benzamide (BA). Images show lipids stained with Oil red O and nuclei stained with 4',6-diamidino-2-phenylindole (DAPI). Cells were imaged after 24h treatment under the following conditions: U untreated replicon cells; M – mock, 1% v/v MeOH; 25 μM BA, 50 μM BA. Lipid levels were increased in the cells treated with BA.

treated with BA. These observations are consistent with the previously stated link between the PPARα receptor and lipid accumulation in clinical HCV infections [36, 37].

To determine if mediation of PPAR signaling affected levels and subcellular localization of the HCV protein NS5B, we preformed protein immunostaining in the replicon bearing Huh-7 cells in the presence of BA. Treatments were conducted for 6h at BA concentrations of 25 μM, 50 μM, and 75 μM. Fluorescence images of these treated cells are shown in Figure 2.11 where NS5B protein is shown in green, nuclei in blue, and lipid droplet in red. Consistent with previous studies [7, 42-44], we observed NS5B subcellular localization in the perinuclear region where membranous web structures are known to reside. The observed decrease in signal intensity for NS5B with increasing doses of benzamide is consistent with the NS3 western blot data (Figure 2.6). Benzamide also appeared to enhance cellular permeability of the antibodies at lower doses. Fluorescence microscopy did not show an alteration of NS5B subcellular localization, although it is possible that NS5B and the associated replication complexes are dispersed upon treatment with BA.

A qualitative investigation of the kinetics of hyperlipidemia was undertaken using a relatively new technique, Coherent Anti-Stokes Raman (CARS) microscopy, in collaboration with Professor Sunney Xie's research group at Harvard. CARS microscopy is a novel technique that images specific molecular vibrations without the need for fluorescence labelling or staining. In conventional Raman spectroscopy, a sample is irradiated with photons. A small proportion of those photons scatter inelastically off the sample, exciting a vibrational motion within the molecule, and emitting a photon with energy equal to the initial photon energy minus energy of the quantized molecular vibration (Scheme 2.4a). By dispersing these scattered photons in a spectrometer, the vibrational spectrum of a particular

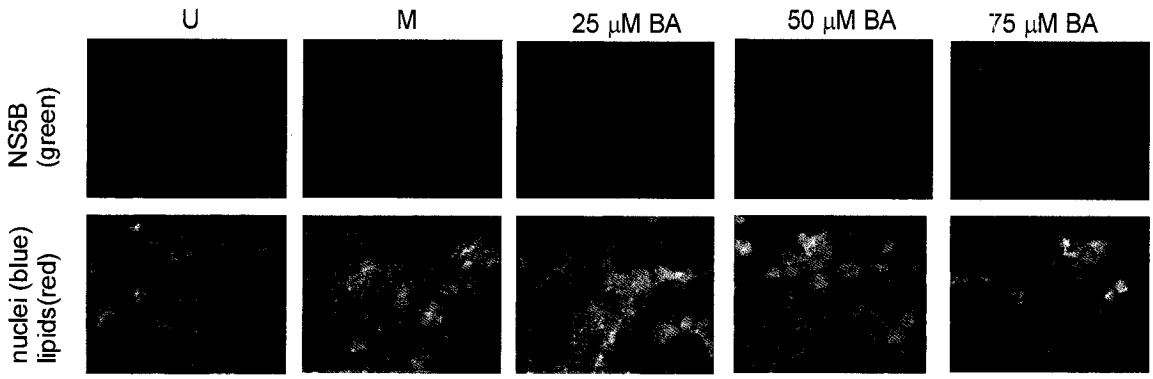

Figure 2.11: Fluorescent microscopy of NS5B protein in Huh-7 replicon cells under various conditions. Images show NS5B (green) immunostained Huh-7 replicon cells, counterstained with oil red O (red) for lipids and 4',6-diamidino-2-phenylindole (DAPI, blue) for nuclei. Huh-7 cells bearing HCV subgenomic replicons were mock treated (M), and treated with 25, 50, and 75 μM of BA for 6h. Images show less NS5B protein in cells treated with 50 and 75 μM of BA which agrees with the decreased level of NS3 protein shown by Western Blotting.

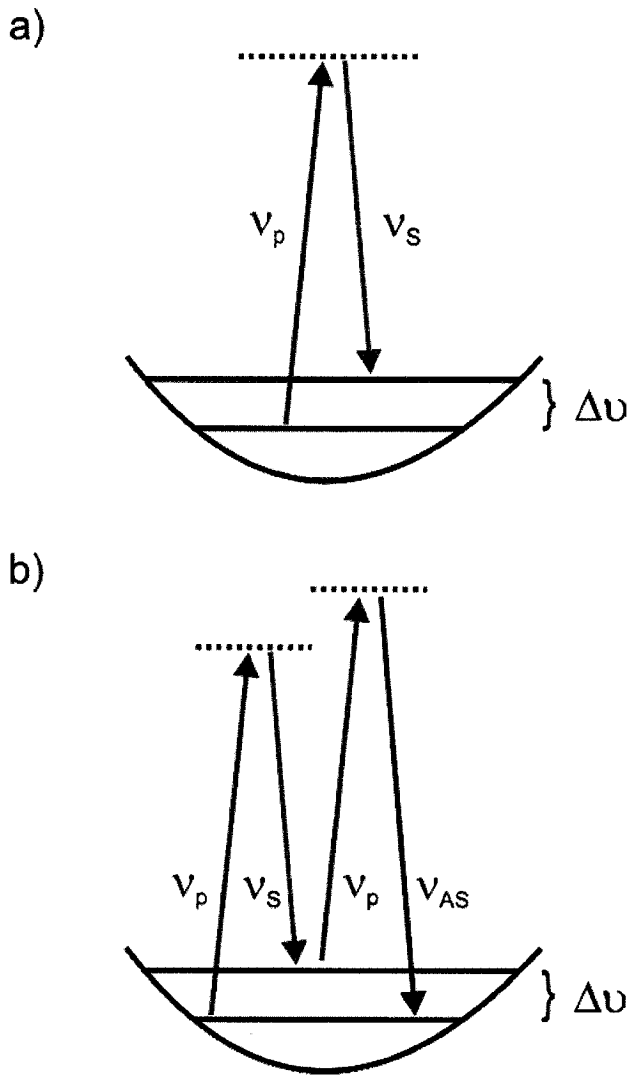

Scheme 2.4: (a) In Raman spectroscopy, photons inelastically scatter off molecules to excite vibrations. The energy difference is equal to the energy of the excited vibration. (b) In CARS spectroscopy, pump and Stokes laser beams stimulate relatively intense emission of anti-Stokes radiation in a well defined direction. ν_P is the pump frequency, ν_S is the Stokes frequency, ν_{AS} is the anti Stokes frequency.

molecule can be obtained. Since all compounds have unique vibrational spectra, it is possible to use Raman spectroscopy to identify molecules unequivocally. The problem with Raman spectroscopy is that it is an inherently weak process, and images for a particular molecule, within a cell for example, will take several hours minimum. CARS overcomes this problem by stimulating the vibrational excitation process using a pair of short pulse lasers with their energy difference precisely equal to the vibrational energy difference of interest (Scheme 2.4b). This means that entire images can be acquired in fractions of a second, allowing cells to be monitored at video rates [45-47]. In addition, since the lasers are focused into the sample using a confocal microsope, and CARS is a nonlinear process, high spatial resolution is achievable. To date, CARS has been primarily used to visualize very abundant CH_2 stretches in lipids and P-O stretches in nucleic acid backbones.

We performed a time course examination of live Huh-7 cells upon treatment with BA using CARS microscopy. The CARS system was tuned to selectively image the strong lipid CH_2 vibrational resonance at 2845 cm^{-1}. Figure 2.12 shows the lipid images at 1h time points measured over 6h after addition of BA. A clear increase in cellular lipids following treatment with BA was observed. In addition, the effects on these live cells were clearly not limited to lipid droplet accumulation. The observed increase in lipid content within the Huh-7 cells can be attributed to decreases in fatty acid activation, transport, β-oxidation, secretion, triglyceride clearance, and cholesterol catabolism, which is consistent with what is known about PPARα signaling in the liver [10, 17, 21, 23]. Results that we obtained from fluorescence microscopy of stained cells and CARS microscopy of live cells treated with BA showed an increase in lipid content within 1-2h following treatment of Huh-7 cells with BA.

Figure 2.12: CARS microscopy images of benzamide effects on lipid homeostasis in Huh-7 cells harbouring subgenomic HCV replicons. Cells were incubated at 37°C with 5% CO2 following treatment with 50 µM 2-Chloro-5-nitro-N-(pyridyl)benzamide. The CARS microscope was tuned to the lipid stretch at 2845 cm-1. Images were acquired at 60 min. intervals over 6h. Immediate changes in lipid distribution and morphology were observed.

There are a number of possible mechanisms by which 2-chloro-5-nitro-N-(pyridyl)benzamide could inhibit HCV replication in the replicon model. While it is possible that this small molecule may interact directly with HCV proteins involved in replication, siRNA PPARα knockdown experiments suggest that the mechanism likely involves the downstream effects of PPARα antagonism. Hyperlipidemia can also disrupt replication complexes by altering the membranous structures where HCV replication occurs [3, 4] or by altering the lipidation of host proteins that are necessary for replication to occur [2, 48]. Previous studies have indicated that genes associated with lipid metabolism such as SCAP and SREBP-regulated genes of the mevalonate pathway are differentially regulated during the initial stages of HCV infection [1]. Lovastatin, a potent inhibitor of HMG-CoA reductase that catalyzes the conversion of HMG-CoA to mevalonic acid (the rate-limiting step in the synthesis of cholesterol) [49] and GGTI-286, an inhibitor of a geranylgeranyl transferase enzyme, also inhibit HCV replication by an indirect route [2, 48]. Transcriptional regulation of hepatocellular genes including lipid transfer genes such as HMG CoA synthase and CPT1A by PPARα is well documented [20-25]. We suggest that the most likely mechanism of anti-HCV action of the benzamide involves post-translational antagonism of PPARα and that this subsequently alters the transcriptional regulation of a number of gene products, including those that regulate lipid metabolism and lipid transfer. The effects are likely enhanced relative to the PPARα siRNA owing to cross reactivity of the small molecule antagonist.

In conclusion, we have demonstrated that both small molecules and siRNA molecules that perturb the function of PPARα also inhibit HCV replication in replicon systems. This activity is linked with a hyperlipidemic condition within the Huh-7 cells although not

necessarily causally related. There exists strong evidence that chronic HCV infections are associated with the impaired expression of PPARα and the likely culprit leading to this host-cell alteration is the core protein of HCV [36, 37]. Our data suggests that the impaired expression of PPARα during chronic infection is not advantageous to HCV propagation. Rather, chronic infection may favour the host rather than the virus in controlling the levels of HCV in the infected liver. This may also be a mechanism by which HCV controls its own levels *in vivo* in an evolutionary attempt to evade the host immune response. Further experiments that examine the precise mechanism by which PPARα inhibits the HCV life cycle may aid in the identification of novel targets for therapeutic intervention.

Materials and Methods

Cell culture

Cell monolayers of the human hepatoma cell line Huh-7 were grown in Dulbecco's modified Eagle's medium (DMEM) (DMEM, Invitrogen, Burlington, ON, Canada) supplemented with 100 nM non-essential amino acids (NEAA, Invitrogen), 50 U/ml penicillin, 50 μg/ml streptomycin (Invitrogen), and 10% fetal bovine serum (FBS, CanSera, Rexdale, ON, Canada). G418 Geneticin® (Gibco, Burlington, ON, Canada) was added to the Huh-7 cells stably expressing HCV replicons at a concentration of 250 μg/ml. Two HCV replicons were used in this thesis. We utilized the Huh-7 cell line stably expressing the HCV subgenomic replicon derived from the pFK-I389neo/NS3-3'/5.1 plasmid that was kindly provided by Ralf Bartenschlager (Institute of Hygiene, University of Heidelberg, Heidelberg, Germany). This is a bicistronic replicon which contains the neomycin phosphotransferase resistance gene (neo^r) at the 5' end, and the HCV genomic sequence that expresses HCV non-structural

proteins from NS3 to the 3' end of the HCV genome. The second HCV cell line, which was primarily used for screening of small molecules and siRNA, harbors the tricistronic replicon constructed from the HCV RNA of the genotype 1b and was derived from the clone pFK-I389neo/luc/NS3-3'/5.1. This cell line was developed in Pezacki's research group [39]. This replicon harbors firefly luciferase reporter gene. In both cells lines translation of the neomycin resistance gene product is mediated by the HCV internal ribosome entry site (IRES), whereas translation of the firefly luciferase gene product and the non-structural HCV proteins is controlled by the encephalomyocarditis virus (EMCV) IRES.

Small molecule treatments

Huh-7 cells harboring HCV subgenomic replicon derived from the clone pFK-I389neo/luc/NS3-3'/5.1 were seeded at $1x10^4$ cells/well in DMEM in a 96-well plate. After 24h, at a confluency of 70 to 80% cells, the medium was aspirated and cells were treated with 2-Chloro-5-nitro-N-(pyridyl)benzamide, (BA), (Calbiochem, San Diego, CA, USA). BA was dissolved in methanol (10 mM stock) and further dilutions were made in DMEM medium that did not contain G418 antibiotic. 100 µl of BA was added in triplicates ranging from 500 µM to 1 µM. Cells were incubated with the small molecule for 24h. The effect of BA on Huh-7 cells was analyzed by firefly luciferase and toxicity assays. Replicon cells were also treated with positive controls: 25-hydroxycholesterol and lovastatin (Calbiochem) and with human interferon γ (IFNγ) (PBL Biomedical Laboratories, Piscataway, NJ, USA) under the same conditions. Before using in cell culture, lovastatin was activated according to previously published procedure [50]. Concentrations of the controls were the following: 25-hydroxycholesterol (2.5 µM), lovastatin (50 mM), and IFNγ (50-500 U/ml).

Overexpression and siRNA transfection in HCV replicon cells

The siRNA duplexes homologous to GL2 and GL3 luciferase were purchased from Dharmacon (Lafayette, CO, USA). The siRNA vector mixes, targeting the PPARα and/or the PPARγ gene, were purchased from Panomics (Redwood City, CA, USA). The siRNA or over-expression vector transfections were routinely done in 96-well plates according to the manufacturer's protocol and assays were carried out at 72h post-transfection. Briefly, Huh-7 cells harboring HCV subgenomic replicon were seeded at $1x10^4$ cells/well in DMEM in a 96-well plate. After 24h, at a confluency of 70 to 80% cells, the medium was aspirated. Cells were washed twice with 1X PBS pH7.4 and once with serum- and antibiotic-free DMEM. siRNA stock solution was incubated for 20 min at 25°C with Lipofectamine 2000 (ratio of siRNA : lipids 1:2). Then the mixture was transferred onto cells. 4h later, DMEM solution with 20% FBS was added. Cells were further incubated for 48-96h posttransfection time.

Firefly luciferase reporter assay and total protein quantification

Huh-7 cells harboring subgenomic replicons derived form the clone pFK-I389neo/luc/NS3-3'/5.1 were transfected with siRNA or treated with the small molecules as described above. At the assay endpoints, 24 or 48h, cells were washed once with 100 µl of 1X PBS and lysed with 100 µl of 1X cell culture lysis buffer (Promega, Madison, WI, USA) for 10 min at room temperature. 50 µl of the lysates per condition were transferred to a Microlite white 96-well plate (VWR International Mont-Royal, PQ, USA) followed by addition of 50 µl of firefly luciferase assay substrate. The substrate for the firefly luciferase assay was prepared fresh for each use. The solution contained 25 mM glycylglycin, 15 mM KH_2PO_4, 4 mM EGTA, 2

mM ATP, 1 mM dithiothreitol (DTT), 15 mM $MgSO_4$, 100 μM acetyl CoA, and 75 μM beetle luciferin (Promega). The final pH was adjusted to 8.0 [51]. Upon substrate addition, the luminescence in relative light units (RLU) was measured after a 2s delay by an Lmax luminometer (Molecular Devices Corporation, Sunnyvale, CA, USA) using SOFTmax Pro software. Luminescence was integrated over 10s. Values were normalized against total protein content for each sample by performing the Bio-Rad DC Protein Assay (Bio-Rad, Mississauga, ON, Canada) according to the manufacturer's protocol. Bovine serum albumin (BSA) was used as the protein standard. This assay is similar to the Lowry assay and it involves addition of a substrate solution which contains alkaline copper tartrate solution and the Folin reagent. The absorbance was read at 720 nm using a Spectramax M2 (Molecular Devices Corporation, Sunnyvale, CA, USA), using SOFTmax Pro software.

Immunoblot Analysis – Western blotting

Huh-7 cells harboring subgenomic replicons derived from the clone pFK-I389neo/NS3-3'/5.1 were seeded in 60 mm dishes, ($1x10^6$ cells per dish) for preparation of western blot lysates. 24h later at 70% confluency, the medium was aspirated and compounds were added at different concentrations. Benzamide was added at 75 μM and 50 μM for the 6h treatments and at 25 μM for the 24h treatment. 25-hydroxycholesterol was added at 2 μM for the 24h treatment, lovastatin was added at 50 μM for the 24h treatment, and IFNγ was added at 50 U for the 72h treatment. At the treatment endpoints, the cells were washed once with 1X PBS and lysed using an SDS lysis buffer consisting of 50 mM Tris-HCl (pH 6.8), 2% SDS, 10% glycerol, 100 mM dithiothreitol (DTT), and 0.1% bromophenol blue. A protease inhibitor cocktail mix (Roche Diagnostics, Penzberg, Germany) was added to each extract. The

protein concentration of each sample was quantified using the Bio-Rad DC Protein Assay according to the manufacturer's protocol. Prior to loading, 10% v/v of DTT and bromophenol blue (1:1) were added to each sample and 60 μg/well was loaded onto a SDS-PAGE gel (10% resolving, 4% stacking gel). The resolved proteins were transferred to a Hybond-P (Amersham Biosciences, Piscataway, NJ, USA) polyvinylidene difluoride membrane. The membrane was probed for HCV NS3 protein using a mouse anti-NS3 primary antibody (1:500 dilution, ViroStat, Portland, ME, USA) followed by secondary (HRP)-conjugated goat anti-mouse IgG antibody (1:1000 dilution) obtained from Jackson ImmunoResearch Laboratories Inc. (Westgrove, PA, USA). The membrane was stripped with ReBlot Plus stripping solution (Chemicon International Inc, Temecula, CA) according to the manufacturer's protocol. To assess loading, membranes were also probed with a mouse PTP1D primary antibody (1:2500 dilution; Sigma, Saint Louis, MO, USA) followed by the same secondary antibody described above. Protein bands were visualized by Western Lightning® Western Blot Chemiluminescence reagents (PerkinElmer Life and Analytical Sciences, Inc, Boston, MA, USA) according to the manufacturer's protocol.

Cytotoxicity Assays

The CytoTox 96® Non-Radioactive Cytotoxicity Assay (Promega) is a colorimetric assay which quantitatively measures lactate dehydrogenase (LDH), a stable cytosolic enzyme that is released upon cell lysis. During 30 min using a coupled enzymatic reaction, released LDH catalyses conversion of lactate into pyruvate and the conversion of a tetrazolium salt (INT) into a red coloured formazan. The intensity of color produced is proportional to the number of lysed cells. Absorbance data at 490 nm were collected using a standard 96 well plate reader.

Huh-7 cells expressing HCV subgenomic replicons were treated with small molecules as described above. At the treatment endpoints, cells were washed three times with 1X PBS. The last wash was left in the plate and 10 µl of 10% Triton-X was added. The cells were lysed for 45 min in an incubator at 37°C under 5% CO_2. 50 µl of the lysate per condition were then transferred into a new 96-well plate followed by addition of 50 µl of the substrate mix to each well. The plate was incubated at room temperature for 30 min and then 50 µl of stop solution was added to each well. The absorbance was read at 490 nm using a Spectramax M2 (Molecular Devices Corporation, Sunnyvale, CA), using SOFTmax Pro software.

Fluorescence Microscopy

Huh-7 cells stably expressing the HCV subgenomic replicon derived from the clone pFK-I389neo/luc/NS3-3'/5.1 were treated with small molecules as described earlier. At the treatment endpoints, cells were washed once with 1X PBS and fixed with 3.7% formaldehyde for 30 min at room temperature. Cells were probed for HCV NS5B protein by overnight incubation at 4°C with 100 µl of mouse anti-NS5B (5B-12B7) primary antibody (1:100 dilution, kindly provided by Darius Moradpour, Department of Medicine II, University of Freiburg, Freiburg, Germany), followed by incubation with Cy2-labeled donkey anti-mouse IgG socondary antibody (1:100 dilution, Jackson ImmunoResearch Laboratories Inc., Westgrove, PA, USA) for 2h at 4°C. After washing three times with 1X PBS, cells were stained for lipids with Oil red O (0.5% in isopropanol, Sigma-Aldrich, Oakville, ON, Canada). Oil red O was prepared by diluting with water (3:2), then filtering through a Whatman filter paper and a 0.45-µm filter. 100 µl of the solution was added per

well and fixed cells were incubated at room temperature for an additional 30 min. Cells were then washed three times with 1X PBS and nuclei were counterstained with 300 nM of 4',6-diamidino-2-phenylindole (DAPI, Invitrogen), 100 µl per well for 2 min. After the final wash, cells were left in 50 µl of 50% glycerol in PBS to keep them hydrated. Fluorescent images were collected using an Axiovert 200M inverted microscope from Zeiss (North York, ON, Canada) with Axiovision 3.1 software. The cells were photographed with an AxioCam connected to the inverted microscope.

CARS imaging of live cells

Huh-7 cells were seeded at $5x10^4$ cells/well in 4.2 cm^2 borosilicate culture vessels (VWR international) and incubated at 37°C under 5% CO_2. At 70 to 80% confluency, the cells were washed once with pre-warmed DMEM. Benzamide, previously dissolved in methanol at 10 mM, was diluted to 100 µM in DMEM and added to the cells. The CARS signal from the cells was collected in the forward direction. Typical pump (711 nm) and Stokes (892 nm) excitation powers were 9 and 3 mW respectively at the sample.

RNA extraction, Reverse transcription and real-time PCR

Total RNAs were extracted using RNeasy kit according to the manufacturer's instructions (Qiagen, Mississauga, ON, Canada). Before reverse transcription, RNAs were treated with DNase following rigorous DNase treatment (Ambion Inc. Woodward, Austin, TX, USA) as described by the manufacturer. RNA concentrations were calculated by measuring absorbance at 260 nm using a Nanodrop-100 Spectrophotometer. Then, 1 µg of RNAs were used to synthesize the cDNAs using the SuperScript™ II RT (Invitrogen) according to the manufacturer's protocol. The cDNAs were cleaned using the Microcon YM-30 (Millipore

Cambridge, ON, Canada) according to the manufacturer's instructions, and cDNAs were eluted with 50 µl of water. The primers used for real-time PCR for amplification of Carnitine palmitoyltransferase-1 (CPT-1) were: (Forward 5'-CGTCTTTTGGGATCCACGATT-3', Reverse 5'-TGTGCTGGATGGTGTCTGTCTC-3') and for Mitochondrial HMG-CoA synthase (HMG-CoAs) were (Forward 5'-TGAGGGCATAGATACCACCAATG, Reverse 5'-TGGCATAACGACCATCCCA-3'). GAPDH primers were from previously published work [52] and the primers for 18S rRNA were: (Forward 5'-GCGATGCGGCGGCGTTATTC-3', Reverse 5'TCAATCTGTCAATCCGTCCGT GTCC-3'). All primers were designed using methods recommended by Bio-Rad. The primers were designed to have a length of about 20-25 bases, a G/C content of around or over 50%, and a Tm of about 60°C. The length of the PCR products ranged between 99 and 203 bp. Real-time PCRs were carried out on a Bio-Rad iCycler with the iQ™ SYBR® Green Supermix (Bio-Rad) in 96-well plates. Master mixes were prepared for each set of primers (12.5 µl of iQ™ SYBR® Green Supermix, 1.2 µl of each primer at 10 µM, 1 µl of the cDNA and 9.1 µl of RNase-free water). Specific cDNAs were amplified by real-time PCR with specific primers (CPT-1, HMG-CoAs and 18S rRNA). Thermal cycling conditions were designated as follows: denaturation at 95°C for 4 min, followed by 40 cycles of 95°C for 30 s, 60°C for 30 s and 72°C for 1 min. Fluorescence measurements were recorded during each cycle. A melting curve was also established to verify the specificity of real-time PCR reaction for each primer pair. Efficiency of amplification was determined by running a standard curve with 10-fold serial dilutions of cDNA. Results were analyzed using the comparative critical threshold (ΔΔCT) method in which the amount of the target RNA was adjusted to a reference (internal target

RNA, 18r RNA). The fold changes were calculated using the $2^{\Delta C_T}$ method as previously described [41].

References:

[1] Su, A. I.; Pezacki, J. P.; Wodicka, L., et al., Genomic analysis of the host response to hepatitis C virus infection. *Proc. Natl. Acad. Sci. U. S. A.* **2002**, *99*, 15669-15674.

[2] Ye, J.; Wang, C. F.; Sumpter, R., et al., Disruption of hepatitis C virus RNA replication through inhibition of host protein geranylgeranylation. *Proc. Natl. Acad. Sci. U. S. A.* **2003**, *100*, 15865-15870.

[3] Moradpour, D.; Gosert, R.; Egger, D., et al., Membrane association of hepatitis C virus nonstructural proteins and identification of the membrane alteration that harbors the viral replication complex. *Antiviral Res.* **2003**, *60*, 103-109.

[4] Gosert, R.; Egger, D.; Lohmann, V., et al., Identification of the hepatitis C virus RNA replication complex in Huh-7 cells harboring subgenomic replicons. *J. Virol.* **2003**, *77*, 5487-5492.

[5] Moriya, K.; Yotsuyanagi, H.; Shintani, Y., et al., Hepatitis C virus core protein induces hepatic steatosis in transgenic mice. *J. Gen. Virol.* **1997**, *78*, 1527-1531.

[6] Hope, R. G.; McLauchlan, J., Sequence motifs required for lipid droplet association and protein stability are unique to the hepatitis C virus core protein. *J. Gen. Virol.* **2000**, *81*, 1913-1925.

[7] Shi, S. T.; Polyak, S. J.; Tu, H., et al., Hepatitis C virus NS5A colocalizes with the core protein on lipid droplets and interacts with apolipoproteins. *Virology* **2002**, *292*, 198-210.

[8] Pfeifer, U.; Thomssen, R.; Legler, K., et al., Experimental Non-a, Non-B Hepatitis - 4 Types of Cytoplasmic Alteration in Hepatocytes of Infected Chimpanzees. *Virchows Arch B Cell Pathol Incl Mol Pathol.* **1980**, *33*, 233-243.

[9] Nakamura, M. T.; Cheon, Y.; Li, Y., et al., Mechanisms of regulation of gene expression by fatty acids. *Lipids* **2004**, *39*, 1077-1083.

[10] Mandard, S.; Muller, M.; Kersten, S., Peroxisome proliferator-activated receptor alpha target genes. *Cell. Mol. Life Sci.* **2004**, *61*, 393-416.

[11] Kliewer, S. A.; Sundseth, S. S.; Jones, S. A., et al., Fatty acids and eicosanoids regulate gene expression through direct interactions with peroxisome proliferator-activated receptors alpha and gamma. *Proc. Natl. Acad. Sci. U. S. A.* **1997**, *94*, 4318-4323.

[12] Hertz, R.; Bisharashieban, J.; Bartana, J., Mode of Action of Peroxisome Proliferators As Hypolipidemic Drugs - Suppression of Apolipoprotein C-Iii. *J. Biol. Chem.* **1995**, *270*, 13470-13475.

[13] Issemann, I.; Green, S., Activation of a Member of the Steroid-Hormone Receptor Superfamily By Peroxisome Proliferators. *Nature* **1990**, *347*, 645-650.

[14] De Duve, C.; Baudhuin, P., Peroxisomes (microbodies and related particles). *Physiol. Rev.* **1966**, *46*, 323-357.

[15] Kovacs, W. J.; Olivier, L. M.; Krisans, S. K., Central role of peroxisomes in isoprenoid biosynthesis. *Prog. Lipid Res.* **2002**, *41*, 369-391.

[16] Auboeuf, D.; Rieusset, J.; Fajas, L., et al., Tissue distribution and quantification of the expression of mRNAs of peroxisome proliferator-activated receptors and liver X receptor-alpha in humans - No alteration in adipose tissue of obese and NIDDM patients. *Diabetes* **1997**, *46*, 1319-1327.

[17] Kliewer, S. A.; Umesono, K.; Noonan, D. J., et al., Convergence of 9-Cis Retinoic Acid and Peroxisome Proliferator Signaling Pathways Through Heterodimer Formation of Their Receptors. *Nature* **1992**, *358*, 771-774.

[18] Lee, G.; Elwood, F.; McNally, J., et al., T0070907, a selective ligand for peroxisome proliferator-activated receptor gamma, functions as an antagonist of biochemical and cellular activities. *J. Biol. Chem.* **2002**, *277*, 19649-19657.

[19] McCarthy, T. C.; Pollak, P. T.; Hanniman, E. A., et al., Disruption of hepatic lipid Homeostasis in mice after amiodarone treatment is associated with peroxisome proliferator-activated receptor-alpha target gene activation. *J. Pharmacol. Exp. Ther.* **2004**, *311*, 864-873.

[20] Miller, R. T.; Glover, S. E.; Stewart, W. S., et al., Effect on the expression of c-met, c-myc and PPAR-alpha in liver and liver tumors from rats chronically exposed to the hepatocarcinogenic peroxisome proliferator WY-14,643. *Carcinogenesis* **1996**, *17*, 1337-1341.

[21] Schoonjans, K.; Staels, B.; Auwerx, J., Role of the peroxisome proliferator-activated receptor (PPAR) in mediating the effects of fibrates and fatty acids on gene expression. *J. Lipid Res.* **1996**, *37*, 907-925.

[22] Lehmann, J. M.; Moore, L. B.; Smitholiver, T. A., et al., An Antidiabetic Thiazolidinedione Is a High-Affinity Ligand For Peroxisome Proliferator-Activated Receptor Gamma(Ppar-Gamma). *J. Biol. Chem.* **1995**, *270*, 12953-12956.

[23] Everett, L.; Galli, A.; Crabb, D., The role of hepatic peroxisome proliferator-activated receptors (PPARs) in health and disease. *Liver* **2000**, *20*, 191-199.

[24] Xu, H. E.; Lambert, M. H.; Montana, V. G., et al., Structural determinants of ligand binding selectivity between the peroxisome proliferator-activated receptors. *Proc. Natl. Acad. Sci. U. S. A.* **2001**, *98*, 13919-13924.

[25] Xu, H. E.; Stanley, T. B.; Montana, V. G., et al., Structural basis for antagonist-mediated recruitment of nuclear co-repressors by PPAR alpha. *Nature* **2002**, *415*, 813-817.

[26] Escher, P.; Wahli, W., Peroxisome proliferator-activated receptors: insight into multiple cellular functions. *Mutat. Res.-Fundam. Mol. Mech. Mutagen.* **2000**, *448*, 121-138.

[27] Vosper, H.; Khoudoli, G. A.; Graham, T. L., et al., Peroxisome proliferator-activated receptor agonists, hyperlipidaemia, and atherosclerosis. *Pharmacol. Ther.* **2002**, *95*, 47-62.

[28] Nolte, R. T.; Wisely, G. B.; Westin, S., et al., Ligand binding and co-activator assembly of the peroxisome proliferator-activated receptor-gamma. *Nature* **1998**, *395*, 137-143.

[29] Oliver, W. R.; Shenk, J. L.; Snaith, M. R., et al., A selective peroxisome proliferator-activated receptor delta agonist promotes reverse cholesterol transport. *Proc. Natl. Acad. Sci. U. S. A.* **2001**, *98*, 5306-5311.

[30] Hsu, M. H.; Savas, V.; Griffin, K. J., et al., Identification of peroxisome proliferator-responsive human genes by elevated expression of the peroxisome proliferator-activated receptor a in HepG2 cells. *J. Biol. Chem.* **2001**, *276*, 27950-27958.

[31] Kersten, S.; Seydoux, J.; Peters, J. M., et al., Peroxisome proliferator-activated receptor alpha mediates the adaptive response to fasting. *J. Clin. Invest.* **1999**, *103*, 1489-1498.

[32] Guo, Y. X.; Chan, S. W.; Kwang, J., Membrane association of greasy grouper nervous necrosis virus protein A and characterization of its mitochondrial localization targeting signal. *J. Virol.* **2004**, *78*, 6498-6508.

[33] Anderson, S. P.; Dunn, C.; Laughter, A., et al., Overlapping transcriptional programs regulated by the nuclear receptors peroxisome proliferator-activated receptor alpha, retinoid X receptor, and liver X receptor in mouse liver. *Mol. Pharmacol.* **2004**, *66*, 1440-1452.

[34] Anderson, S. P.; Yoon, L.; Richard, E. B., et al., Delayed liver regeneration in peroxisome proliferator-activated receptor-alpha-null mice. *Hepatology* **2002**, *36*, 544-554.

[35] Hashimoto, T.; Cook, W. S.; Qi, C., et al., Defect in peroxisome proliferator-activated receptor alpha-inducible fatty acid oxidation determines the severity of hepatic steatosis in response to fasting. *J. Biol. Chem.* **2000**, *275*, 28918-28928.

[36] Dharancy, S.; Malapel, M.; Perlemuter, G., et al., Impaired expression of the peroxisome proliferator-activated receptor alpha during hepatitis C virus infection. *Gastroenterology* **2005**, *128*, 334-342.

[37] Dharaney, S.; Malapel, M.; Roskams, T., et al., Impaired liver expression of the peroxysome proliferator-activated receptor (PPAR)-A, modulates liver steatosis and inflammation during hepatitis C virus (HCV) infection. *Hepatology* **2002**, *36*, 264A-264A.

[38] Bredel, M.; Jacoby, E., Chemogenomics: An emerging strategy for rapid target and drug discovery. *Nat. Rev. Genet.* **2004**, *5*, 262-275.

[39] Sagan, S. M.; Rouleau, Y.; Leggiadro, C., et al., The influence of cholesterol and lipid metabolism on host cell structure and hepatitis C virus replication. *Biochem. Cell Biol.* **2006**, *84*, 67-79.

[40] Guzman, M.; Cortes, J. P.; Castro, J., Effects of Lovastatin On Hepatic Fatty-Acid Metabolism. *Lipids* **1993**, *28*, 1087-1093.

[41] Livak, K. J.; Schmittgen, T. D., Analysis of relative gene expression data using real-time quantitative PCR and the 2(T)(-Delta Delta C) method. *Methods* **2001**, *25*, 402-408.

[42] Moradpour, D.; Brass, V.; Bieck, E., et al., Membrane association of the RNA-dependent RNA polymerase is essential for hepatitis C virus RNA replication. *J. Virol.* **2004**, *78*, 13278-13284.

[43] Reigadas, S.; Ventura, M.; Sarih-Cottin, L., et al., HCV RNA-dependent RNA polymerase replicates in vitro the 3 ' terminal region of the minus-strand viral RNA more efficiently than the 3 ' terminal region of the plus RNA. *Eur. J. Biochem.* **2001**, *268*, 5857-5867.

[44] Takigawa, Y.; Nagano-Fujii, M.; Deng, L., et al., Suppression of hepatitis C virus replicon by RNA interference directed against the NS3 and NS5B regions of the viral genome. *Microbiol. Immunol.* **2004**, *48*, 591-598.

[45] Cheng, J. X.; Xie, X. S., Coherent anti-Stokes Raman scattering microscopy: Instrumentation, theory, and applications. *J. Phys. Chem. B* **2004**, *108*, 827-840.

[46] Nan, X. L.; Cheng, J. X.; Xie, X. S., Vibrational imaging of lipid droplets in live fibroblast cells with coherent anti-Stokes Raman scattering microscopy. *J. Lipid Res.* **2003**, *44*, 2202-2208.

[47] Evans, C. L.; Potma, E. O.; Puoris'haag, M., et al., Chemical imaging of tissue in vivo with video-rate coherent anti-Stokes Raman scattering microscopy. *Proc. Natl. Acad. Sci. U. S. A.* **2005**, *102*, 16807-16812.

[48] Kapadia, S. B.; Chisari, F. V., Hepatitis C virus RNA replication is regulated by host geranylgeranylation and fatty acids. *Proc. Natl. Acad. Sci. U. S. A.* **2005**, *102*, 2561-2566.

[49] Grimbert, S.; Pessayre, D.; Degott, C., et al., Acute Hepatitis Induced By Hmg-Coa Reductase Inhibitor, Lovastatin. *Dig. Dis. Sci.* **1994**, *39*, 2032-2033.

[50] Kita, T.; Brown, M. S.; Goldstein, J. L., Feedback-Regulation of 3-Hydroxy-3-Methyglutaryl Coenzyme a Reductase in Livers of Mice Treated with Mevinolin, a Competitive Inhibitor of the Reductase. *J. Clin. Invest.* **1980**, *66*, 1094-1100.

[51] Dyer, B. W.; Ferrer, F. A.; Klinedinst, D. K., et al., A noncommercial dual luciferase enzyme assay system for reporter gene analysis. *Anal. Biochem.* **2000**, *282*, 158-161.

[52] Lawrence, J. W.; Li, Y.; Chen, S. Y., et al., Differential gene regulation in human versus rodent hepatocytes by peroxisome proliferator-activated receptor (PPAR) alpha - PPAR alpha fails to induce peroxisome proliferation-associated genes in human cells independently of the level of receptor expression. *J. Biol. Chem.* **2001**, *276*, 31521-31527.

3

Applying Forward Chemical Genetics using Abscisic Acid Analogs

Introduction

High throughput techniques including gene expression profiling and proteomics approaches have identified a number of important host-virus interactions in cell culture models for HCV replication, and in HCV infection [1-3]. Small molecule-based antiviral strategies have also demonstrated success in inhibiting HCV in clinical infections [4]. There is much promise in using chemical genetic approaches [5] to study host-pathogen interactions because many dynamic molecular interactions are not easily identified.

In this study chemical genetic approaches have been applied to examine host-virus interactions in HCV replicons. More precisely, we used a forward chemical genetics approach to identify natural product-like inhibitors of HCV replication and to identify the target proteins to which these inhibitors bind. Forward chemical genetic approaches have uncovered cell-permeable small molecules that disrupt protein function in cellular processes such as mitosis [6], cell signaling [7], and tissue regeneration [8]. In forward chemical genetics, a desired phenotype of interest is first defined. This phenotype can be cell growth,

cell proliferation, cell death, protein trafficking, disease inhibition, or any other change that reflects biological processes. Examples of phenotypic assays include microarrays, in which a small molecule library is immobilized onto an array surface and screened for a variety of proteins that fluoresce upon binding [9]. Other ways of screening are Enzyme-Linked Immunosorbent Assay (ELISA) methods, in which cells are treated with compounds, followed by fixing and staining with an antibody to an epitope that elicits the desired phenotype [9]. Morphological changes in screened cells can also be detected using imaging techniques [10]. Genetic reporters encoded in cell replicons, whose activity is correlated with a particular phenotype change, can also be used in high-throughput screening. In our study we measured luciferase protein levels to detect HCV inhibition. The phenotype here is replication competency of HCV replicon RNA in Huh-7 cells.

Forward chemical genetics uses high-throughput screening of libraries to select molecules inducing the desired phenotype. These libraries should include structurally diverse and structurally complex molecules. There are several sources of libraries that can be used for high-throughput screening [11]. Small molecule libraries can consist of natural products. However, many natural compounds occur as mixtures of various isomers, which make the identification of active molecules quite difficult. Furthermore, natural compounds are often isolated in low yield and their structural and stereochemical complexity can be problematic in synthetic design. Synthetic small molecule libraries can be divided in two groups: focused and diversity oriented libraries [12, 13]. Focused libraries are based on natural compound scaffolds and use their further functionalization to target specific classes of proteins. In contrast, diversity oriented synthesis (DOS) creates libraries of compounds with maximal diverse stereochemistry and functional groups, based on synthetic algorithms.

Most often, compounds from DOS libraries contain cores resembling natural product classes (eg. indole, or glycal template), and are not biased toward any protein class in particular [14, 15]. Usually, library generation involves a model compound synthesis in solution followed by solid phase synthesis using the so called split-pool method [11]. Although the outcome is a large number of compounds for biological study, library generation requires optimization of each step from solution to solid phase, and proper choice of orthogonal functional groups. Therefore, it is time consuming. An example of a small molecule identified from a DOS library is galanthamine, which inhibits protein trafficking [16].

The small molecule library that we used in our study was a collection of synthesized small molecules based on the scaffold of a plant hormone, (+)-S-abscisic acid (ABA), which is a carotenoid-derived sesquiterpene (Figure 3.1). This library was obtained from the Abrams' research group at the National Research Council, Plant Biotechnology Institute, Saskatoon. ABA is involved in the regulation of numerous physiological processes in plant growth and development, including embryo and seed development, protein storage, and stress responses [17]. Many analogs of ABA have been synthesized for structure-activity studies, and for developing growth regulators with enhanced and prolonged activity [18-21]. These make up a focused library of natural product like compounds. ABA has a high degree of structural similarity to terpenoid ligands such as retinoic acid, as well as synthetic mammalian nuclear hormone receptor ligands (retinoic acid and retinoids) (Figure 3.2) [22, 23]. These ligands bind to retinoic acid receptor α (RXRα). We were interested to see if any of the ABA compounds inhibit HCV viral replication in the replicon cells by directly affecting the HCV proteins or by showing reactivity towards mammalian nuclear hormone receptors (PPAR or RXRα). We have already shown that modulation of peroxisome

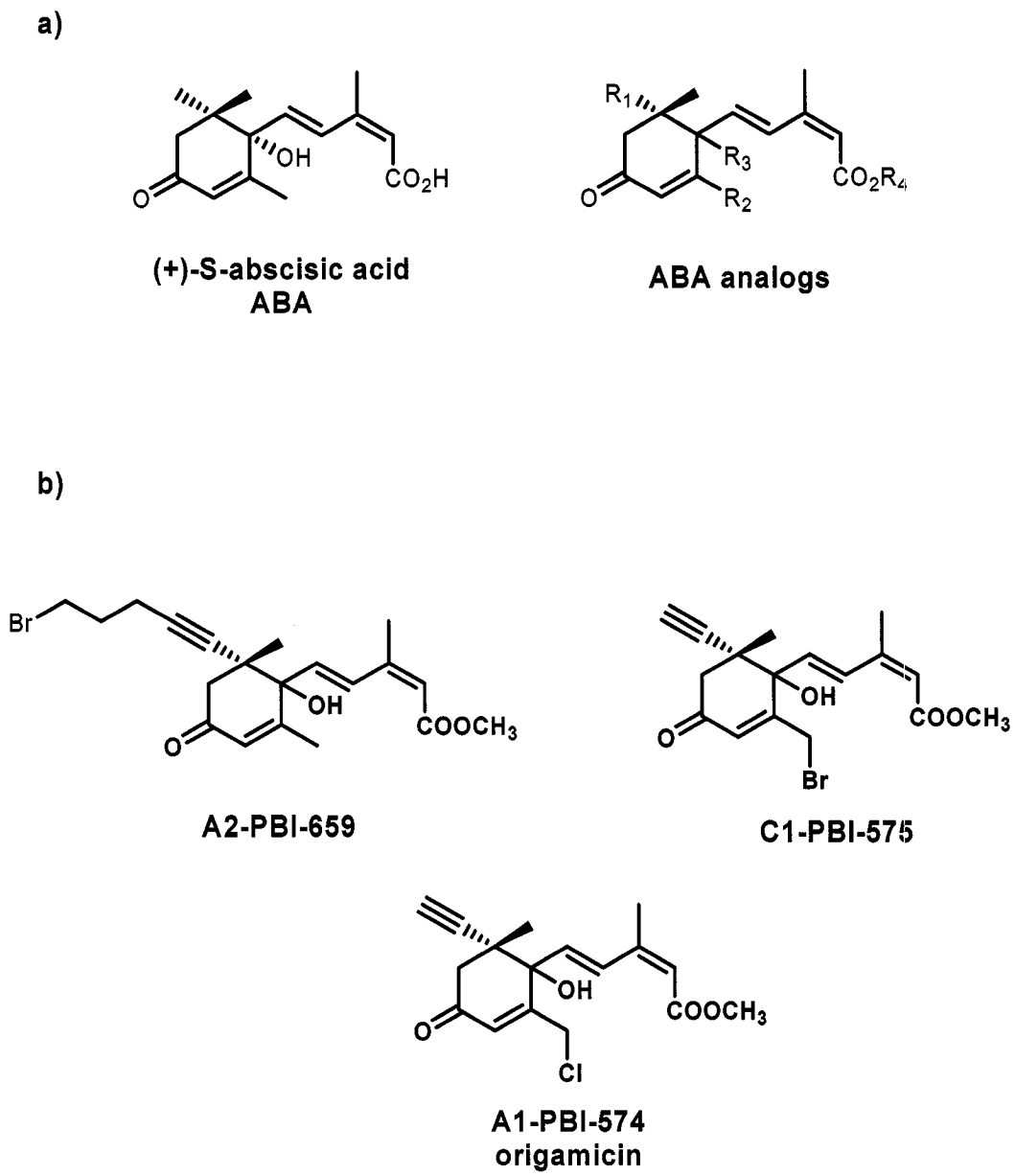

Figure 3.1: Chemical structures of abscisic acid (ABA), analogs scaffold, and three ABA analogs.

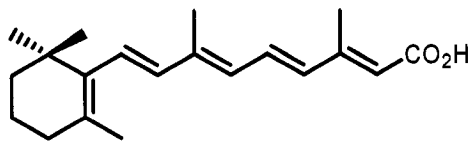

Retinoic Acid

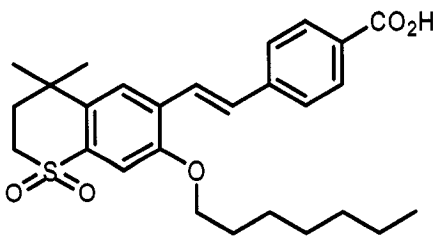

RARα-selective antagonist
J.Med.Chem. **2004**, *47*, 4360

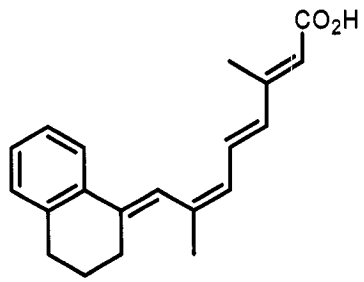

9cUAB30
RXR-selective retinoid
chemopreventive agent for breast cancer
J.Med.Chem. **2004**, *46*, 3766

Figure 3.2: Chemical structure of the retinoic acid and retinoids.

proliferator-activated receptor (PPAR) blocked HCV replication [24], however, the RXRα pathway is not directly connected with HCV replication.

Results and Discussion

For preliminary assessments of ABA analog activity against HCV RNA replication in Huh-7 replicon cells, a library of 100 ABA analogs was screened at the high dose of 100 μM. HCV RNA inhibition was determined by performing firefly luciferase assays utilizing the tricistronic subgenomic HCV replicon previously explained in Chapter 2 and shown in Figure 3.3. All of the ABA analogs contained the six-membered ring and the unsaturated side chain with a variety of substituents. The general structure is shown in Figure 3.1.

Initial screening identified 18 ABA analogs that showed significant inhibitory activity via the firefly luciferase assay after 24h treatment (Figure 3.4). These analogs were then tested for cytotoxicity at the same concentration, 100 μM, by quantifying LDH activity, which directly measures cell viability. Experiments showed that all of the 18 compounds identified as having anti-HCV activity in the firefly luciferase assay displayed some degree of cytotoxicity at 100 μM concentrations, with cell viabilities ranging from 9.4% to 70% compared to untreated cells (Figure 3.5). To determine whether any of the 18 compounds showed activity at lower concentrations, we repeated the assay between 100 μM and 50 nM concentrations. The firefly luciferase and cytotoxicity assays of these compounds showed that A1-PBI-574, which we named origamicin, A2-PBI-659, and C1-PBI-575 had the greatest antiviral activity and only C1-PBI-575 showed adverse cytotoxicity at concentrations less than 100 μM.

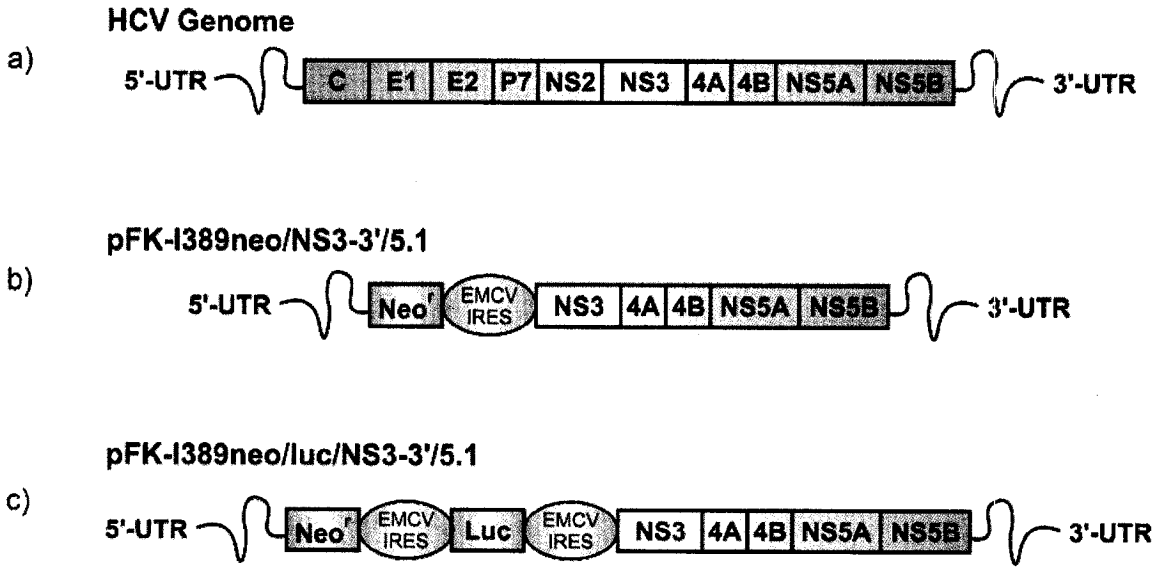

Figure 3.3: Schematic representation of the HCV genome and the subgenomic replicons used in the abscisic acid analog screening study. a) HCV genome with genes expressing structural and non-structural proteins. b) pFK-I389neo/NS3-3'/5.1 bicistronic sub-genomic replicon. c) pFK-I389neo/luc/NS3-3'/5.1 tricistronic sub-genomic replicon containing the firefly luciferase gene used in screening experiments.

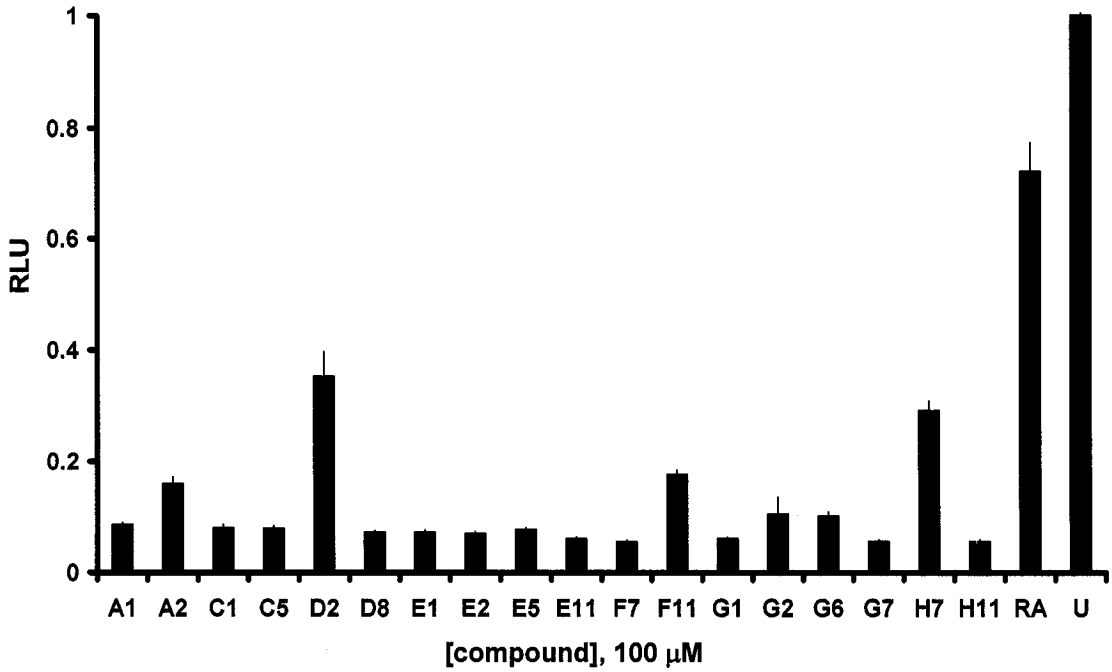

Figure 3.4: Firefly luciferase data of Huh-7 replicon cells treated with 18 ABA analogs. Activity was determined following 24h treatment with the ABA analogs and RA at 100 μM. Letter-number combinations indicate ABA analogs; RA-retinoic acid; U-untreated Huh7 subgenomic replicon cells. All of the compounds show significant activity in inhibiting HCV. This is apparent from the small levels of luminescence from cells treated with the ABA analogs relative to that of the untreated cells. Error bars represent the mean ± SD.

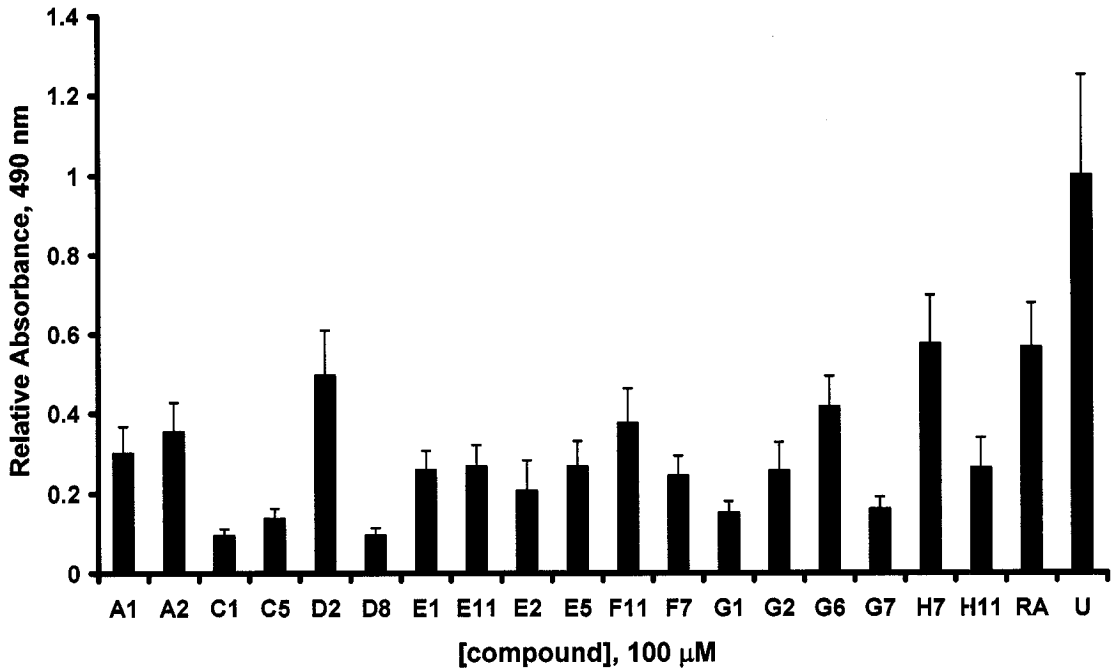

Figure 3.5: Cytotoxicity data of Huh-7 replicon cells treated with 18 ABA analogs. Cytotoxicity was determined by LDH assay after 24h cells treatment with compounds at 100 μM and is measured in Relative Absorbance units at 490 nm. Letter-number combinations indicate ABA analogs; RA-retinoic acid; U-untreated Huh7 subgenomic replicon cells. All of the compounds show high cytotoxicity to Huh-7 replicon cells at their high dose, as indicated by their small absorbance values relative to untreated cells. Error bars represent the mean ± SD.

We decided to evaluate the efficacy of the three ABA analogs shown in Figure 3.1, towards HCV inhibition in more detail by measuring HCV replication ability over a wide range of concentrations in order to determine the IC_{50} replicon values. Plots of firefly luciferase activity versus ABA analog concentration shown in Figure 3.6 were used to determine IC_{50} values of 20.5 ± 2.5 μM, 10.6 ± 6.5 μM, and 1.98 ± 0.42 μM for origamicin, A2-PBI-659, and C1-PBI-575, respectively. Structures of origamicin and C1-PBI-575 differ only in their halogen substituent. Origamicin has chlorine atom where C1-PBI-575 has a bromine atom. However, IC_{50} values, as well as single point measurements show that C1-PBI-575 has the same effect on HCV as origamicin at ten times lower concentration. Bromine is a better leaving group and the activity of the two compounds can be possibly associated with metabolism of the two compounds. Similarly to activity results, cytotoxicity assay for the three analogs showed concentration dependence and greater toxicity of the brominated C1-PBI-575 compound (Figure 3.7). We further compared the activity of the three ABA analogs to the activity of the previously mentioned small molecules lovastatin and 25-hydroxycholesterol, which inhibit HCV replication in cell cultures by modulating lipid metabolism. At concentrations where cell viability was comparable, these analogs showed similar or superior inhibitory effects compared to 25-hydroxycholesterol (2.5 μM), and lovastatin (50 μM) (Figure 3.6 and Figure 3.7) [25, 26]. We also compared the activity of the three active ABA analogs to retinoic acid, a mammalian ortholog of ABA. Experiments showed that the ABA analogs have similar cytotoxicity to that of retinoic acid, however, retinoic acid showed much lower activity at 100 μM compared to the other small molecules (see Figure 3.8 and Figure 3.9). Retinoic acid induces cell differentiation; however, the effect was not large enough to result in changes in HCV replication.

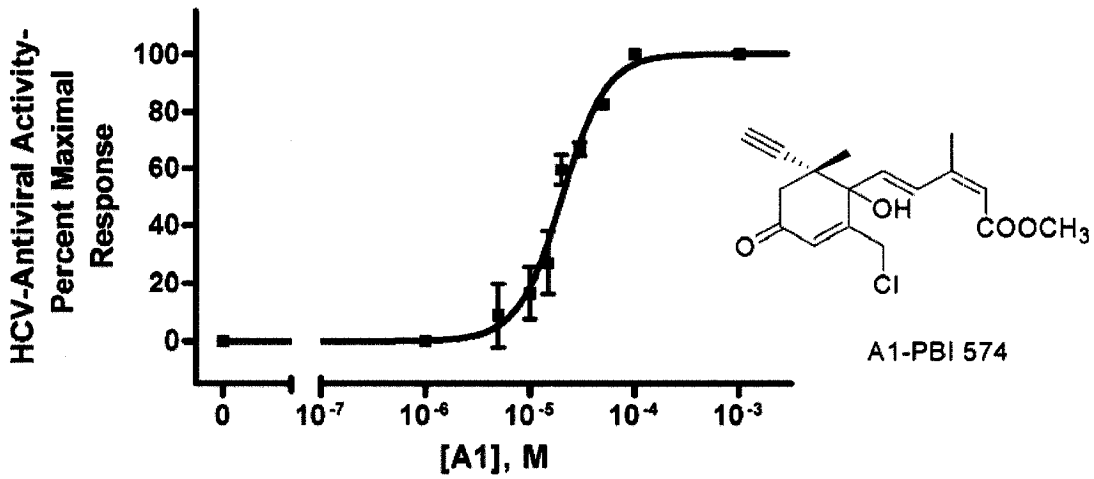
HCV-Antiviral Activity-
Percent Maximal
Response
100
80
60
40
20
0
0
10-7
10-6
10-5
10-4
10-3
[A1], M
OH
COOCH3
O
Cl
A1-PBI 574

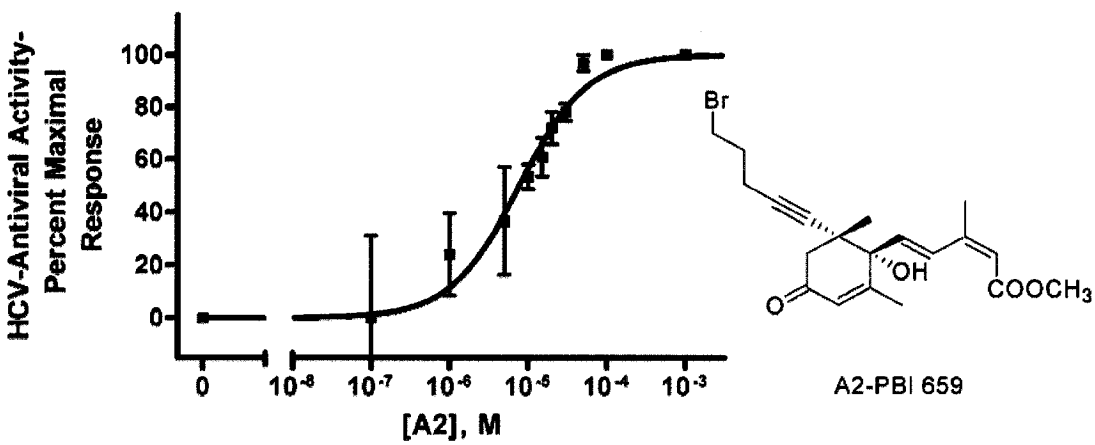
HCV-Antiviral Activity-
Percent Maximal
Response
100
80
60
40
20
0
0
10-8
10-7
10-6
10-5
10-4
10-3
[A2], M
Br
OH
COOCH3
O
A2-PBI 659

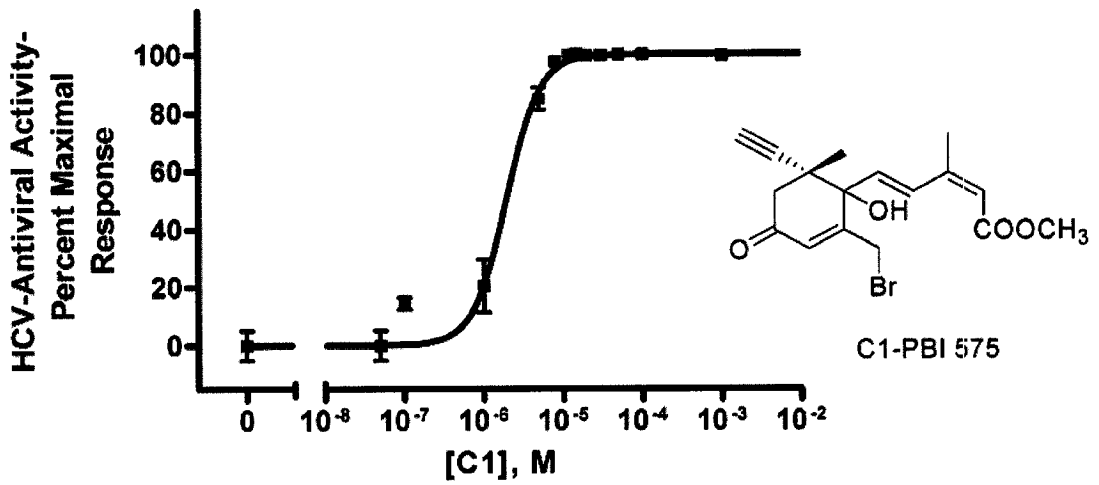

Figure 3.6: Activity data of A1-PBI-574 (origamicin), A2-PBI-659 and C1-PBI-575 expressed as IC_{50}. The data shows the concentration-dependent inhibition of HCV replication by three ABA analogs in the sub-genomic replicon system after 24h treatment. 0% and 100% response correspond to no effect on and complete inhibition of HCV replication respectively. The IC_{50} values for origamicin, A2-PBI-659, and C1-PBI-575 were determined to be 20.5 ± 2.5 μM, 10.6 ± 6.5 μM, and 1.98 ± 0.42 μM respectively. Error bars represent the mean ± SD.

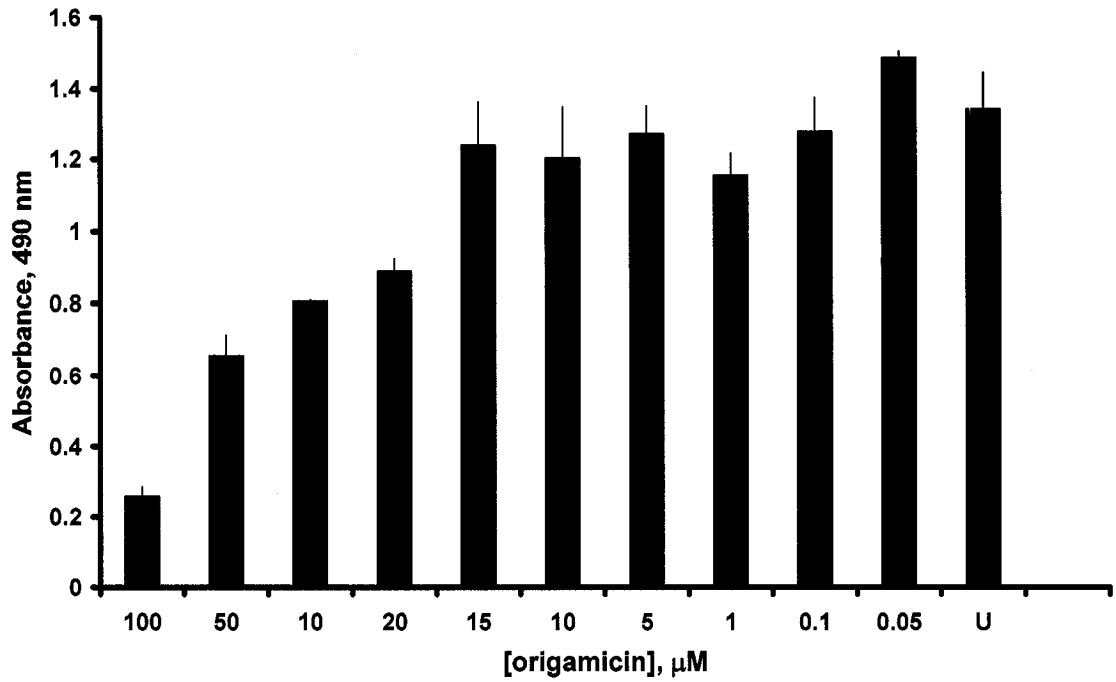
Absorbance, 490 nm
1.6
1.4
1.2
1
0.8
0.6
0.4
0.2
0
100
50
10
20
15
10
5
1
0.1
0.05
U
[origamicin], μM

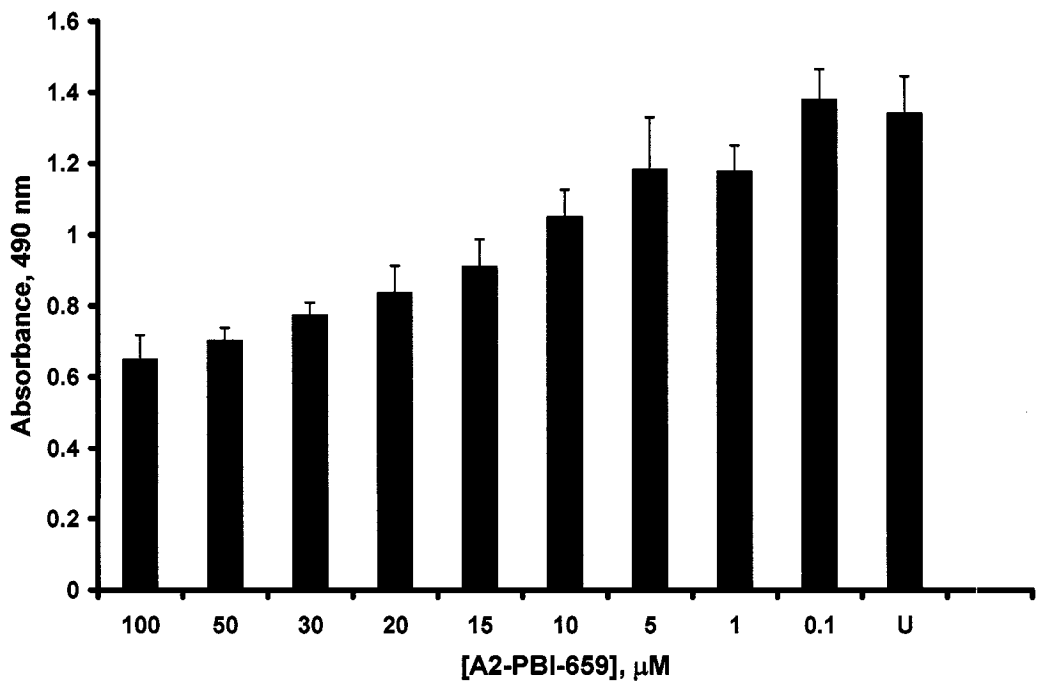
Absorbance, 490 nm
1.6
1.4
1.2
1
0.8
0.6
0.4
0.2
0
100
50
30
20
15
10
5
1
0.1
U
[A2-PBI-659], μM

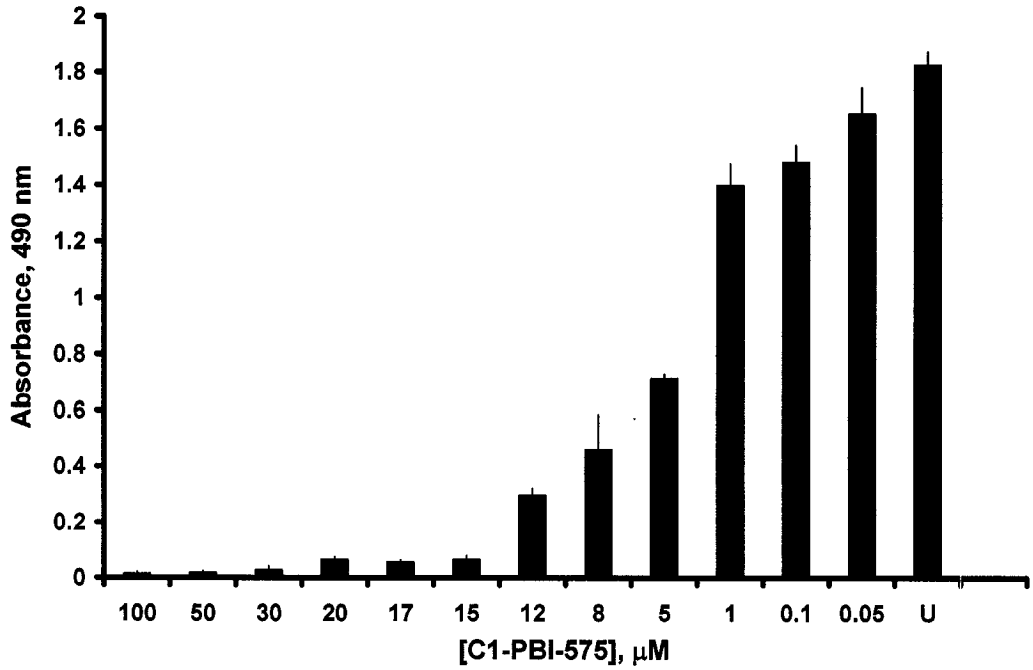

Figure 3.7: Cytotoxicity profiles of Huh7 cells stably expressing an HCV subgenomic replicon treated with origamicin, A1-PBI-659 and C1-PBI-575 at various concentrations. U-untreated Huh7 subgenomic replicon cells. Cytotoxicity was determined by LDH assay following 24h cell treatment. The data shows that cell viability was strongly depended on compound concentration. Error bars represent the mean ± SD.

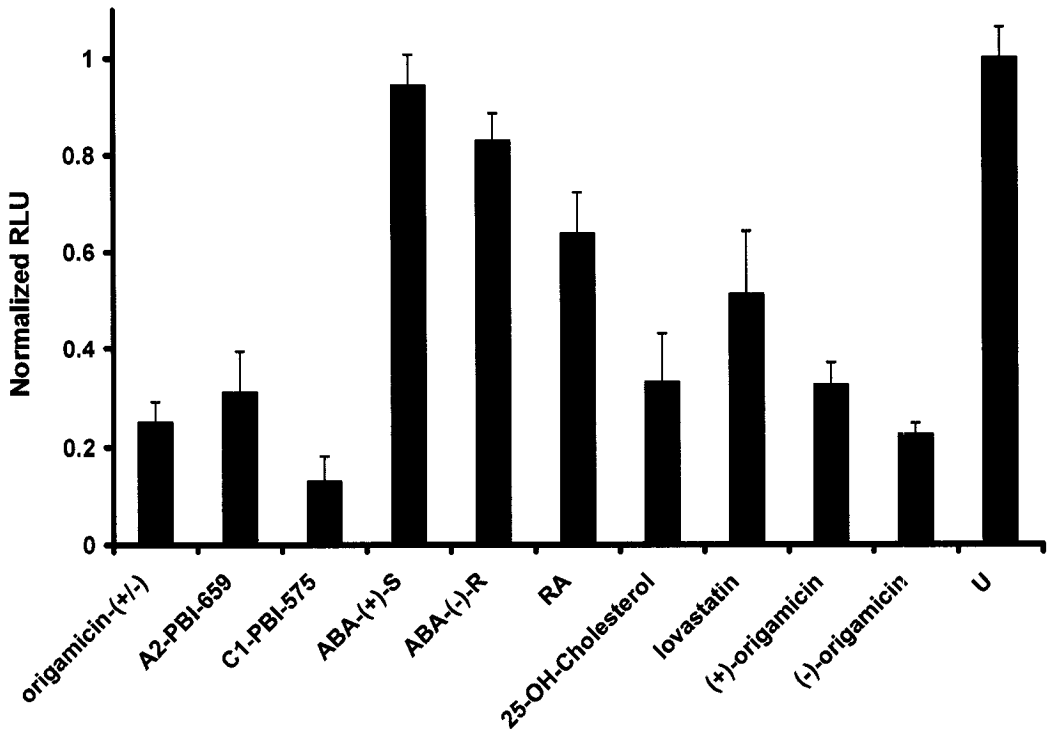

Figure 3.8: Normalized firefly luciferase data of Huh-7 replicon cells treated with ABA and its analogs, RA, lovastatin and 25-hydroxycholesterol. Activity was determined after 24h treatment with compounds at the following concentrations: origamicin, (±) 30 μM; A2-PBI-569, 20 μM; C1-PBI-575, 5 μM; ABA-(+)-S- abscisic acid, 100 μM; ABA- (-)-R- abscisic acid, 100 μM; RA- retinoic acid, 100 μM; 25-OH-Cholesterol-25-hydroxycholesterol, 2.5 μM; lovastatin, 50 μM; U-untreated cells. The data shows similar activity for the ABA analogs, 25-hydroxycholesterol and lovastatin. (±) ABA did not significantly affect HCV replication. Error bars represent the mean ± SD.

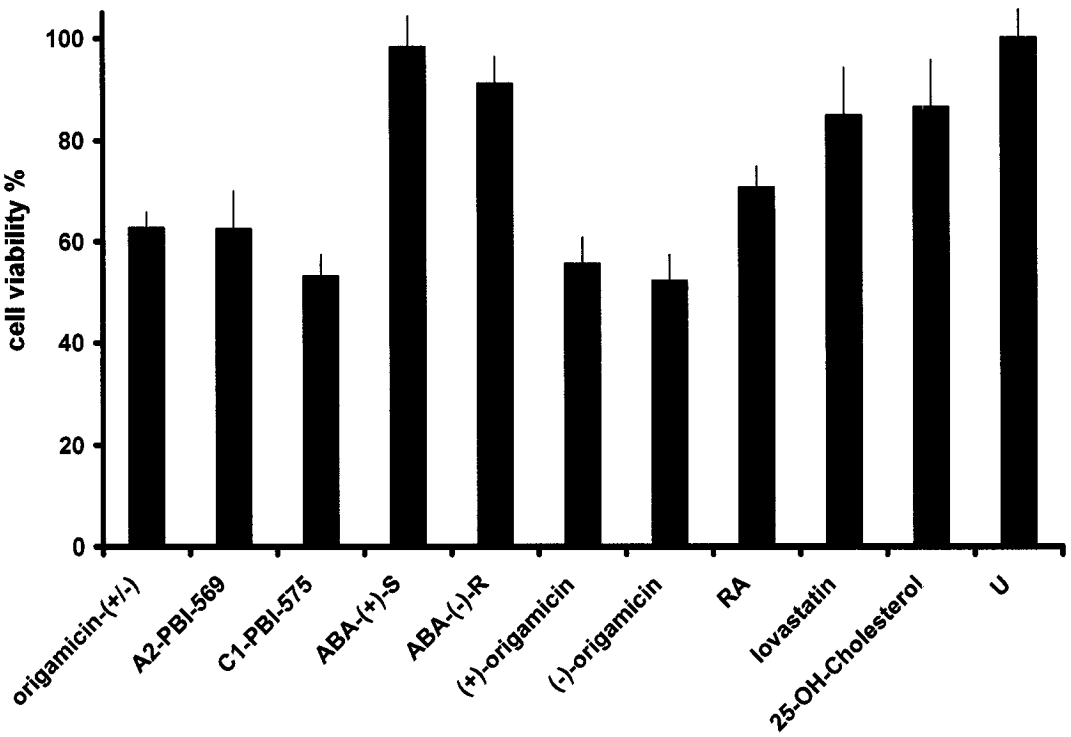

Figure 3.9: Cell viability data of Huh-7 replicon cells treated with ABA and its analogs, retinoic acid, lovastatin and 25-hydroxy cholesterol. Cell viability is expressed as a percentage after 24h treatment with compounds at the following concentrations: origamicin, (±) 30 μM; A2-PBI-569, 20 μM; C1-PBI-575, 5 μM; ABA-(+)-S- abscisic acid, 100 μM; ABA- (-)-R- abscisic acid, 100 μM; RA- retinoic acid, 100 μM; 25-OH-25-hydroxycholesterol, 2.5 μM; lovastatin, 50 μM; U-untreated cells. The data shows that the ABA analogs were slightly more toxic towards the Huh-7 replicon cells than lovastatin and 25-hydroxycholesterol for a single point measurement. Error bars represent the mean ± SD.

The activity experiment also showed that treatment of the HCV replicon with 100 μM (+)-S-abscisic acid and (-)-R-abscisic acid did not have affect on HCV replication. This suggested the there were some unique structural elements in the ABA analogs that result in their activity. Concentration dependant experiments with the R and S isomers of origamicin indicated that their antiviral properties towards the HCV replicon were not dependent on stereochemistry. Comparing the activities of the 18 ABA analogs based on their structure, we concluded that the position of the halogen in origamicin was critical for its biological activity. Although cytotoxicity of halogenated electrophiles towards human liver cells has been established previously [27], we observed for example, that replacing the allylic halide in origamicin or C1-PBI-575 with a propyl halide eliminated the biological activity.

In order to validate the luciferase assay data, the effects of ABA analogs origamicin, A2-PBI-659, and C1-PBI-575, on expression levels of HCV proteins were measured using a bicistronic HCV replicon previously explained in Chapter 2 (Figure 3.3b). Huh-7 cells stably supporting HCV replicon propagation were treated with the three ABA analogs for 12-30h, after which the cells were lysed and the cellular proteins were collected and quantified. Western blots were then performed and probed for HCV NS3 and NS5A proteins using mouse anti-NS3 and anti-NS5A primary antibodies. Antibodies against the protein tyrosin phosphatase 1D (PTP1D) verified equal loading of the proteins on the blots, and showed that the concentrations used were not toxic for the cells (Figure 3.10). The western blots showed that the compounds origamicin, A2-PBI-659, and C1-PBI-575 inhibited HCV NS5A protein production by approximately 80%, 75%, and greater than 90%, respectively. This inhibition was comparable to that exhibited by antiviral cytokine interferon gamma (IFNγ), which was used as a positive control for viral inhibition.

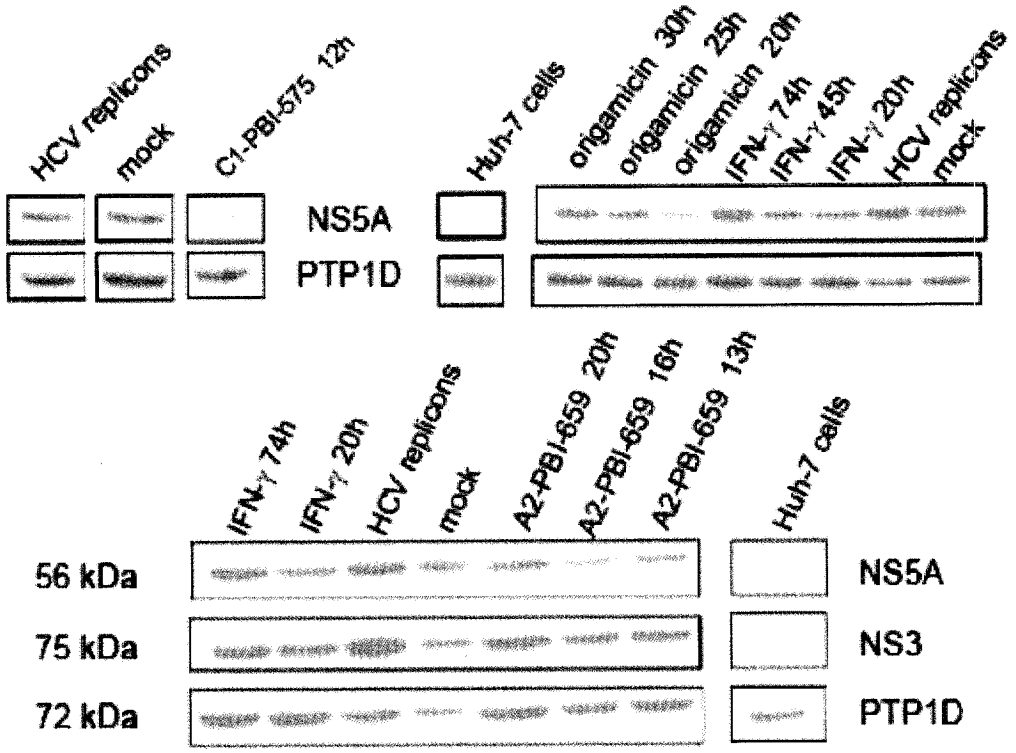

Figure 3.10: Western blots indicating the expression of NS5A and NS3 proteins of Huh-7 replicon cells treated with ABA analogs and IFNγ under various conditions. The lanes for C1-PBI-574 (upper left) are: HCV replicons- untreated cells; Mock-1% v/v MeOH; C1-PBI-575, 15μM, 12h treatment. For origamicin (upper right) the lanes are: Huh-7 cells; origamicin, 50 μM after 30h, 25h and 20h treatment respectively; IFNγ 5 U/ml after 74h, 45h and 20h treatment respectively; HCV replicons - untreated cells; Mock-1% v/v MeOH. For A2-PBI-569 (lower middle) the lanes are: IFNγ 5 U/ml after 74h and 20h treatment respectively; HCV replicons- untreated cells; Mock-1% v/v MeOH; A2-PBI-569, 50 μM after 20h, 16h and 13h treatment respectively; Huh-7 cells. Expression of PTP1D protein was used as a loading control. The blots show reduced expression of NS5A and to lesser extent NS3 protein in replicon cells treated with the ABA analogs and with the positive control, IFNγ. Expression level of NS5A protein recovered in cells treated with origamicin and A2-PBI-659 over time.

In this experiment, origamicin and A2-PBI-659 were used at 50 μM, and C1-PBI-575 at 15 μM. These concentrations were higher than the previously measured IC_{50} using the tricistronic replicon and might have been expected to cause high levels of cellular toxicity. However, this effect was not observed as proved by control antibodies for cellular PTP1D protein. This is presumably due to the fact that the bicistronic replicon used for these Western blot experiments expresses much more HCV proteins and behaves differently in cell culture than the tricistronic one. Interestingly, with origamicin and A2-PBI-659, the replicon cells recovered over time and HCV replication resumed. In contrast, cells could be cured of HCV replicons using ABA analog C1-PBI-575 (Figure 3.10).

In order to determine if the inhibition of HCV replication was linked with changes in cellular viability or morphology, we performed fluorescence microscopy experiments on the tricistronic HCV replicon treated with origamicin at 20 μM, A2-PBI-659 at 20 μM, and C1-PBI-575 at 7 μM. Cells were treated for 48h, after which the cells were stained with a mouse anti-NS5B primary antibody and a fluorescein labeled anti-mouse secondary antibody, followed by counterstaining with DAPI for nuclei; and Oil-Red O for lipid droplets. We observed decreases in NS5B protein with all three ABA analogs compared to untreated cells (Figure 3.11). Fluorescence microscopy also showed that at these concentrations there was no change in nuclear morphology (based on DAPI) indicating no change in cellular viability. We did not observe changes in the lipid content between treated and non-treated cells. This led us to the conclusion that the ABA analog's efficacy was not due to modulation of the cholesterol or PPARα pathways as we previously hypothesized.

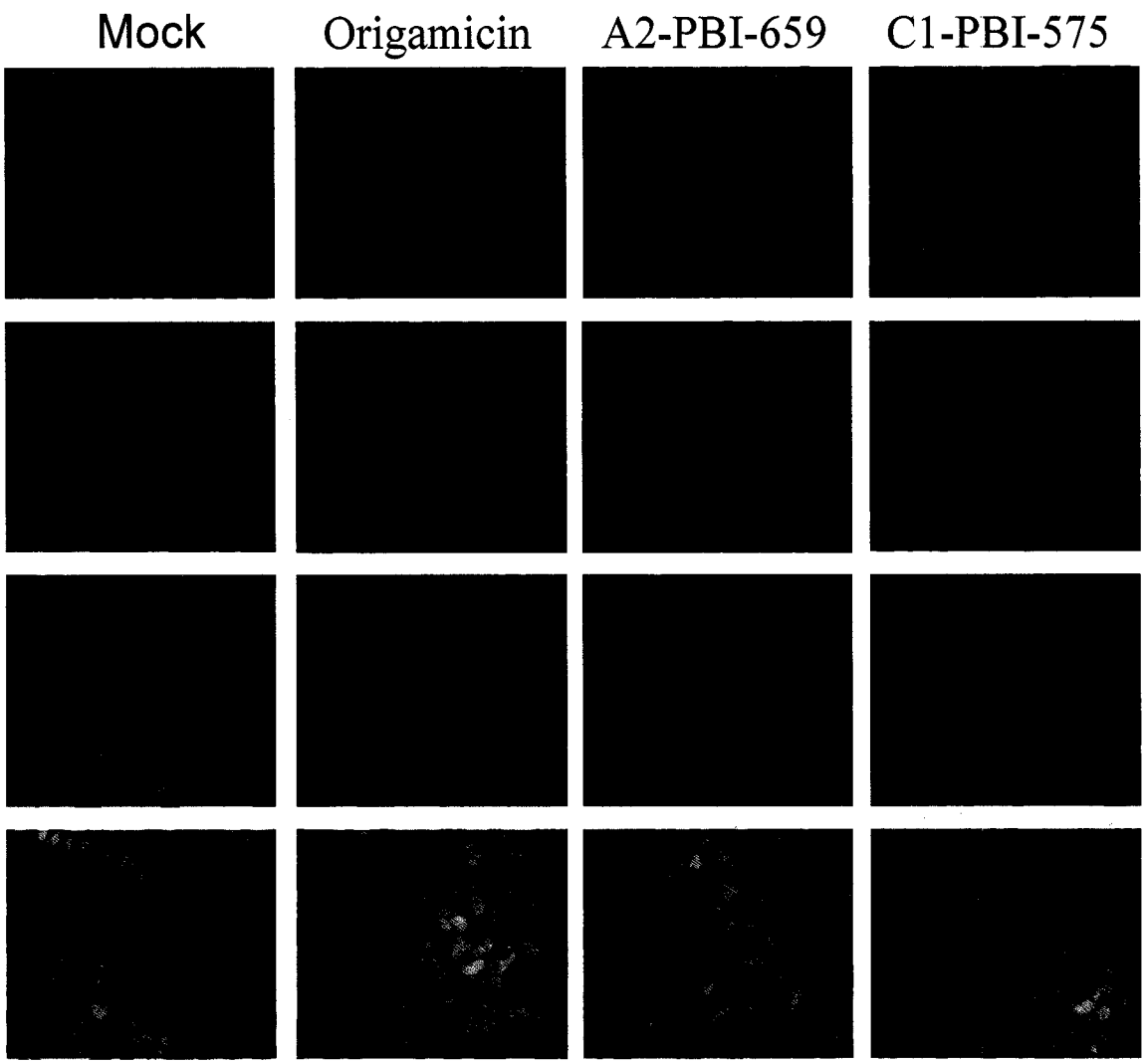

Figure 3.11: Fluorescent microscopy of NS5B protein in Huh-7 replicon cells treated with origamicin, A2-PBI-659 and C1-PBI-575. Images show NS5B (green) immunostained Huh-7 replicon cells, counterstained with 4',6-diamino-2-phenylindole (DAPI, blue) for nuclei, and lipids stained with oil red O (red). The last row shows the three colour overlay. Mock is 1% v/v MeOH; origamicin analog, 20 μM, 48h treatment; A2-PBI-569 analog 20 μM, 48h treatment; and C1-PBI-575 analog at 7 μM, 48h treatment. All images show reduced level of NS5B protein expression after ABA analog treatment compared to Mock treated cells.

To investigate if HCV inhibition by the active ABA analogs was due to interactions with the host Huh-7 human hepatoma proteins, or whether their activity and cytotoxicity were due to a specific interaction with HCV, their cytotoxic effects were screened against a panel of human cell lines. These cell lines included Huh-7, HepG2, C3A human hepatocarcinoma, MDA-MB-435 human melanoma, HEK293 human epithelial kidney, and HeLa cervical carcinoma cells (Figure 3.12). The results suggest that the host cell effects of origamicin, A2-PBI-659, and C1-PBI-575 are cell-type specific. Hepatoma and kidney cells appeared to be most sensitive to the effects of the ABA analogs, whereas HeLa cells showed virtually no cytotoxicity upon treatment with the ABA analogs, excepting high doses of C1-PBI-575 ($\geq$100 μM). Therefore, we concluded that cytotoxic effects at higher concentrations of ABA analogs were dependent on cell type but do not require the expression of HCV proteins.

As ABA and its analogs have similar molecular structures to retinoic acid and other nuclear hormone receptor ligands, they may show reactivity toward these mammalian receptors. By binding to the RXRα receptor, retinoic acid regulates cell processes such as vertebrate growth and development, stem cell differentiation, embryonic development, vision, immune response, and reproduction [23]. In order to test whether the ABA analogs affect the (RXRα) signaling pathway, we performed the Enzyme-Linked Immunosorbent Assay (ELISA) for albumin. The ELISA method allows detecting and quantifying substances such as peptides, proteins, antibodies and hormones. It is widely used in biology, immunology and medicine. In an ELISA, an antigen (primary or coating antibody) is first immobilized on a solid surface. Most often 96-well or 384-well plates are used, allowing for high-throughput screening assays. The antigen (in this case albumin) is then complexed with

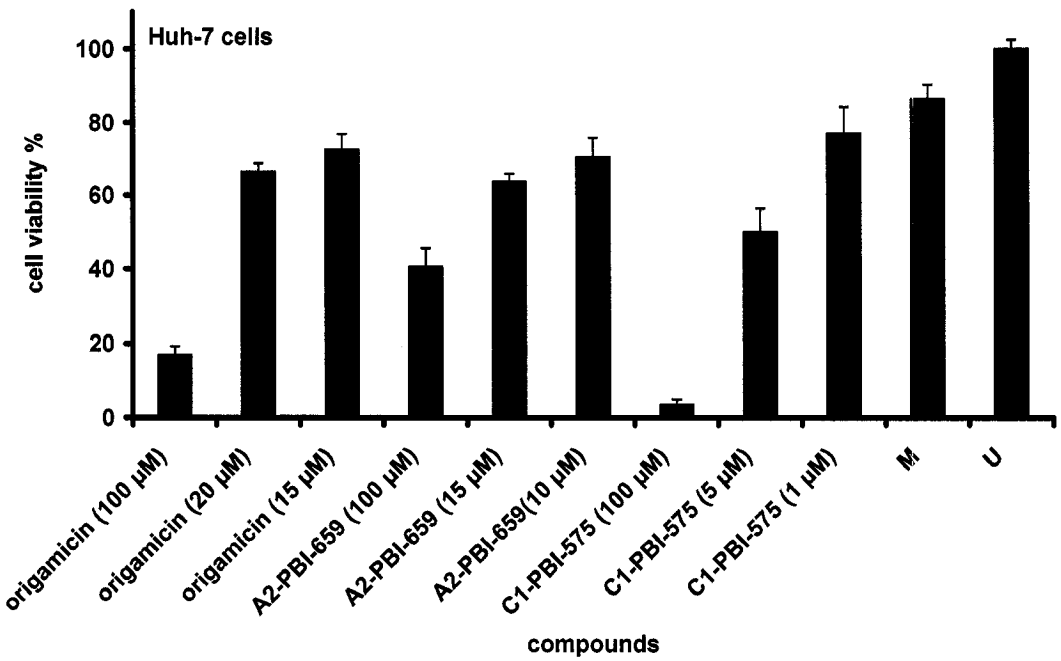
Huh-7 cells
cell viability %
100
80
60
40
20
0
origamicin (100 µM)
origamicin (20 µM)
origamicin (15 µM)
A2-PBI-659 (100 µM)
A2-PBI-659 (15 µM)
A2-PBI-659(10 µM)
C1-PBI-575 (100 µM)
C1-PBI-575 (5 µM)
C1-PBI-575 (1 µM)
M
U
compounds

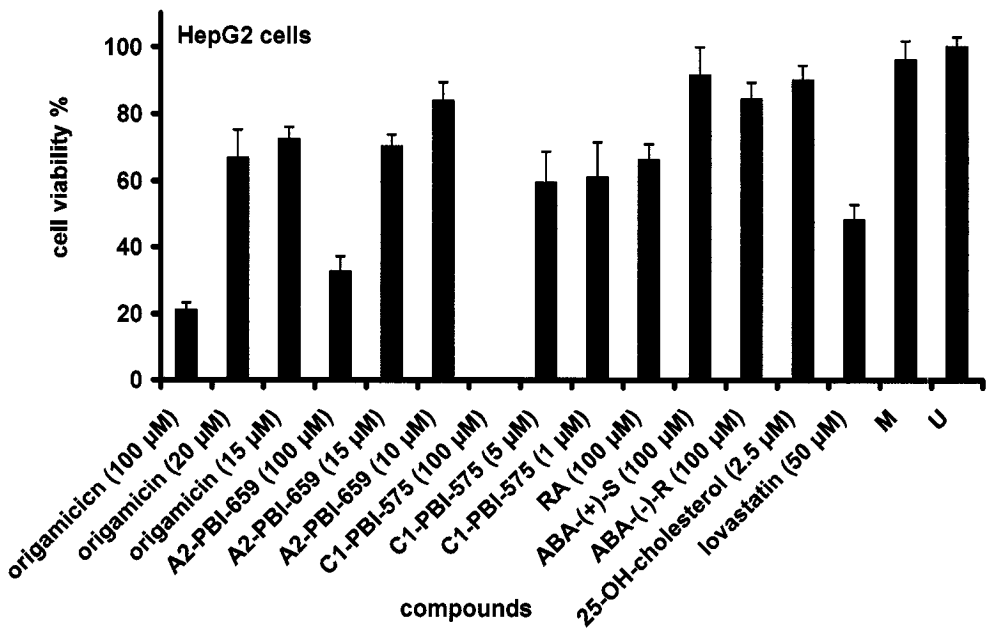
HepG2 cells
cell viability %
100
80
60
40
20
0
origamicicn (100 µM)
origamicin (20 µM)
origamicin (15 µM)
A2-PBI-659 (100 µM)
A2-PBI-659 (15 µM)
A2-PBI-659 (10 µM)
C1-PBI-575 (100 µM)
C1-PBI-575 (5 µM)
C1-PBI-575 (1 µM)
RA (100 µM)
ABA-(+)-S (100 µM)
ABA-(-)-R (100 µM)
25-OH-cholesterol (2.5 µM)
lovastatin (50 µM)
M
U
compounds

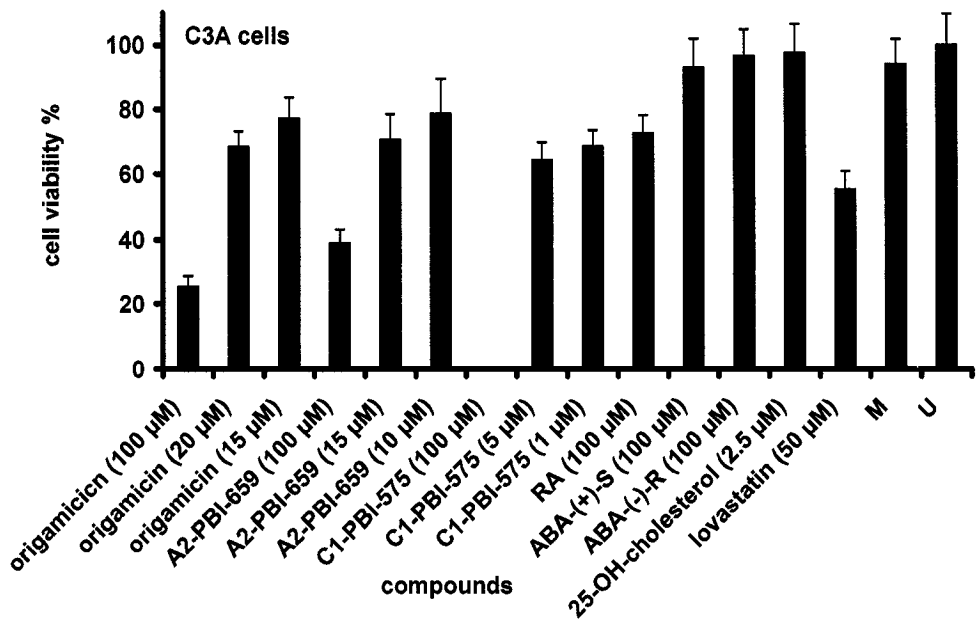
C3A cells
cell viability %
100
80
60
40
20
0
origamicicn (100 µM)
origamicin (20 µM)
origamicin (15 µM)
A2-PBI-659 (100 µM)
A2-PBI-659 (15 µM)
A2-PBI-659 (10 µM)
C1-PBI-575 (100 µM)
C1-PBI-575 (5 µM)
C1-PBI-575 (1 µM)
RA (100 µM)
ABA-(+)-S (100 µM)
ABA-(-)-R (100 µM)
25-OH-cholesterol (2.5 µM)
lovastatin (50 µM)
M
U
compounds

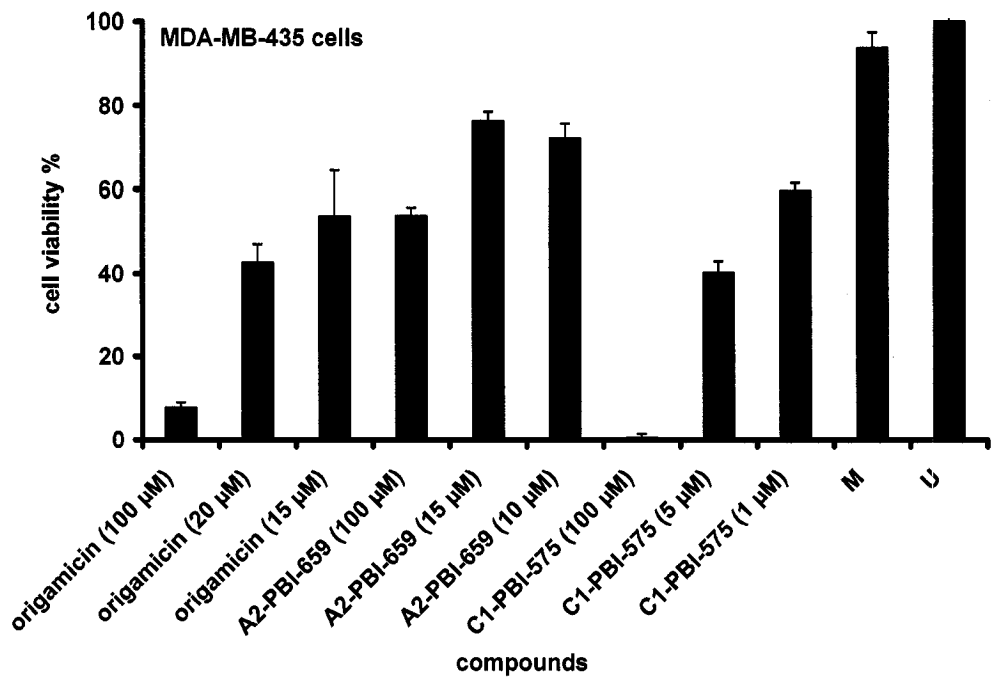
MDA-MB-435 cells
cell viability %
100
80
60
40
20
0
origamicin (100 µM)
origamicin (20 µM)
origamicin (15 µM)
A2-PBI-659 (100 µM)
A2-PBI-659 (15 µM)
A2-PBI-659 (10 µM)
C1-PBI-575 (100 µM)
C1-PBI-575 (5 µM)
C1-PBI-575 (1 µM)
M
U
compounds

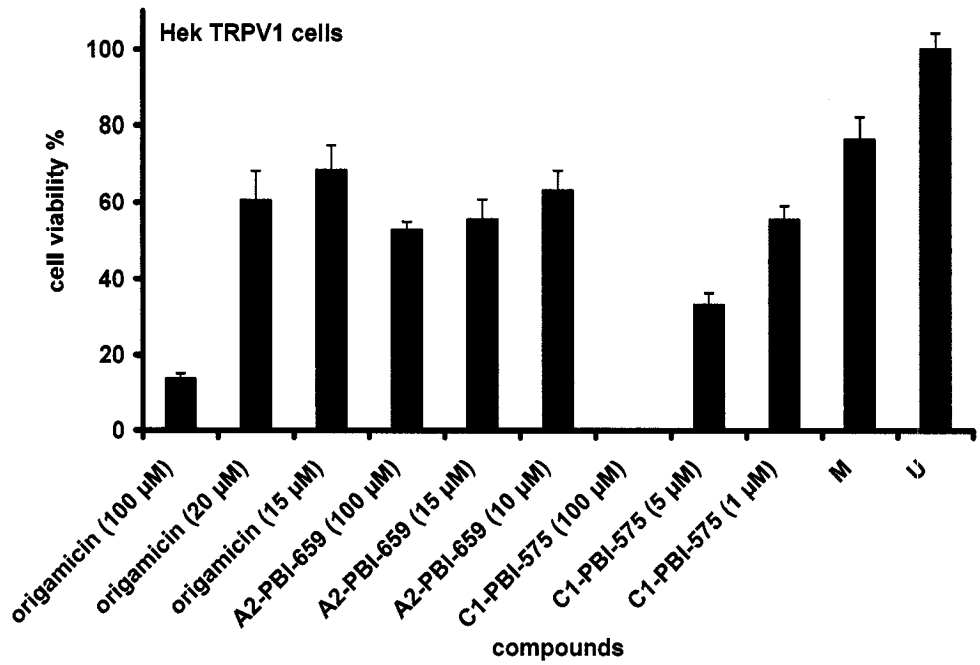
Hek TRPV1 cells
cell viability %
100
80
60
40
20
0
origamicin (100 µM)
origamicin (20 µM)
origamicin (15 µM)
A2-PBI-659 (100 µM)
A2-PBI-659 (15 µM)
A2-PBI-659 (10 µM)
C1-PBI-575 (100 µM)
C1-PBI-575 (5 µM)
C1-PBI-575 (1 µM)
M
U
compounds

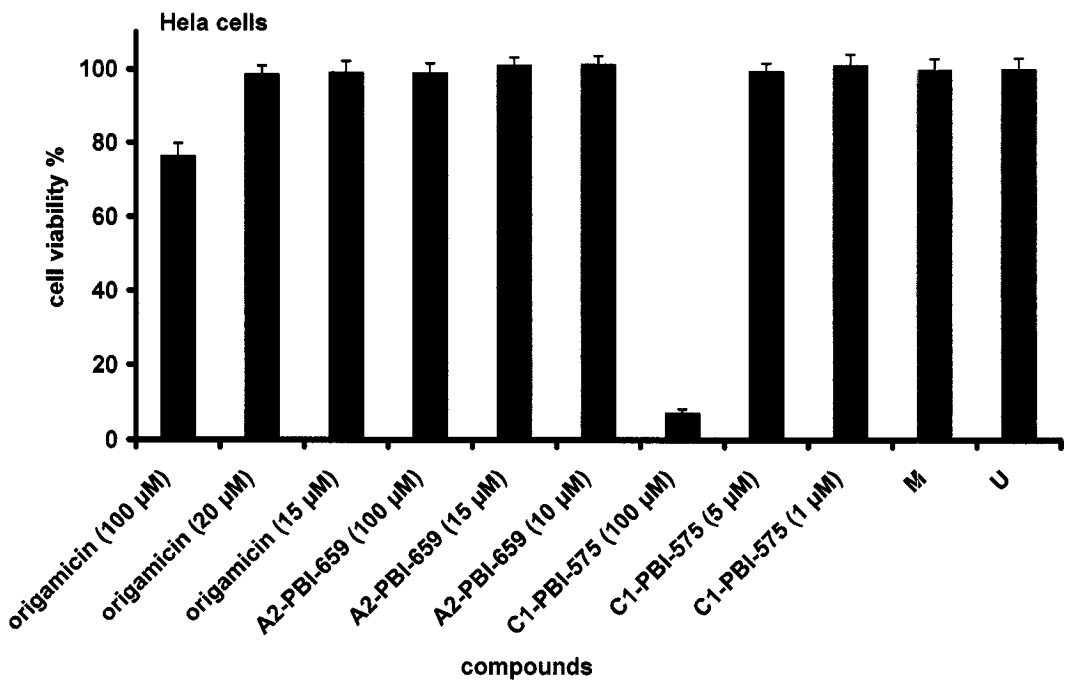
Hela cells
cell viability %
100
80
60
40
20
0
origamicin (100 µM)
origamicin (20 µM)
origamicin (15 µM)
A2-PBI-659 (100 µM)
A2-PBI-659 (15 µM)
A2-PBI-659 (10 µM)
C1-PBI-575 (100 µM)
C1-PBI-575 (5 µM)
C1-PBI-575 (1 µM)
M
U
compounds

Figure 3.12: Cytotoxicity profiles of different cell lines after treatments with ABA analogs as measured by LDH assay. The figures show cytotoxicity profiles for Huh-7 cells, HepG2, C3A human hepatocarcinoma, MDA-MB-435 human melanoma, HEK293 human epithelial kidney, and Hela cervical carcinoma cells, respectively. Cell viability is expressed as a percentage relative to untreated cells (U) measured after 24h treatment with the ABA analogs. M-1% v/v MeOH. The compound concentration is shown in parentheses. Error bars represent the mean ± SD.

an antibody that is linked to an enzyme. Detection is accomplished by incubating this enzyme-complex with a substrate that produces colour. Albumin levels can be determined by measuring the absorbance of the samples. We chose to investigate albumin levels because their secretion is known to be directly modulated by retinoic acid. Also, changes in albumin levels can be associated with other effects on cell proliferation and differentiation by ABA and its analogs [22, 28, 29].

The ELISA was performed with the supernatant of ABA analogs origamicin (20 μM and 15 μM), A2-PBI-659 (15 μM and 10 μM), C1-PBI-575 (5 μM and 1 μM), as well as lovastatin (50 μM), 25-hydroxycholesterol (2.5 μM), R and S abscisic acid (100 μM), retinoic acid (100 μM), mock treated and untreated HCV replicon cells. Huh-7 cells stably expressing HCV replicons were treated with the small molecules for 24h, after which the amount of secreted albumin was measured. No significant reduction in albumin was observed upon treatment with ABA or the three analogs that showed anti-HCV activity, verified by performing one way ANalysis Of Variance (ANOVA) statistical test, in contrast to retinoic acid, which did lower the secreted albumin levels as expected (Figure 3.13).

No change in albumin levels suggests that the ABA analogs do not behave as their mammalian orthologs (retinoids) and that their inhibitory effect must be due to specific interactions with HCV proteins and/or host proteins involved in the HCV replication cycle. Also, fluorescence images showing that the ABA analogs do not disrupt membrane lipid content support the evidence that the compounds do not bind to nuclear hormone receptors. Unfortunately, this contradicted our original hypothesis. However, we were very interested to understand the inhibitory effect of the three ABA analogs and we decided to perform

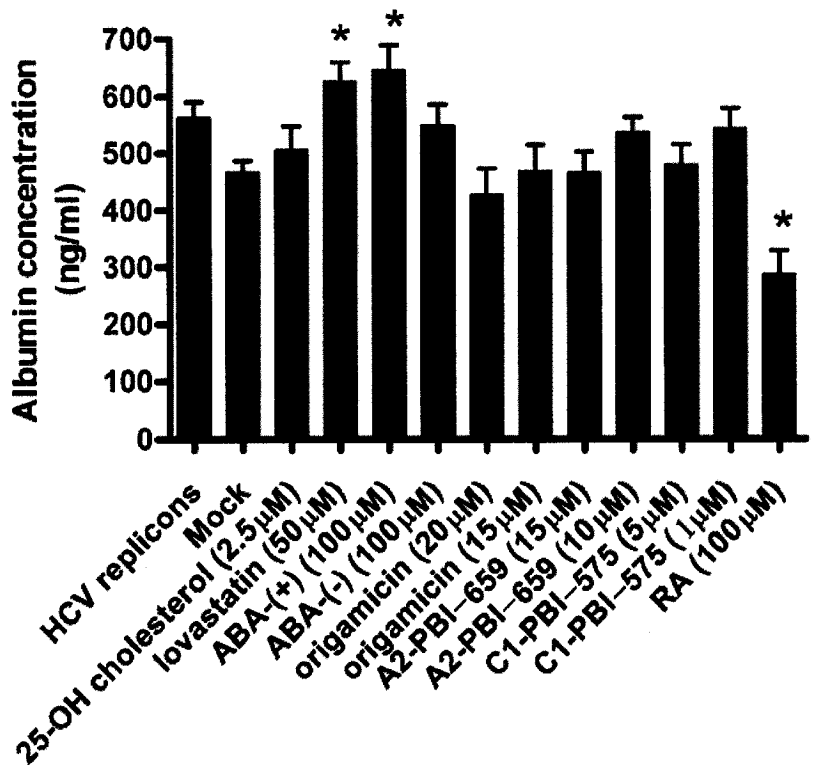

Figure 3.13: Albumin concentration (ng/ml) of HCV replicon bearing cells after 24h cells treatment under different conditions. Analog concentrations are shown in parentheses. Only retinoic acid (RA) significantly reduced level of albumin protein comparing to Mock treated replicon cells. Mock-1% v/v MeOH. Statistical analyses were carried out using GraphPad Prism software (version 4.01, GraphPad Software, San Diego, CA, USA). Mean quantitative values were compared to Mock using the Dunnett's Multiple Comparison Test. All P values less than 0.05 were accepted as statistically significant (*).

proteomics studies and to identify their targeted proteins. These proteomics studies are described in Chapter 4.

Materials and Methods

Cell culture

Cell monolayers of the human hepatoma cell line Huh-7 and Huh-7 cells stably expressing HCV replicons were grown in complete Dulbecco's modified minimal essential medium (DMEM) supplemented with G418. For further details please refer to Materials and Methods in Chapter 2.

Replicon treatment with ABA analogs and HCV inhibitors

The ABA compounds were dissolved in methanol at 10 mM stock solution and further dilutions were made in DMEM medium. Huh-7 cells harboring HCV were seeded at $1x10^4$cells/well in DMEM without G 418 in 96-well plates. After 24h, at a confluency of 70 to 80%, the cells were treated with 100 µl of the ABA analogs for 24h or 48h. The same conditions were followed for treatments with 25-hydroxycholesterol (2.5 µM), lovastatin (50 µM), and retinoic acid (100 µM).

Luciferase reporter assay and total protein quantification

Huh-7 cells stably expressing HCV subgenomic replicons were treated with ABA analogs as described above. At the assay time point, cells were washed once with 1X PBS and lysed with cell culture lysis buffer (Promega) for 10 min at room temperature (RT). For detailed information on the experimental protocol please refer to Materials and Methods in Chapter 2. Values were normalized against total protein content that were determined using the Bio-Rad

DC protein assay (Bio-Rad) according to the manufacturer's protocol. Normalized values of each sample are shown as the mean ± standard deviation. IC_{50} curves were obtained using GraphPadPrism 4 software.

Cytotoxicity assay

Huh-7 cells expressing HCV subgenomic replicons were treated with the ABA analogs as described above. After 24h or 48h, the cells were processed for the CytoTox 96 Non-Radioactive Cytotoxicity Assay (Promega) according to the manufacturer's protocol. The absorbance was read at 490 nm using the SPECTRAmax M2 plate reader and SOFTmax Pro software. Values of each experiment are shown as the mean ± standard deviation. For more details please refer to Materials and Methods in Chapter 2.

Fluorescence microscopy

The Huh-7 cells stably expressing HCV sub-genomic replicons were treated with ABA analogs as described above. Cells were probed with mouse NS5B primary antibody (1:100 dilution) followed by incubation with CyTM2 conjugated AffiniPure Donkey Anti-Mouse IG secondary antibody (1:100 dilution, Jackson ImmunoResearch Laboratories Inc.). Nuclei were stained with DAPI (300 nM), and lipids were stained with Oil Red O (0.5% in isopropanol). Fluorescent images were collected using an Aziovert 200M inverted microscope from Zeiss with Axiovision 3.1 software. The cells were photographed with an AxioCam connected to the inverted microscope. For detailed information on cell staining please refer to Chapter 2.

Western Blotting

Huh-7 cells harboring subgenomic replicona derived from the clone pFK-I389neo/NS3-3'/5.1 ($1x10^6$ cells) were seeded in 60 mm dishes for preparation of western blot lysates. After 24h, the cells were treated with origamicin (50 μM), A2-PBI-659 (50 μM), C1-PBI-575 (15 μM) and interferon γ (IFNγ), 5 U/ml. At specified treatment time points: C1-PBI-575, 12h; origamicin, 20h, 25h and 40h; A2-PBI-659, 13h, 16h and 20h; and IFNγ, 20h, 45h and 74h, the cells were washed and lysed using an SDS lysis buffer consisting of 50 mM Tris-HCl (pH 6.8), 2% SDS, and 10% glycerol. The page gel and blotting were then run as described previously in Chapter 2. The membranes were probed for HCV NS5A and HCV NS3 protein using a mouse anti-NS5A primary antibody and a mouse anti-NS3 primary antibody (1:500 dilution, Virostat). As a loading control, a mouse PTP1D primary antibody (1:2500 dilution; Sigma) was used. For more details please refer to Materials and Methods in Chapter 2.

Albumin ELISA

Huh-7 cells harbouring subgenomic replicons were treated with origamicin (15 μM and 20 μM); A2-PBI-659 (10 μM and 15 μM); C1-PBI-575 (1 μM and 5 μM); (±) ABA (100 μM); lovastatin (50 μM); 25-hydroxycholesteron (2.5 μM), and retinoic acid (100 μM) as previously described. The albumin ELISA was performed using the human albumin ELISA quantification kit (Bethyl laboratories, TX, USA) as follows. 1 μl of goat anti-human albumin (1 mg/ml) was added to 100 μl coating buffer (0.05 M carbonate-bicarbonate, pH 9.6) and 100 μl of such diluted coating antibody was added to each well in a 96 well plate for 1h incubation period at room temperature. Experiments were done in triplicates. Excess of coating antibody was washed three times with washing solution (50 mM Tris-HCl, 0.14 M

NaCl, 0.05% Tween-20, pH 8) followed by 30 min incubation with 200 µl/well of blocking-postcoat solution (50 mM Tris-HCl, 0.14 M NaCl, 1% BSA, pH 8). After washing three times with 200 µl/well washing solution, 100 µl of standard solutions (human reference serum, 25 mg/ml albumin) and 100 µl of the small molecule supernatants from cell treatments were added and incubated 1h at room temperature. The excess of uncoated reagents were removed by washing five times with 100 µl of wash solution followed by addition of 100 µl/well secondary HRP detection antibody (goat anti-human- HRP conjugate, 1 mg/ml, dilution 1:50000) for 1h at room temperature. The excess of secondary antibody was aspirated and wells washed in the usual way. Peroxide substrate solution was prepared by mixing equal volumes of 3,3',5,5'-tetramethylbenzidine (0.4 g/l in an organic base) and 0.02% H_2O_2 in a citric acid buffer. 100 µl/well of solution were added followed by incubation at room temperature until the colours became blue, to a maximum of 30 min. The enzyme substrate reaction was stopped by adding 100 µl/well of stop solution (2M H_2SO_4) and absorbance was read at 450 nm using a Spectramax M2 (Molecular Devices Corporation, Sunnyvale, CA). Albumin concentrations are expressed as ng/ml. Statistical analyses were done using GraphPad Prism software (version 4.01, GraphPad Software, San Diego, CA).

References:

[1] Yan, W.; Lee, H.; Yi, E. C., et al., System-based proteomic analysis of the interferon response in human liver cells. *Genome Biol.* **2004**, *5*.

[2] Dimitrova, M.; Imbert, I.; Kieny, M. P., et al., Protein-protein interactions between hepatitis C virus nonstructural proteins. *J. Virol.* **2003**, *77*, 5401-5414.

[3] Flajolet, M.; Rotondo, G.; Daviet, L., et al., A genomic approach of the hepatitis C virus generates a protein interaction map. *Gene* **2000**, *242*, 369-379.

[4] Lamarre, D., An NS3 protease inhibitor with antiviral effects in humans infected with hepatitis C virus. *Nature* **2003**, *426*, 186-189.

[5] Bredel, M.; Jacoby, E., Chemogenomics: An emerging strategy for rapid target and drug discovery. *Nat. Rev. Genet.* **2004**, *5*, 262-275.

[6] Mayer, T. U.; Kapoor, T. M.; Haggarty, S. J., et al., Small molecule inhibitor of mitotic spindle bipolarity identified in a phenotype-based screen. *Science* **1999**, *286*, 971-974.

[7] Gray, N. S.; Wodicka, L.; Thunnissen, A., et al., Exploiting chemical libraries, structure, and genomics in the search for kinase inhibitors. *Science* **1998**, *281*, 533-538.

[8] Rosania, G. R.; Chang, Y. T.; Perez, O., et al., Myoseverin, a microtubule-binding molecule with novel cellular effects. *Nat. Biotechnol.* **2000**, *18*, 304-308.

[9] Spring, D. R., Chemical genetics to chemical genomics: small molecules offer big insights. *Chem. Soc. Rev.* **2005**, *34*, 472-482.

[10] Lokey, R. S., Forward chemical genetics: progress and obstacles on the path to a new pharmacopoeia. *Curr. Opin. Chem. Biol.* **2003**, *7*, 91-96.

[11] Arya, P.; Joseph, R.; Gan, Z. H., et al., Exploring new chemical space by stereocontrolled diversity-oriented synthesis. *Chem. Biol.* **2005**, *12*, 163-180.

[12] Schreiber, S. L., Target-oriented and diversity-oriented organic synthesis in drug discovery. *Science* **2000**, *287*, 1964-1969.

[13] Young, S. S.; Ge, N. X., Design of diversity and focused combinatorial libraries in drug discovery. *Curr. Opin. Drug Discovery Dev.* **2004**, *7*, 318-324.

[14] Arya, P.; Couve-Bonnaire, S.; Durieux, P., et al., Solution- and solid-phase synthesis of natural product-like tetrahydroquinoline-based polycyclics having a medium size ring. *J. Comb. Chem.* **2004**, *6*, 735-745.

[15] Kubota, H.; Lim, J.; Depew, K. M., et al., Pathway development and pilot library realization in diversity-oriented synthesis: Exploring Ferrier and Pauson-Khand reactions on a glycal template. *Chem. Biol.* **2002**, *9*, 265-276.

[16] Pelish, H. E.; Westwood, N. J.; Feng, Y., et al., Use of Biomimetic Diversity-Oriented Synthesis to Discover Galanthamine-Like Molecules with Biological Properties beyond Those of the Natural Product. *J. Am. Chem. Soc.* **2001**, *123*, 6740-6741.

[17] Razem, F. A.; El-Kereamy, A.; Abrams, S. R., et al., The RNA-binding protein FCA is an abscisic acid receptor. *Nature* **2006**, *439*, 290-294.

[18] Abrams, S. R.; Rose, P. A.; Cutler, A. J., et al., 8'-methylene abscisic acid - An effective and persistent analog of abscisic acid. *Plant Physiol.* **1997**, *114*, 89-97.

[19] Abrams, S. R.; Milborrow, B. V., Synthesis and Biological-Activity of Allenic Analogs of Abscisic-Acid. *Phytochemistry* **1991**, *30*, 3189-3195.

[20] Cutler, A. J.; Krochko, J. E., Formation and breakdown of ABA. *Trends Plant Sci.* **1999**, *4*, 472-478.

[21] Cutler, A. J.; Rose, P. A.; Squires, T. M., et al., Inhibitors of abscisic acid 8 '-hydroxylase. *Biochemistry* **2000**, *39*, 13614-13624.

[22] Elstner, E.; Muller, C.; Koshizuka, K., et al., Ligands for peroxisome proliferator-activated receptor gamma and retinoic acid receptor inhibit growth and induce apoptosis of human breast cancer cells in vitro and in BNX mice. *Proc. Natl. Acad. Sci. U. S. A.* **1998**, *95*, 8806-8811.

[23] Berger, J.; Moller, D. E., The mechanisms of action of PPARs. *Annu. Rev. Med.* **2002**, *53*, 409-435.

[24] Rakic, B.; Sagan, S. M.; Noestheden, M., et al., Peroxisome Proliferator-Activated Receptor [alpha] Antagonism Inhibits Hepatitis C Virus Replication. *Chem. Biol.* **2006**, *13*, 23-30.

[25] Su, A. I.; Pezacki, J. P.; Wodicka, L., et al., Genomic analysis of the host response to hepatitis C virus infection. *Proc. Natl. Acad. Sci. U. S. A.* **2002**, *99*, 15669-15674.

[26] Ye, J.; Wang, C. F.; Sumpter, R., et al., Disruption of hepatitis C virus RNA replication through inhibition of host protein geranylgeranylation. *Proc. Natl. Acad. Sci. U. S. A.* **2003**, *100*, 15865-15870.

[27] Kalgutkar, A. S.; Gardner, I.; Obach, R. S., et al., A comprehensive listing of bioactivation pathways of organic functional groups. *Curr. Drug Metab.* **2005**, *6*, 161-225.

[28] Kliewer, S. A.; Umesono, K.; Noonan, D. J., et al., Convergence of 9-Cis Retinoic Acid and Peroxisome Proliferator Signaling Pathways through Heterodimer Formation of Their Receptors. *Nature* **1992**, *358*, 771-774.

[29] Hamamoto, S.; Fukuda, R.; Ishimura, N., et al., 9-cis Retinoic acid enhances the antiviral effect of interferon on hepatitis C virus replication through increased expression of type I interferon receptor. *J. Lab. Clin. Med.* **2003**, *141*, 58-66.

4

Proteomics Study with PBI-574 ABA analog-Origamicin

Introduction

The cell based screen using the HCV replicon encoding a firefly luciferase genetic reporter identified three ABA compounds that inhibited HCV viral replication. This inhibition was confirmed by measuring reduced expression levels of NS3 and NS5A nonstructural HCV proteins in western blots of replicon bearing cells, treated with origamicin, A2-PBI-659 and C1-PBI-575 compounds. Furthermore, inhibition was confirmed by changes in the expression level of NS5B protein, which was shown by fluorescent microscopy. However, the protein target or targets, whose functions were mediated by the ABA analogs, had to be identified. This, often difficult identification process was necessary to uncover the mechanism by which ABA analog molecular activity arises. We focused our study on identifying the targeted proteins of origamicin by applying an inhibitor based protein profiling approach and using gel electrophoresis techniques combined with nano LC-MS-MS. Somewhat surprisingly, we found that origamicin showed antiviral activity through the inhibition of host proteins involved in protein folding rather

than viral proteins. This pathway has never before been directly linked to HCV replication.

There are several different approaches to target identification. They can be classified as either biochemical or genetic approaches. The most commonly used method involves derivatization of the active molecule by attaching a tag (radioactive, biotin or, fluorescent moiety) or a cross-linker that covalently binds a protein following activation with UV light [1]. Some examples of the successful application of biotin tags for protein target identification using affinity purification include Crews and coworkers study of the anti-angiogenic agent fumagillin, which covalently binds and inhibits methionine aminopeptidase, MetAP-2 in yeast [2]; and Schultz and coworker's study on myoseverin, which reversibly binds to tubulin and promotes cell proliferation [3].

Other methods for target identification include "drug Westerns" [4], three-hybrid assays, and phage display [5-7]. Microarray screening of nucleic acids, cells, tissues, and proteins are also used for target identification [8]. DNA microarrays have been shown to identify changes in gene expression patterns that occur in response to small molecule treatment of cells [9]. An example by Chen *et al* showed the application of protein microarrays as an activity-based approach, where several classes of enzymes were immobilized on a glass slide, and high-throughput screening identified enzyme suicide inhibitors [10].

Although the previously described classical methods of identifying targeted proteins and assigning their function are successful, these approaches have some limitations. One obvious limitation is the requirement for derivatisation of the active small molecule. This can be a problem because it is not always easy to install a tag on the small molecule without

modifying the molecule's activity. Also, most target identifications with tagged compounds are performed *in vitro,* under conditions that may be different from cellular protein function. Thus, they may not truly represent small molecule-protein interactions. This is due to the fact that proteins usually function as part of a complex network of metabolic and signaling pathways, where interactions with other proteins and subcellular localization are important. Additionally, proteins undergo covalent post-translational modification, and reversible interactions such as phosphorylation. They also have endogenous inhibitors that mediate their function. This dynamic kaleidoscope of events is often misrepresented with *in vitro* binding experiments. Nevertheless, "fishing" for targets using individual proteins of cell lysates can give important information about the reactivity of a given small molecule towards classes of protein targets.

Alternatively, there are methods that do not require active molecule derivatisation for assigning proteins and their function. One of these is a hypothesis-based approach and was demonstrated by the identification of Eg5, a monestrol targeted protein [11]. Other methods include genetic techniques, such as small interfering RNA in which gene silencing gives the same phenotype as the activity of the small molecule that targets the gene's product [12]. These approaches provide indirect evidence of the potential targets of small molecules.

The method of target identification that we have used in our study was based on the copper (I)-catalyzed 1,3-Huisgen dipolar cycloaddition ('click reaction') of alkyne and azide moieties [13]. Although this reaction was discovered more than fifty years ago, it was not widely used, primarily due to safety concerns about working with organic azides. Fortunately, it has been recently rediscovered by Sharpless and coworkers and has found many applications. Azides are easy to introduce into organic molecules by nucleophilic

substitution of halides or by ring opening of epoxides with sodium azide [14]. They are inert toward biological molecules and towards reaction conditions inside living cells (water, oxygen, pH) [14]. In the presence of good dipolarophiles such as terminal alkynes, azides undergo formation of 1,2,3-triazoles. However, this reaction is rather slow at room temperature and requires heating. There are no side reactions, but mixtures of 1,5- and 1,4-regioisomers are formed under these conditions. Sharpless and Meldal discovered that the reaction is faster if catalyzed by copper (I) ions, and further, does not require heating and gives only 1,4-disubstituted triazoles [15, 16]. They postulate a stepwise mechanism of reaction, shown in Scheme 4.1. $CuSO_4 \cdot 5H_2O$ in the presence of sodium ascorbate as a reducing agent proved to be the best source of Cu(I) catalyst. The reaction takes place in water and also proceeds well in mixtures of water and alcohol (t-butanol or ethanol). It can also be run as a suspension. It generally takes between 6h and 36h and tolerates a large pH range (4-12). The reaction is also compatible with a number of functional groups including: thioethers, carboxylic acids, esters, amides, ethers, thiols, alcohols, phenols, amines, guanidines, and carbamates [17]. Recently, a few ligands were synthesized that enhance the reaction rate and inhibit alkyne oxidative coupling. All of the reported ligands are oligotriazoles derived from propargyl amine. They chelate to Cu(I), forming a five-member chelate between the N-3 in the triazole and the amine. The best ligand was found to be tris-(benzyltriazolylmethyl) amine, (TBTA) [18]. Once formed, the 1,4- triazole cannot be cleaved hydrolytically or otherwise, and is stable under oxidative and reductive conditions.

Due to their inertness towards biological molecules inside the cell, alkynes and azides are an ideal pair for probing complex biological systems. Thus, it is not surprising that the 'click reaction' has found extensive application in chemical biology. For example, Sharpless

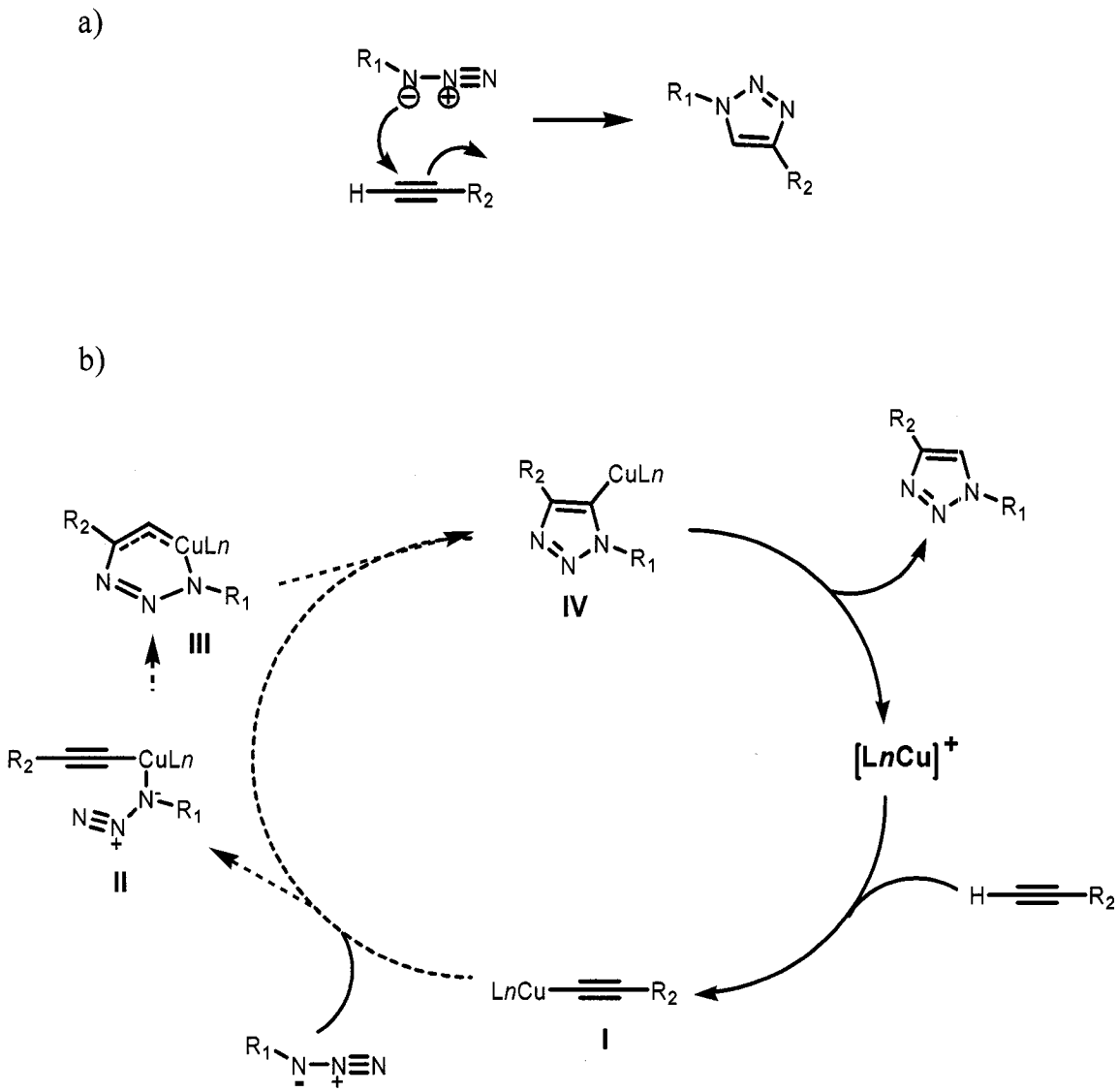

Scheme 4.1: 1,3-Huisgen dipolar cycloaddition ('click reaction') and a catalytic cycle of the reaction. Density theory calculations suggest stepwise cycloaddition mechanism from copper (I) acetylide I to triazole IV (I-II-III-IV).

and coworkers used it for target-guided synthesis of acetylcholinesterase (AchE) enzyme inhibitor [19]. They synthesized a number of tacrine and phenanthridinium analogs having alkyne or azides chains of different length as building blocks. Neither azide/alkyne combination gave any triazole at room temperature in the absence of the enzyme. However, the reaction was possible if the building blocks were in close proximity enforced by interactions with the AchE active site. One combination gave a triazole product that fit well into the binding pocket of AchE, thus inhibiting its activity. The enzyme suppression with the triazole was the most potent obtained so far with femtomolar K_d. In another example, Finn and coworkers used the copper catalyzed azide alkyne cycloaddition reaction for labeling Cowpea mosaic virus particles (CPMV) [20]. CPMV's capsid encapsulates a single stranded RNA virus and consists of sixty copies of asymmetric two-protein units, each containing single reactive Cys and Lys amino acids. Using bioconjugation reactions, the azide moiety was attached to all reactive thiols and amines on the capsid, and subjected to the 'click reaction' with fluorescein alkyne.

The 'click reaction' has also found important application in activity-based profiling of proteins (ABPP). The ABPP approach utilizes chemical probes that react with an active site in complex proteoms, and can be used as effective tools in functional proteomics [21]. The ABPP probe consists of a reactive group (usually a moderate electrophile), a linker, and a tag (biotin and/or fluorophore), for protein detection and isolation. In directed ABPP, probes are rationally designed to target specific classes of enzymes according to the catalytic active site. This has allowed functional assignment of many enzyme classes such as serine hydrolases, cystein proteases, metaloproteases, kinases, as well as many others [22]. Many ABPP experiments have been performed *in vitro* because the bulky biotin or fluorescent tag

can cause physical disruption of cells and tissues. Also, bulky reporter tags may inhibit cellular uptake of the probe causing varying probe distributions within the cell. The discovery of the copper-catalyzed click reaction has allowed enzymes to be profiled *in vivo*. This was first demonstrated by Speers *et al* using an azide-derivatized phenylsulphonate ester as a tag-free probe and rhodamine alkyne [23]. They were able to visualize *in vitro* glutathione S-transferases, aldehyde dehydrogenase, and enoyl CoA hydratase. Importantly, they have also been able to covalently label the same proteins in cells and in mice, and to visualize them by performing click reactions after cell lysis or tissue isolation, respectively.

Although the 3 HCV active ABA analog compounds were shown to be very active in functional assays, we only focused on origamicin to investigate the small molecule-protein interactions. All three ABA analogs have an alkyne group in a side chain at C8'. Origamicin was chosen for the proteomics studies because it has a terminal alkyne, which is compatible to the 'click chemistry' approach. Origamicin is a Michael acceptor: it has a double bond conjugated with an ester in the side chain, and a double bond conjugated with a ketone in the six membered ring. Origamicin also has a chloride which can undergo substitution. All aforementioned groups can serve as potential reactive sites *in vivo*. ABA analog C1-PBI-575 has a bromide in place of the chlorine in origamicin, which is more reactive, as well as more toxic in human cells that we tested. Targeted proteins of C1-PBI-575 could potentially be the same as for origamicin and their identification will be pursued in future studies.

To understand the possible mechanisms from which the ABA analogs derive their anti-HCV activity, we utilized a chemical proteomics strategy to determine the protein targets within the entire proteome [24]. We applied principles of ABPP, to investigate interactions of the ABA analog origamicin with both host and viral proteins isolated from the

replicon systems. We named our approach inhibitor-based protein profiling. We exploited the alkyne functionality present in origamicin to conjugate via 'click chemistry' both rhodamine for in-gel fluorescence experiments and biotin for affinity chromatography experiments [23].

Results and Discussion

Our first experiments to identify the ABA targets involved *in vitro* labeling of cytosolic and membrane proteins from Huh-7 cells harboring HCV replicons. The experiments are referred as *in vitro* because the labeling reaction between small molecule probes and the proteins from replicon bearing cells had been performed outside cells, more specifically with isolated cytosolic and membrane proteins. In order to perform *in vitro* experiments we synthesized two probes. One probe was named origamicin-Rh and was synthesized in a 'click reaction' between the origamicin alkyne moiety and rhodamine azide (Scheme 4.2). This probe allowed visualization of labeled proteins by fluorescence. The second probe that we synthesized in the 'click reaction' between the origamicin alkyne moiety and biotin azide was named origamicin-Biotin (Scheme 4.2). We used this probe to isolate proteins that were labeled with origamicin-biotin by streptavidin. Schematic presentation of *in vitro* experiments is shown in Scheme 4.3. We also synthesized a 'click' compound, in the reaction between octyl azide and origamicin, that we fully characterized (Scheme 4.2). This compound was not used in our biological studies.

Four strong bands were observed on the silver stained gel upon incubation of the biotin labeled probe origamicin-biotin with cytosolic proteins (Figure 4.1). These bands were isolated and identified via mass spectrometry. A list of these protein IDs is shown in

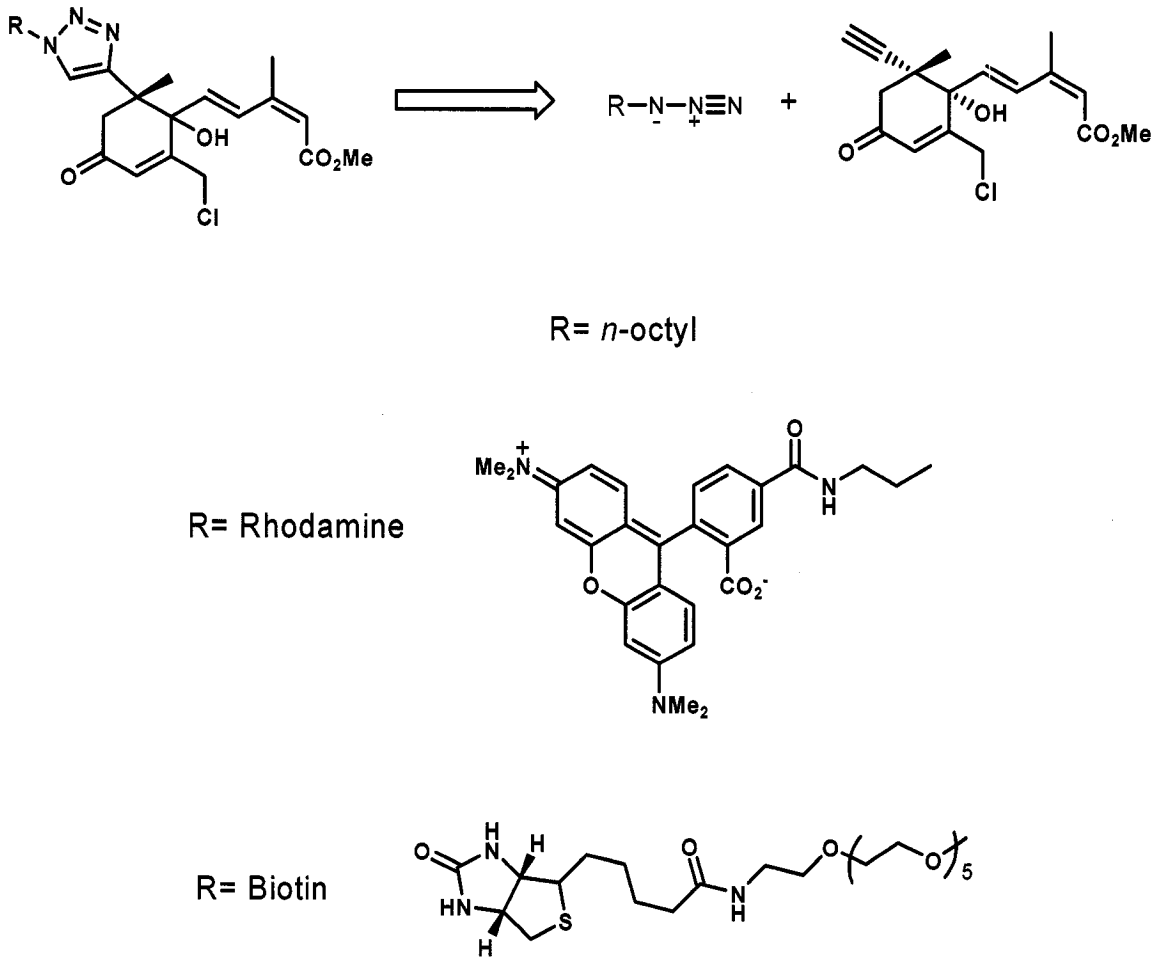

Scheme 4.2: Retrosynthesis of origamicin-rhodamine click, origamicin-biotin click, and octyl-origamicin click probes.

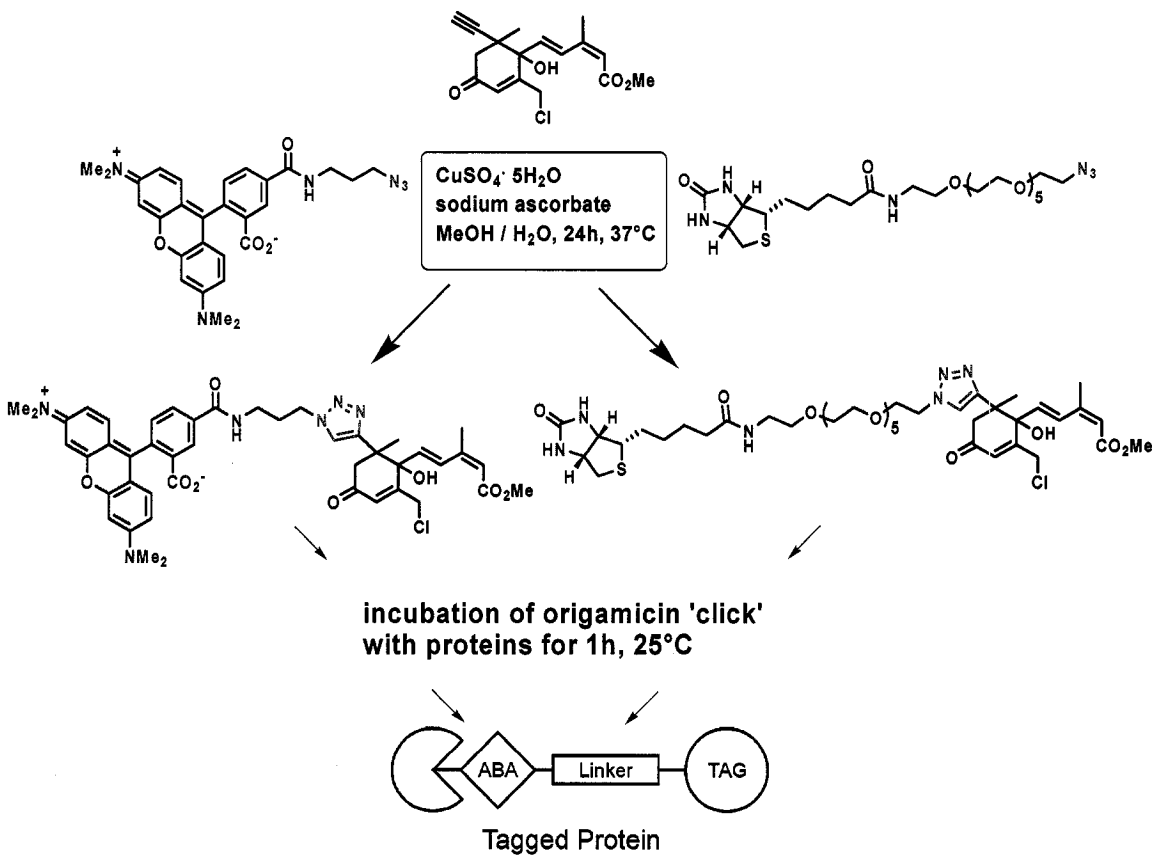

Scheme 4.3: In-vitro inhibitor based proteomics approach with origamicin-rhodamine click, and origamicin-biotin click probes. Proteins were isolated from HCV replicon cells and incubated with 'clicked' probes for 1h at 25°C, followed by fluorescence imaging or streptavidin purification of labeled proteins.

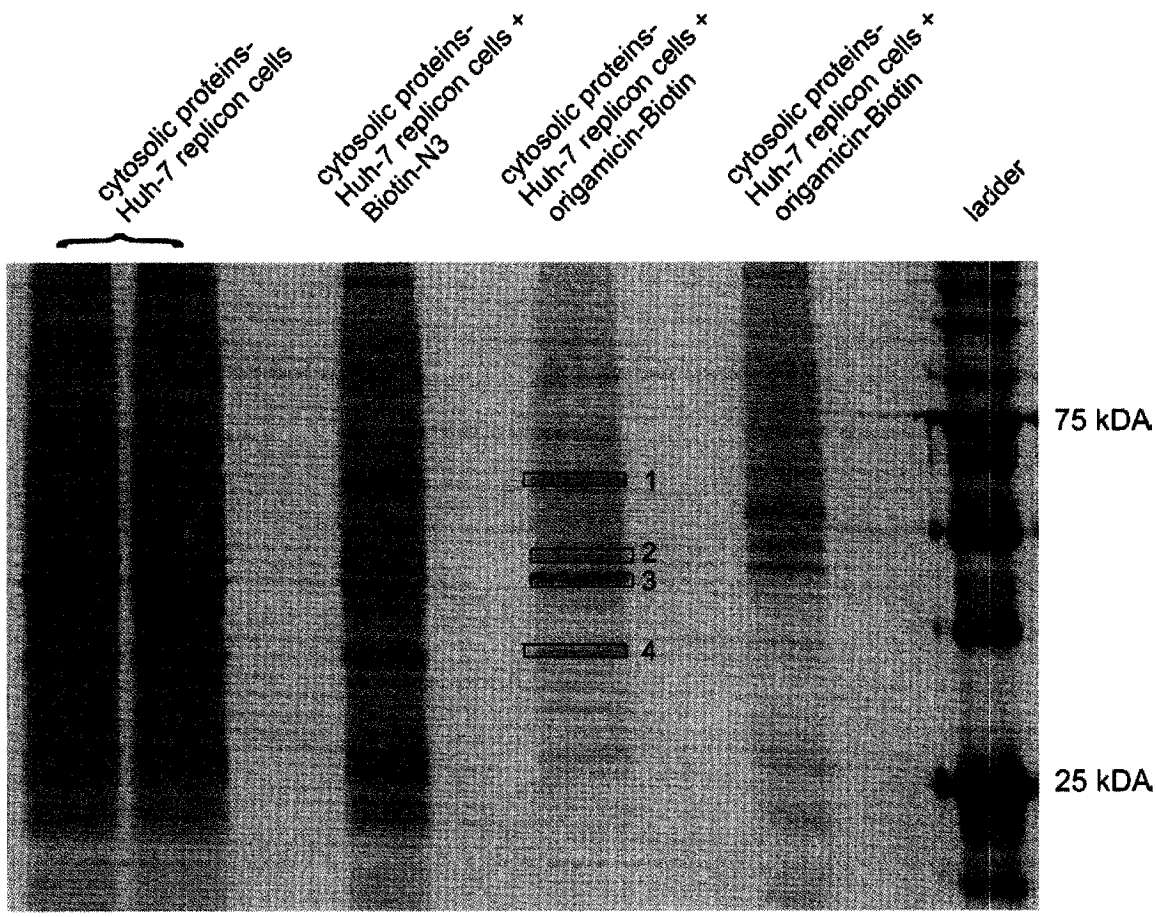

Figure 4.1: In-vitro labeling of cytosolic proteins with origamicin-biotin probe-silver stained gel. Lanes from left to right: cytosolic proteins isolated from Huh-7 replicon cells (lane 1, 2); cytosolic proteins isolated from Huh-7 replicon cells and incubated with biotin azide followed by avidin purification (lane 4); cytosolic proteins isolated from Huh-7 replicon cells and incubated with origamicin-biotin 'click' probe followed by avidin purification (lane 4, 5). Highlighted bands (1, 2, 3, 4) were isolated and analyzed by mass spectrometry.

Appendix 1. Interestingly, the four proteins were all host proteins important to protein folding and trafficking, specifically heat shock proteins, and protein disulfide isomerase. We postulated that origamicin reacted with these targets as an electrophile. The electrophilic sites can be blocked with a nucleophile, which can potentially reduce the activity of origamicin. To test our hypothesis, we pre-incubated origamicin with cystene for 2h, and looked if the activity of origamicin had changed. Firefly luciferase assays involving the HCV replicon indicated that pre-incubation of origamicin at 30 μM with cysteine significantly reduced origamicin activity, whereas incubation of origamicin at 50 μM with cysteine only partially affected the activity of origamicin. Since 6 mol equivalents of cysteine were incubated with origamicin, this can be attributed to reversible interconversion between cysteine and origamicin (Figure 4.2). Statistical analysis showed that incubation with cysteine significantly reduced the activity and toxicity of origamicin ($P < 0.05$), however, some activity was retained and cell viability did not completely recover in the presence of cysteine. This indicated that cysteine alone was insufficient to irreversibly block origamicin's inhibitory activity. This is not the first example where small molecule inhibitors are modified prior to their interaction with their target protein. For example, lactacystin is known to undergo reversible interconversion between a lactone and thioacyl intermediates [25-27].

In order to more specifically characterize the protein targets of the ABA analog origamicin, *in situ* inhibitor-based protein profiling experiments were conducted (Scheme 4.4). HCV replicon bearing cells were treated for 24h with origamicin (30 μM), and origamicin pre-incubated with cysteine (30 μM). The cytosolic proteins were then extracted and copper-catalyzed 'click reactions' were conducted for 1h to conjugate rhodamine to the

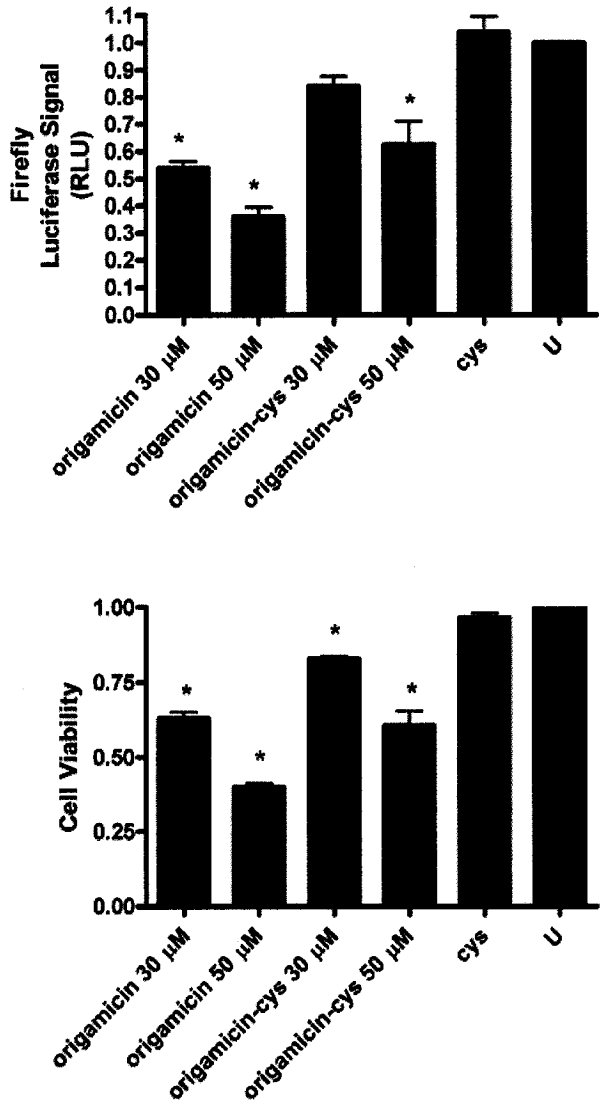

Figure 4.2: Normalized firefly luciferase and cell viability data of Huh-7 replicon cells treated with origamicin compound in the presence of cysteine. The data shows that 24h cell treatment with origamicin compounds preincubated with cysteine significantly reduced the activity of origamicin at 30 µM but not at 50 µM. Preincubation with cysteine did not fully restore the cell viability. Statistical analyses were carried out using GraphPad Prism software (version 4.01, GraphPad Software, San Diego, CA, USA). Mean quantitative values were compared to untreated using the Dunnett's Multiple Comparison Test. All P values less than 0.05 were accepted as statistically significant (*).

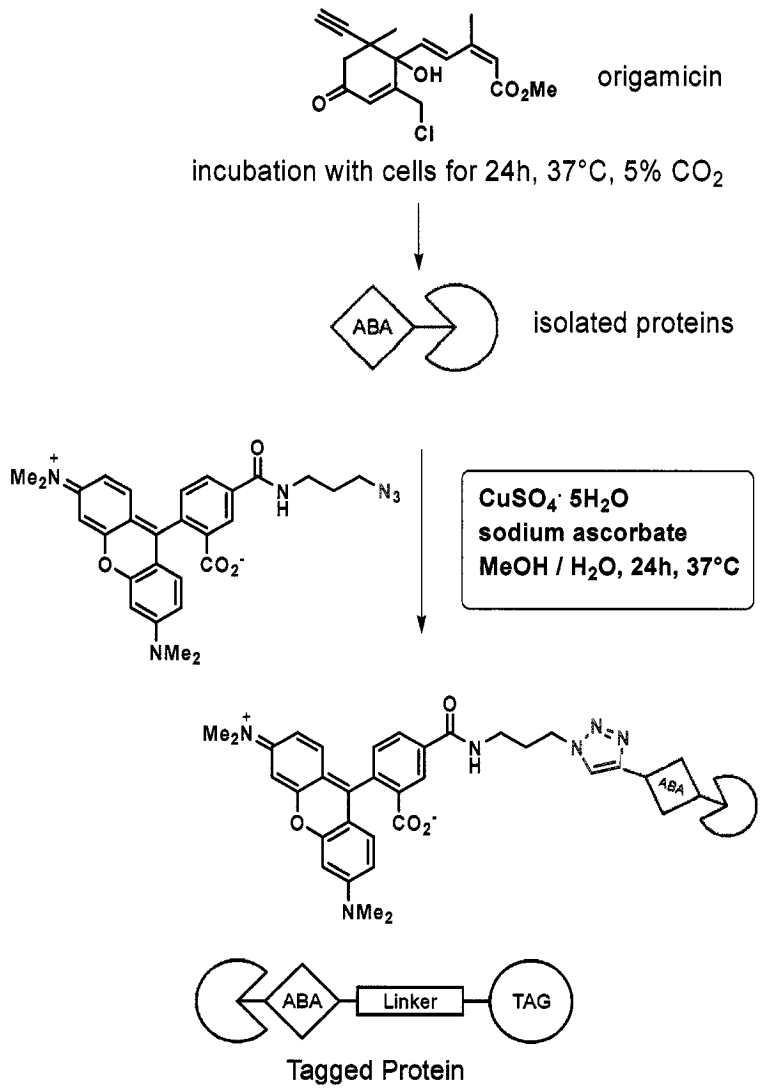

Scheme 4.4: In-situ inhibitor based proteomics approach with origamicin and rhodamine azide. Huh-7 cells were incubated with origamicin for 24h at 37°C. Proteins were then isolated from the treated cells and incubated with rhodamine azide for 1h at 25°C. Labeled proteins were visualized by fluorescence.

proteins that were bound to the origamicin. In-gel fluorescence showed that origamicin again interacted strongly with the same four specific proteins (Figure 4.3). Control experiment showed that Rhodamine azide did not label any proteins, as we expected. The fluorescent gel showed that pre-incubation of origamicin with cysteine did not cause much difference in protein labeling, which once again suggested that cysteine reversibly reactes with origamicin. We repeated *in situ* experiments with Huh-7 cells that do not contain any HCV replicon, and in-gel fluorescence showed a similar labeling pattern. This suggested that origamicin affects non-HCV proteins. These protein targets were still unidentified.

In order to confirm the specificity and to determine other possible protein targets for origamicin, we performed 2-dimensional gel electrophoresis experiments (Figure 4.4). In the 2D, fluorescently labeled gel, we observed 8 strongly fluorescently label proteins and 16 weakly labeled proteins. Proteins that were identified by nanoLC-MS/MS either had a cysteine-containing active site (e.g. Protein disulfide isomerase (PDI) family, and to a lesser extent, peroxiredoxin 1), or were known phosphoproteins (e.g. heat shock protein beta-1, cofilin-1, and nucleophosmin). The strongest fluorescence, and thus the highest selectivity in labeling was observed with spots containing proteins of the PDI family (PDIA1, PDIA3, PDIA4 and PDIA6), which all have two cysteine-containing active sites. The targeting of PDI proteins by origamicin is consistent with the reactivity of other simpler halogenated organic molecules that demonstrate a lower degree of target specificity and a much higher degree of cytotoxicity [28-30]. The full list of protein identities is provided in Table 4.1. One of the cysteine-containing active site proteins that was identified was retinal dehydrogenase 1. This is consistent with our original hypothesis that the ABA analogs may show cross-reactivity with retinoic acid-binding proteins.

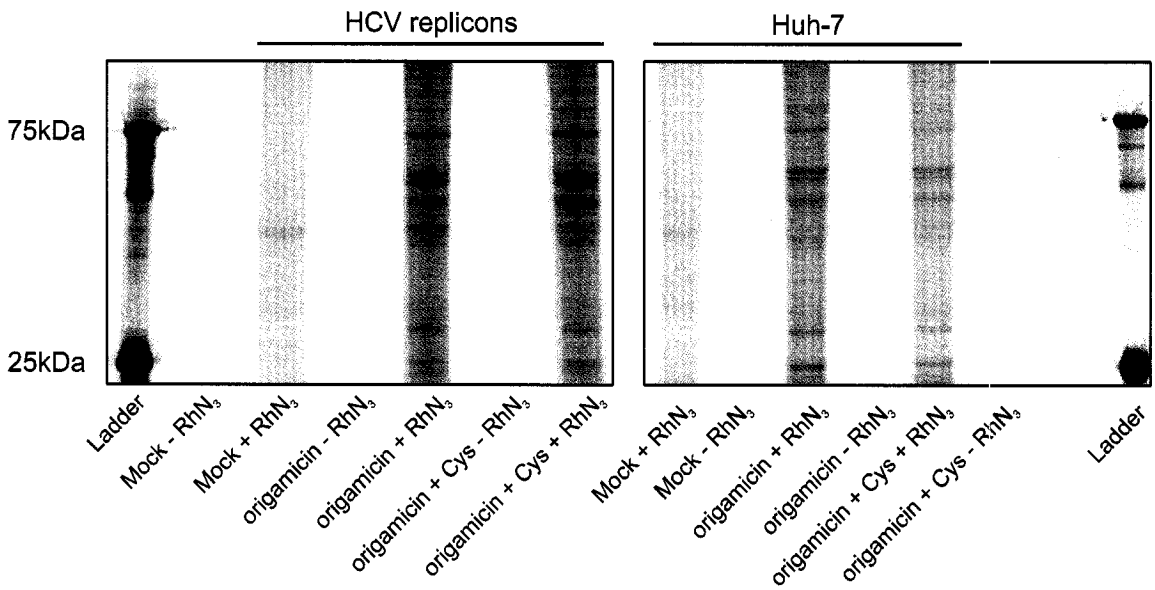

Figure 4.3: In-gel fluorescence images of 1D-page gel containing Huh-7 and Huh-7 replicons cytosolic proteins reacted with Rhodamine azide. Huh-7 replicon bearing cells and Huh-7 cells were treated with origamicin at 30 μM, and origimicin pre-incubated with cystein at 30 μM for 24h. Cytosolic proteins were then isolated and 'click' reaction with rhodamine azide (RhN_3) was conducted. Mock refers to cytosolic proteins isolated from non-treated cells. Fluorescence images show no bands in the absence of RhN_3 (control bands). Only one band was observed in the click reaction between Mock cytosolic proteins and RhN_3. Cytosolic proteins isolated form cells treated with origamicin or origamicin-cysteine for 24h showed several fluorescent bands. This indicates that the small molecule covalently reacted with several proteins and that the 'click' reaction between the alkyne functionality in origamicin and RhN_3 was successful for visualization. Labeling pattern is similar between proteins from Huh-7 cells and from replicon cells and does not differ from the origamicin-cystein treatments.

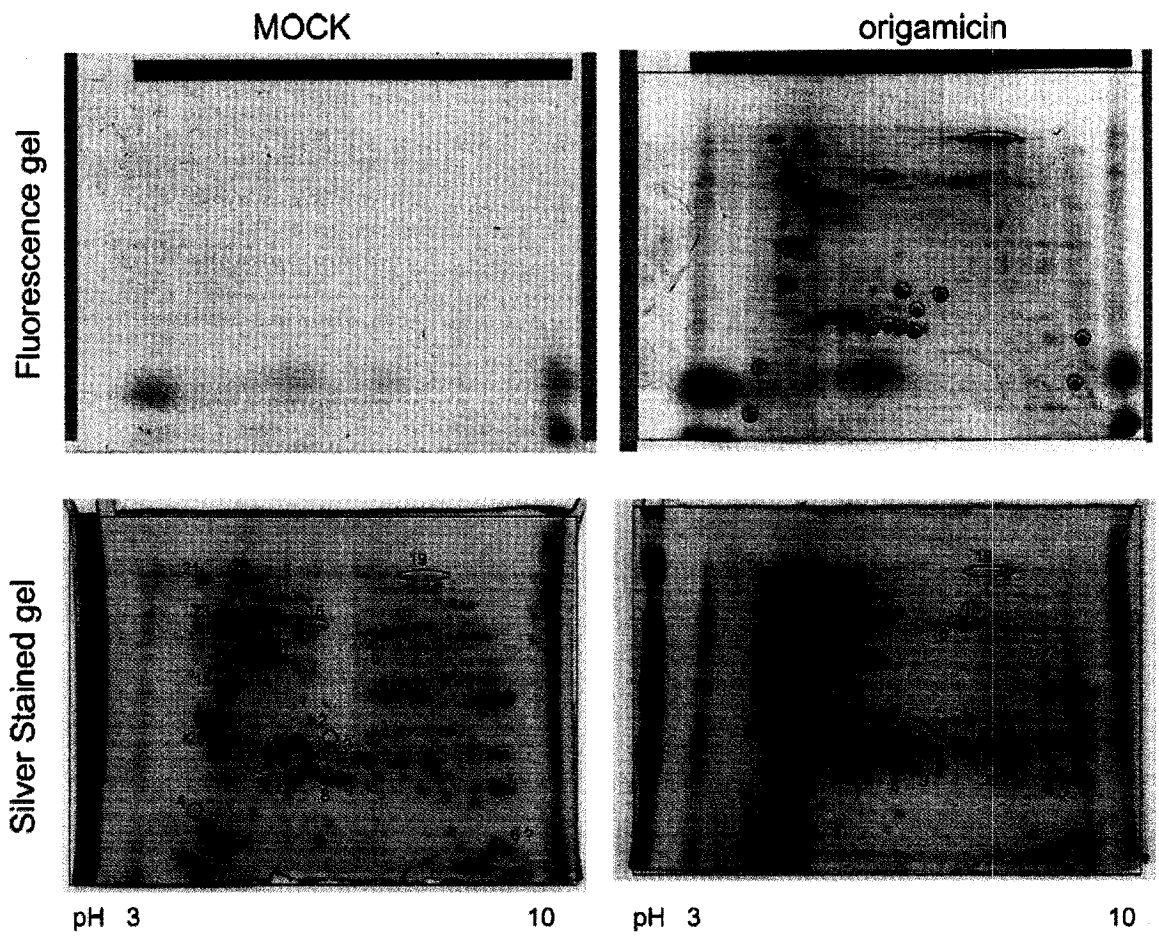

Figure 4.4: Fluorescent and silver stained 2D-gel images of untreated control (Mock) and treated (origamicin) Huh-7 replicon cytosolic proteins. Silver staining shows all proteins while fluorescence images only show proteins that reacted with RhN_3 in the 'click' reaction. Huh-7 replicon cells were treated for 24h with origamicin, 30 μM followed by protein extraction and 'click' reaction of the isolated cytosolic proteins with RhN_3. The Mock gel was done with proteins extracted from untreated cells that were submitted to the same 'click' reaction conditions. The gel was run from pH 3-10. Circled spots were cut and proteins were identification by LC-MS/MS. The number beside the circles corresponds to the isolated proteins in Table 4.1.

Spot #	Identified Protein	Accession no. [a]	Theoretical MW/pI [b]	Score/ coverage % [c]	Properties [d]
1	(P78417) Glutathione transferase omega 1	GSTO1_HUMAN	27548/6.23	237/19	Cys-ACS
2	(P78417) Glutathione transferase omega 1	GSTO1_HUMAN	27548/6.23	180/17	Cys-ACS
3	(P04792) Heat-shock protein beta-1	HSPB1_HUMAN	22768/5.98	165/19	Phospho
4	(Q15185) Telomerase-binding protein p23	TEBP_HUMAN	18685/4.35	290/39	Phospho
5	(P05386) 60S acidic ribosomal protein P1	RLA1_HUMAN	11507/4.26	54/14	Phospho
6	(P23528) Cofilin-1	COF1_HUMAN	18360/8.26	473/53	Phospho
7	Q06830) Peroxiredoxin 1	PRDX1_HUMAN	22096/8.27	395/41	Cys-ACS + Phospho
8	(Q99497) Protein DJ-1	PARK7_HUMAN	19878/6.33	204/31	Phospho
	(P30048) Thioredoxin-dependent peroxide reductase, mitochondrial	PRDX3_HUMAN	27675/7.67	138/13	Cys-ACS
9	(P30048) Thioredoxin-dependent peroxide reductase, mitochondrial	PRDX3_HUMAN	27675/7.67	222/25	Cys-ACS
10	(P30048) Thioredoxin-dependent peroxide reductase, mitochondrial	PRDX3_HUMAN	27675/7.67	194/21	Cys-ACS
11	(P09211) Glutathione S-transferase P	GSTP1_HUMAN	23210/5.44	506/49	
	(P30048) Thioredoxin-dependent peroxide reductase, mitochondrial	PRDX3_HUMAN	27675/7.67	157/18	Cys-ACS
12	(P09936) Ubiquitin carboxyl-terminal hydrolase isozyme L1	UCHL1_HUMAN	24808/5.33	117/8	Cys-ACS
13	(P06748) Nucleophosmin	NPM_HUMAN	32555/4.64	440/39	Phospho
14	(P09936) Ubiquitin carboxyl-terminal hydrolase isozyme L1	UCHL1_HUMAN	24808/5.33	193/32	Cys-ACS
15 [e]	(P30101) Protein disulfide-isomerase A3	PDIA3_HUMAN	56747/5.98	592/36	Cys-ACS
16	(P00352) Retinal dehydrogenase 1	AL1A1_HUMAN	54696/6.29	490/19	Cys-ACS
17 [e]	(Q15084) Protein disulfide-isomerase A6	PDIA6_HUMAN	48091/4.95	333/18	Cys-ACS
	(Q8NBS9) Thioredoxin domain-containing protein 5	TXND5_HUMAN	47599/5.63	212/14	
18	(P00352) Retinal dehydrogenase 1	AL1A1_HUMAN	54696/6.29	817/36	Cys-ACS
19	(P13639) Elongation factor 2	EF2_HUMAN	95146/6.42	569/16	Phospho
20	(P08238) Heat shock protein HSP 90-beta	HS90B_HUMAN	83081/4.97	836/26	Phospho
21	(P14314) Glucosidase II beta subunit precursor	GLU2B_HUMAN	59259/4.34	494/22	Phospho
	(Q16643) Drebrin	DREB_HUMAN	71250/4.41	163/14	Phospho
22 [e]	(P11021) 78 kDa glucose-regulated protein precursor	GRP78_HUMAN	72288/5.07	1253/43	
	(P13667) Protein disulfide-isomerase A4	PDIA4_HUMAN	72887/4.96	260/13	Cys-ACS
23 [e]	P07237) Protein disulfide-isomerase	PDIA1_HUMAN	57081/4.76	1118/51	Cys-ACS
24	(P06576) ATP synthase beta chain, mitochondrial	ATPB_HUMAN	56525/5.26	1265/63	
	(Q15084) Protein disulfide-isomerase A6	PDIA6_HUMAN	48091/4.95	211/12	Cys-ACS
25 [e]	(P62258) 14-3-3 protein epsilon	1433E_HUMAN	29155/4.63	498/43	
	(P24534) Elongation factor 1-beta	EF1B_HUMAN	24617/4.5	496/49	Phospho

[a] Accession number according to Swissprot.
[b] Theoretical mass (Da) and pI calculated from translated gene sequence.
[c] Mascot score, sequence coverage (%).
[d] Cys-ACS indicates that the protein has one or more cysteine containing active site. Phospho indicate that the protein is a known phosphoprotein.
[e] spots 15,17,22,23,24 showed significant and maximal fluorescence labeling by origamicin and represent the primary targets.

Table 4.1: List of proteins present in the fluorescent spots excised from the origamicin-labeled cytosolic protein 2D-gel.

Since origamicin was found to interact strongly with the protein disulfide isomerase family, we examined its interaction with yeast PDI *in vitro*. We incubated PDI yeast protein for 1h with different concentrations of the origamicin-Rh probe and visualized labeling of PDI by fluorescence gels. Although we have not determined the binding constant of origamicin-Rh to PDI, fluorescent gel showed that their interaction is depended on the origamicin-Rh concentration. We saw almost no binding at 2 μM origamicin-Rh and very strong binding at 500 μM (Figure 4.5).

We also examined whether origamicin showed subcellular localization in the endoplasmic reticulum (ER) where protein synthesis and folding occurs. We performed fluorescence microscopy on HCV replicon cells treated with origamicin-Rh and counterstained with antibodies against PDI. Figure 4.6 shows that Origamicin-Rh does localize in the ER and colocalizes with PDI. It is known that a number of HCV proteins also colocalize with PDI in the ER. Therefore small molecule perturbations of PDI and the resultant induction of ER stress [31-35] could affect both the proper maturation of HCV proteins and disrupt the environment of HCV replication complexes. The disruption of the human immunodeficiency virus (HIV) life cycle by blocking PDI function has been demonstrated using the antimicrobial peptide bacitracin and anti-PDI antibodies [34]. In HIV, protein-disulfide isomerase function is required to reduce two disulfide bonds of the HIV envelope glycoprotein 120 to allow entry [31].

Small molecules that target the ER have great potential as tools for cell biology because numerous fundamental processes occur on the ER membrane. This is particularly true for HCV as well as many other RNA viruses that replicate on the ER and those that require the cell protein folding machinery for proper assembly of virion particles. The

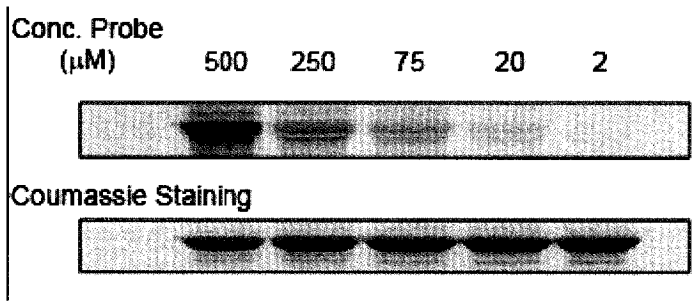

Figure 4.5: In-gel fluorescence image and a Coumassie staining image of page gel containing yeast PDI protein treated with origamicin-Rh 'click' probe at various concentrations. Coumassie staining shows equal loading of PDI proteins for all conditions. The fluorescence image shows that reaction of probe with PDI protein is concentration dependent and increases from 2 μM to 500 μM.

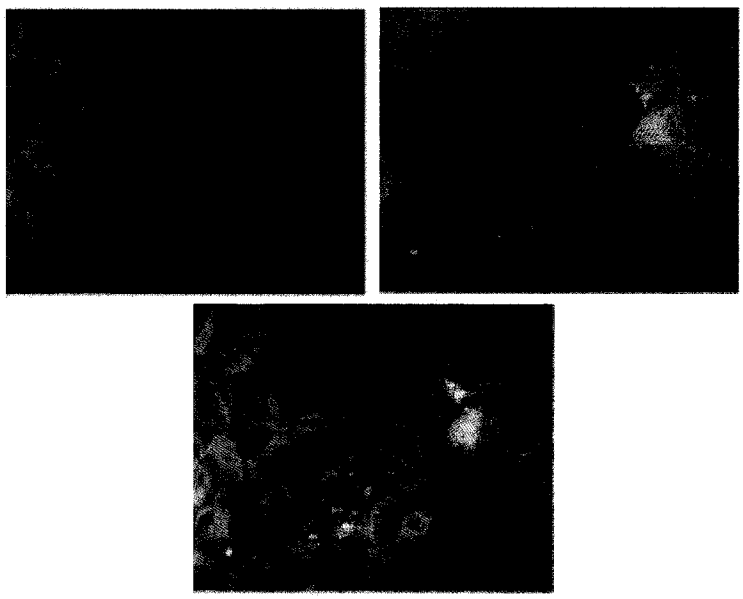

Figure 4.6: Fluorescence microscopy images of Huh-7 replicon bearing cells treated with origamicin-Rh 'click' probe. Images show cells stained with origamicin-Rh (red, upper right) and counterstained with antibodies against PDI (green, upper left). Nuclei (blue) are stained with 4',6-diamino-2-phenylindole (DAPI). The overlay in the lower panel shows that nearly all origamicin-Rh is localized in the ER and colocalized with PDI.

subcellular localization of origamicin is most likely linked to the high degree of specificity that it displays towards isoforms of PDI that reside in the ER. This feature helps establish it as a tool for understanding PDI function.

Origamicin's main protein targets in Huh-7 cells are the isoforms of protein disulfide isomerase. Dysfunction of the protein family can lead to ER stress due to the misfolding of both host and virus proteins that lead to unfolded protein response. Our hypothesis is that HCV replicon RNA can be translated by ribosomes, and post-translationally processed into immature proteins, but that origamicin prevents the proper folding of the precursor proteins, thus preventing the formation of mature viral proteins. Our proposed model for the mechanism by which origamicin inhibits HCV replication is presented in Scheme 4.5. It is known that HCV gene expression occurs on the ER and itself induces ER stress. It has also been demonstrated in replicon systems that HCV blocks the normal unfolded protein response, and also suppresses the subsequent protein degradation by the IRE1-XBP1 pathway [9]. The cellular protein folding machinery is essential for maturation of the HCV proteome. There are a number of disulfide bonds that are critical to HCV proteins, including the envelope proteins E1 and E2, as well as the NS5A protein [36]. The HCV NS3 serine protease and NS4A cofactor both colocalize with PDI, suggesting that their assembly and function are linked to these ER proteins. It is possible that a specific isoform of PDI is responsible and this is the subject of the further study.

In conclusion, we have used chemical genetics approaches to discover a new cell permeable small molecule modulator of protein folding that also acts as an inhibitor of HCV replication by blocking a critical host cell pathway that is essential to the viral lifecycle. The protein targets of origamicin were determined using inhibitor-based protein profiling

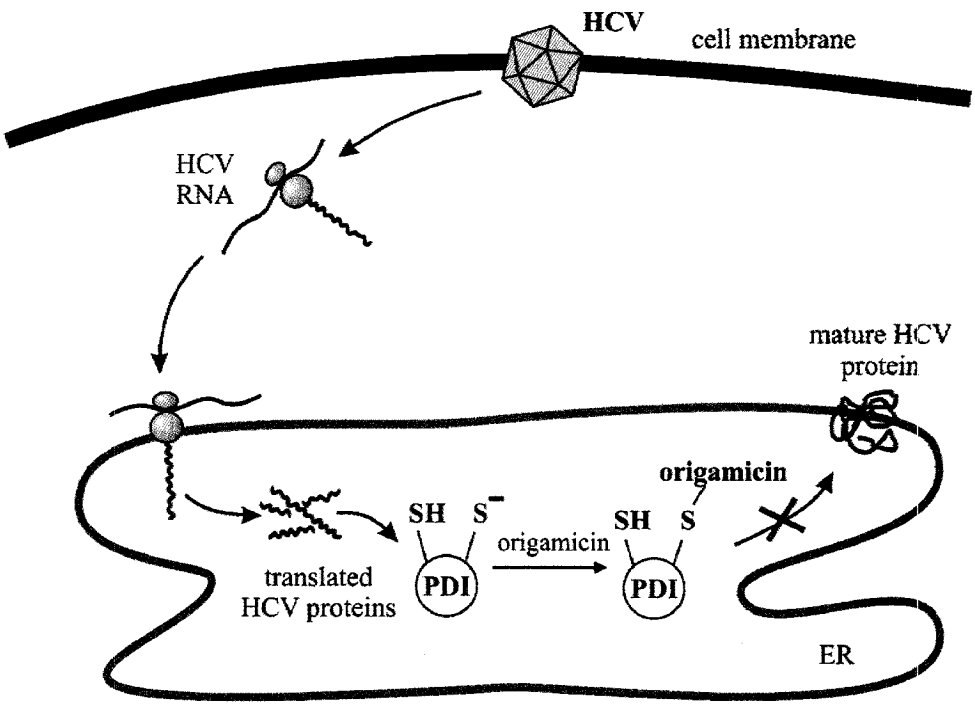

Scheme 4.5: A proposed mechanism by which origamicin inhibits HCV replication in Huh-7 replicon bearing cells. We propose that origamicin binds to PDI and thus prevents the proper folding of HCV translated proteins into mature HCV proteins.

techniques that utilized *in vivo* reactions of origamicin with the HCV replicon cells, followed by 'click reaction' of the extracted proteins with either rhodamine or biotin labels. The major target for origamicin was found to be protein disulfide isomerase, a major component of the ER. Here, we establish a new way of targeting these specific ER proteins. We demonstrate that transient blocking of this host protein can block HCV replication in HCV replicons without permanently influencing cell viability and establish a novel strategy for anti-HCV compound development. Since origamicin is a close structural analog of a naturally occurring plant metabolite, originally developed as a plant growth regulator, its potency and specificity towards human proteins is surprising. These results demonstrate the opportunities for utilizing molecular scaffolds for multiple unrelated targets.

Although we have strong evidence that PDI targeting by origamicin causes HCV inhibition, further confirmation of the proposed mechanism is desired. Future investigations will have to identify the amino acid residues that react with origamicin by mass spectrometry. Furthermore, we will need to confirm the specificity of origamicin towards PDI by lowering the compound concentration and using small interfering RNA against the PDI genes.

Materials and Methods

Activity-based protein profiling:

The proteins of HCV replicon bearing Huh-7 cells as well as the parental cell line were probed under a variety of conditions. To confirm the product of 'click' reactions, we conducted a reaction with a model alkyl azide and fully characterized this adduct.

Preparation of cell line soluble proteins:

The Huh-7 cell line and the Huh-7 cell line stably expressing HCV replicon were grown in 10 cm dishes ($1.5x10^6$cells/dish) in Dulbecco's modified minimal essential medium (DMEM) (Invitrogen) supplemented with 100 nM non-essential amino acids, 50 U/ml penicillin, 50 mg/ml streptomycin, and 10% fetal bovine serum (FBS) (Cansera). At the 80% confluency, cells were treated with 30 μM origamicin for 24h at 37°C. Cells were then washed with cold PBS and harvested in 10 mM sodium/potassium phosphate buffer (PB) pH 8 for Rhodamine experiments, or 50 mM Tris-HCl buffer pH 7.5 for biotin experiments. Cells were then sonicated, homogenized and ultracetrifuged at 100,000g for 45 min at 4°C to isolate the supernatant fraction (cytosolic proteins). For collecting the membrane proteins the pellet was rinsed with H_2O, resuspended in 0.3 ml of cold buffer + 1% Triton X-100, and homogenized for 25-30s. Proteins were then rotated on a shaker at 4°C for 1h followed by centrifuging at 100,000g for 45 min at 4°C. Cytosolic and membrane proteins were quantified using a Bio-Rad DC protein assay. Mock controls were prepared the same way, however cells were not treated with the small molecule.

***In Vitro* experiment with origamicin-Rh probe:**

20 μg of cytosolic proteome was incubated with origamicin-Rh (final concentration 200 μM) for 1h at 25°C. Samples which included unlabeled proteome as a negative control, and labeled proteome, were denaturated at 95°C for 10 min. Equal amounts of 2XSDS loading buffer were added to each sample. Proteins were separated by 1D-SDS-PAGE (10% resolving, 4% stacking) and visualized using an in-gel fluorescence scanner (Typhoon Trio Scanner, 532nm laser, Cy3 filter, PMT = 450V).

***In Vitro* labeling of cytosolic proteins with origamicin-biotin probe:**

Cytosolic protein extract, 759 μg, was reacted with the origamicin-Biotin probe (200 μM final concentration) for 2h at 25°C. The combined proteins and probe were then mixed with 100 μl streptavidin-agarose gel (Amersham Biosciences) and shaken on a rotator for 2h at 25°C. The sample was then centrifuged at 750g for 3 min, and the supernatant removed. Agarose gel was washed three times with 50 mM Tris hydrochloride buffer (pH 8) supplemented with 100 mM guanidine-HCl, and then washed twice with 50 mM Tris-HCl [37]. The pellet was resuspended in 50 μl of 2XSDS loading buffer, heated for 5 min at 95°C, cooled at RT, and loaded onto gel. Proteins were separated by 1D-SDS-PAGE (10% resolving, 4% stacking) for 1.5h at 100V. The gel was stained with silver nitrate and bands were cut and submitted for mass spectrometry analysis.

***In Vivo* labeling of Huh-7 cells with origamicin followed by cycloaddition click reaction of labeled proteins with rhodamine azide. In-Gel fluorescence scanning:**

Cells were treated with origamicin (30 μM) and 24h later, the labeled cytosolic proteins were isolated using above mentioned method. Into 100 μg of cytosolic proteins was added rhodamine azide (Rh-N_3), final concentration 200 μM (50 mM stock in methanol), followed by addition of 2 mM sodium ascorbate (32 mM stock in water), 2 mM copper (II) sulfate (32 mM stock in water), and 205 μM TBTA ligand (50 mM stock of t-butanol:water, 4:1), to a final volume of 80 μl. The reaction mixture was incubated for 1h at 25°C. The same protocol was repeated with cytosolic proteins isolated from cells that were not treated with origamicin as a negative control. After the reaction was finished, samples were centrifuged (5900g, 4 min, 4°C) to pellet the proteins, and excess of cycloaddition reagents were

removed followed by addition of 50 µl of cold methanol. Protein pellets were resuspended and centrifuged (5900g, 4 min, 4°C) and supernatant removed. The samples were finally resuspended in 20 µl of phosphate buffer pH 8 and denatured for 10 min at 95°C followed by addition of equal amounts of 2XSDS loading buffer to each sample. Proteins were separated by 1D-SDS-PAGE (10% resolving, 4% stacking) and visualized in-gel using a fluorescence scanner (Typhoon Trio Scanner, 532 nm laser, Cy3 filter, PMT = 450V). Bands were Comassie stained and cut for mass spectrometry analysis.

2D gel proteomics experiments:

Cytosolic proteins were isolated from cells treated with origamicin as well as from non treated cells after 24h treatment. Proteins were stored in phosphate buffer pH 8. For the 2D gel experiment, samples were subjected to cycloaddition click reaction with RhN_3 (100 µg of protein) for 1h at 25°C. After the reaction was finished, proteins were pelleted and supernatant removed followed by washing to remove extra RhN_3. Precipitated protein pellets from Mock and origamicin samples were each resuspended in 125 µl of IEF buffer (7M Urea, 2M thiourea, 4%CHAPS, 1%DTT) and Ampholytes pH 3-10 (biolytes, Bio-Rad) were added to a final concentration of 0.2%. IPG Strips pH 3-10NL, 7 cm (Bio-Rad) were rehydrated with samples passively for 16h. The strips were then submitted to Isoelectric focusing (IEF) in the Protean IEF Cell (Bio-Rad) using the following program: 200V rapid ramp for 30min, 500V rapid ramp for 30min, 2h linear ramp to 6500V, 2h focusing (rapid ramp) at 6500V. Final VH was 17 500. Prior to SDS-PAGE separation, proteins immobilized on the IPG strips were reduced (1% DTT) and alkylated (4% iodoacetamide) in SDS equilibration buffer (6 M urea, 30% glycerol, 2% SDS, 50 mM tris-HCl, pH 8.8). The

SDS-PAGE separation was performed on a 10% gel (1 mm thick) at constant 150 volts per gel. The gels were first left between the glass plates to be scanned for fluorescence with the Typhoon (GE Healthcare) then they were placed in fixing solution (50% ethanol-5% acetic acid) overnight. The gels were stained with silver nitrate and scanned using the Fluor-S imager (Biorad) to visualize all the protein spots.

Protein identification of spots excised from 2D-gel:

The fluorescent gel image was aligned with the silver stain gel image to locate the labeled protein spots. Selected spots were excised manually under a laminar flow hood. Gels spots were destained with potassium ferricyanide solution (15 mM potassium ferricyanide-50 mM sodium thiosulfate) then rinsed three times with water and shrunk with acetonitrile. The gel pieces were reswelled with 20 µl of trypsin solution (0.01 µg/µl in 50 mM ammonium bicarbonate), and incubated overnight at 37°C. The in-gel digests were analyzed by nanoLC-MS/MS using a "CapLC" capillary liquid chromatography system (Waters) coupled to a "Q-TOF Ultima" hybrid quadrupole time-of-flight mass spectrometer (Waters). MS/MS spectra were acquired on doubly, triply and quadruply charged-ions. Proteins were identified by matching the sequences derived from peptide MS/MS spectra with the NCBI and the Swissprot protein sequence database using Mascot™ database searching software (Matrix Science) to extract and tabulate the significant sequence matches from multiple Mascot result files.

***In Vitro* labeling of PDI protein with different concentrations of origamicin-rhodamine.**

In-Gel fluorescence scanning:

Protein disulfide isomerase (PDI) from bovine liver (Sigma) was reconstituted in water (1mg/ml). 20 μg of PDI was incubated with the following concentrations of origamicin-Rh (500 μM, 250 μM, 75 μM, 20 μM, and 2 μM final concentrations). After stirring for 1h at 25°C equal amount of 2XSDS loading buffer were added to each sample. Proteins were separated by 1D-SDS-PAGE (10% resolving, 4% stacking) for 1h at 100 V and visualized in-gel using a fluorescence scanner (Typhoon Trio Scanner, 532 nm laser, Cy3 filter, PMT = 530 V). Gels were then Comassie stained.

Fluorescent imaging of endoplasmic reticulum of Huh-7 cells stably expressing HCV: Huh-7 cells were grown in a 96 well plate ($1x10^4$ cells/well). At 70-80% confluency the cells were treated with 30 μM origamicin-Rh for 30 min. Cells were fixed and stained according to the Molecular Probes protocol: Select FXTM Alexa Fluor 488 Endoplasmic Reticulum Labeling Kit (S34200). Briefly, cells were washed with warm 1X PBS and fixed with 1X fixative solution at 37°C for 15 min. Cells were then permeabilized for 5 min. For ER staining, cells were blocked with the blocking solution and stained with anti-PDI primary antibody (1:1000 dilution) for 2h at 25°C. Cells were then treated with secondary antibody Alexa Fluor 488® at 25°C for 30 min. After washing with 1X PBS, the cells were kept in 50% glycerol and visualized using an Axiovert 200M inverted microscope from Zeiss (North York, ON) with Axiovision 3.1 software. The cells were photographed with an AxioCam connected to the inverted microscope.

Click chemistry Synthesis:

Rhodamine azide was synthesized according to the previously reported procedure by Speers et al [38]. ES-MS: (*m/z*) 513.3 (MH^+).

TBTA ligand for the cycloaddition reaction was prepared according to the procedure of Chan *et al* [39]. ES-MS (*m/z*) 531 (MH^+), Mp: 137°C.

Cycloaddition click reaction between origamicin and rhodamine azide:

Cycloaddition click reaction was performed between origamicin (3 mg, $9.3x10^{-6}$ mol), and RhN_3, (4.7 mg, $9.3x10^{-6}$ mol, 50 mmol stock solution). Into the reaction mixture were added sodium ascorbate (5 mol%, 50 mmol stock solution in water), $CuSO_4$ (5 mol%, 50 mmol stock solution in water), and TBTA ligand (10 mol%, 50 mmol stock solution in ^{t}BuOH/water). The final volume included 300 µl of methanol and 100 µl of water. The reaction mixture was stirred at 37°C for 24h and then purified by reverse HPLC column (NovaPak HR-C18, Waters, Milford Massachusetts USA, 3.9x300 mm, 6 µm) using 20-95% MeCN/water/0.1%TFA gradient in 20 min at 1 ml/min. The retention time of the purified origamicin-Rh isomers under these conditions were 18.1 min and 19.1 min, Ex = 543 nm, Em = 573 nm. HPLC purification afforded origamicin-Rh 'click' compound as a pink oil (3 mg, 39%). ES-MS: (m/z) 835.5 (MH+).

Biotin azide:

Azido PEG amine (60mg, $1.99x10^{-4}$ mol), (purchased from Polypure) was dissolved in 5 ml of dry DMF and then the flask was cooled at 0°C. Biotin succinimide (68 mg, $1.93x10^{-4}$ mol), (purched from Nova Biochem) was added to the reaction. After 2h, the solvent was removed under reduced pressure and the crude compound was purified by column chromatography (10% methanol/dichloromethane) affording biotin azide (69 mg, 60% as a colorless oil. ES-MS: (m/z) 577.3 (MH+).

Cycloaddition click reaction between origamicin and biotin azide:

Biotin azide (4.5mg, $7.8x10^{-6}$ mol, 0.5 M stock in methanol) was added into a solution of origamicin in methanol (2.5 mg, $7.8x10^{-6}$ mol, 0.13 M), followed by addition of sodium ascorbate (30 mol%, 0.4 M stock solution in water) and CuSO4 (20 mol%, 0.25 M stock solution in water). Reaction mixture was stirred at 37°C for 20h followed by purification on reverse HPLC column: (NovaPak HR-C18, Waters, 3.9x300 mm, 6 μm) using gradient 35-45% MeCN/water/0.1%TFA in 20 min then 95% MeCN/water/0.1%TFA in 3 min. The retention time under these conditions was 8.7 min affording origamicin-biotin (2 mg, 30%) as colorless oil. ES-MS: (m/z) 899.4 (MH+).

Cycloaddition click reaction between origamicin and octyl azide:

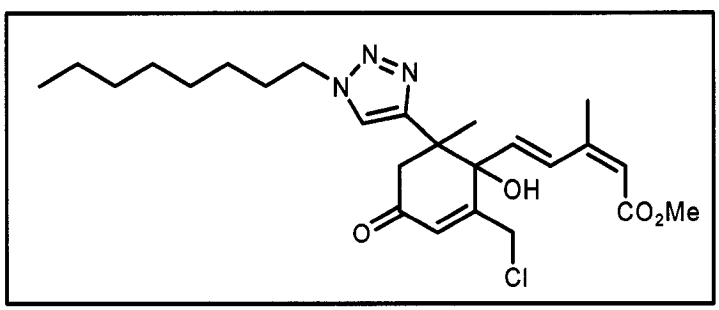

Octyl azide was synthesized following the previously reported procedure [40]. ES-MS: (*m/z*) 157.1 (MH^+). Into 50 μl of *t*-BuOH and 30 μl of water, origamicin (5 mg, $1.5x10^{-5}$ mol) was added followed by addition of octyl azide (2.4 mg, $1.5x10^{-5}$mol). Into the reaction mixture was then added sodium ascorbate (10 mol%, 1 M stock solution in water), and $CuSO_4$ (1 mol%, 0.3 M stock solution in water). The reaction mixture was stirred at 37°C for 20h followed by reverse HPLC column purification (NovaPak HR-C18, 3.9x300 mm, 6 μm) using 75% MeCN/water/0.1%TFA in 10 min. The retention time under these conditions was

4.1 min affording origamicin-octyl click (4 mg, 54%) as colorless oil. ^{1}H NMR (400 MHz, $CDCl_3$), δ = 7.96 (d, J = 16.0 Hz, 1H), 7.33 (s, 1H), 6.23 (s, 1H), 6.16 (d, J = 16.0 Hz, 1H), 5.81 (s, 1H), 4.38-4.20 (m, 4H), 3.73 (s, 3H), 2.86 (dd, J = 17.5, 49.3 Hz, 2H), 2.07 (s, 3H), 1.90-1.84 (m, 2H), 1.43 (s, 3H), 1.33-1.28 (m, 10H), 0.90 (q, J = 6.7, 3H). ^{13}C-NMR: (100 MHz, $CDCl_3$) δ = 196.9, 166.6, 163.1, 153.4, 149.1, 134.1, 131.1, 126.7, 121.4, 119.6, 80.3, 51.7, 51.2, 48.4, 45.2, 43.3, 32.0, 30.4, 29.4, 29.2, 26.8, 24.7, 23.0, 21.6, 14.5. ES-MS: (*m/z*) 478.4(MH^+).

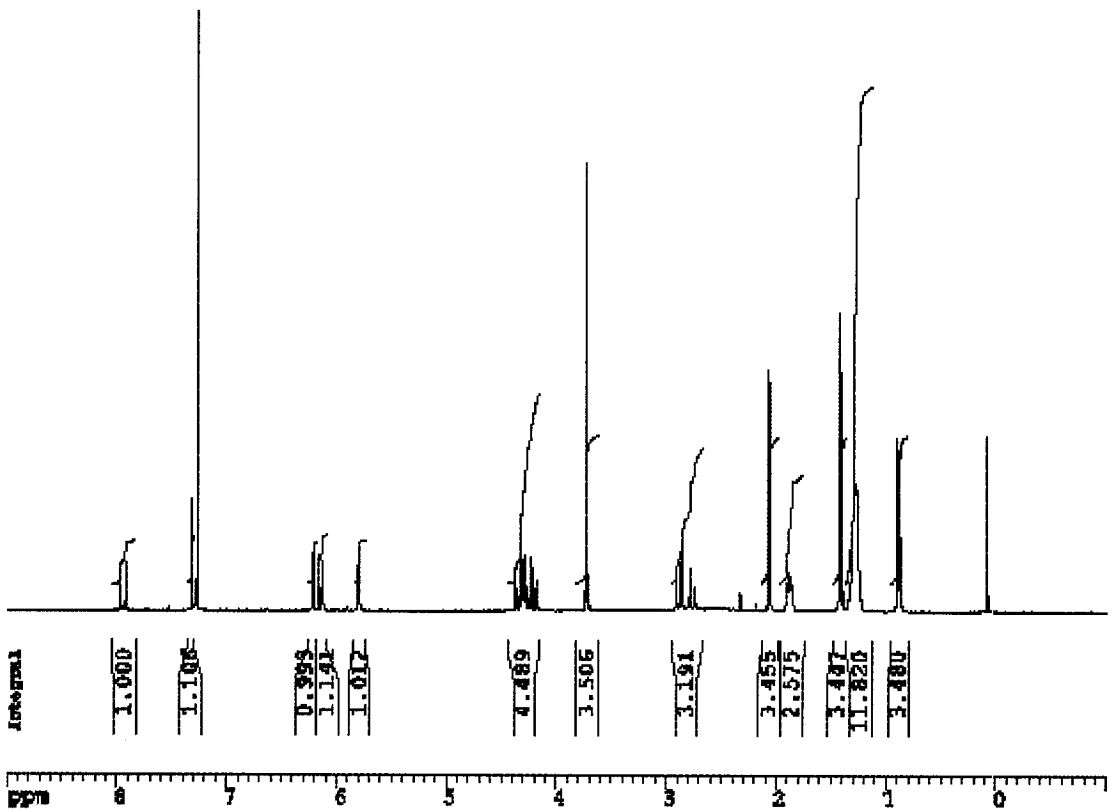

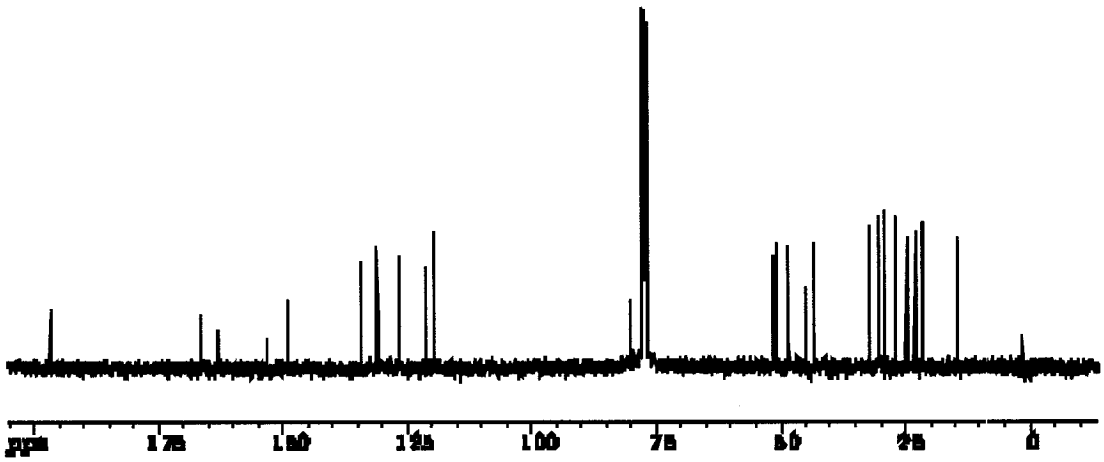

References:

[1] Burdine, L.; Kodadek, T., Target identification in chemical genetics: The (often) missing link. *Chem. Biol.* **2004**, *11*, 593-597.

[2] Sin, N.; Meng, L.; Wang, M. Q. W., et al., The anti-angiogenic agent fumagillin covalently binds and inhibits the methionine aminopeptidase, MetAP-2. *Proc. Natl. Acad. Sci. U. S. A.* **1997**, *94*, 6099-6103.

[3] Rosania, G. R.; Chang, Y. T.; Perez, O., et al., Myoseverin, a microtubule-binding molecule with novel cellular effects. *Nat. Biotechnol.* **2000**, *18*, 304-308.

[4] Tanaka, H.; Ohshima, N.; Hidaka, H., Isolation of cDNAs Encoding Cellular Drug-Binding Proteins Using a Novel Expression Cloning Procedure: Drug-Western. *Mol. Pharmacol.* **1999**, *55*, 356-363.

[5] Sche, P. P.; McKenzie, K. M.; White, J. D., et al., Display cloning: functional identification of natural product receptors using cDNA-phage display. *Chem. Biol.* **1999**, *6*, 707-716.

[6] King, R. W., Chemistry or biology: which comes first after the genome is sequenced? *Chem. Biol.* **1999**, *6*, R327-R333.

[7] Henthorn, D. C.; Jaxa-Chamiec, A. A.; Meldrum, E., A GAL4-based yeast three-hybrid system for the identification of small molecule-target protein interactions. *Biochem. Pharmacol.* **2002**, *63*, 1619-1628.

[8] Zhu, H.; Snyder, M., Protein chip technology. *Curr. Opin. Chem. Biol.* **2003**, *7*, 55-63.

[9] Zheng, X. F. S.; Chan, T. F.; Zhou, H. H., Genetic and genomic approaches to identify and study the targets of bioactive small molecules. *Chem. Biol.* **2004**, *11*, 609-618.

[10] Chen, G. Y. J.; Uttamchandani, M.; Zhu, Q., et al., Developing a strategy for activity-based detection of enzymes in a protein microarray. *Chembiochem* **2003**, *4*, 336-339.

[11] Mayer, T. U.; Kapoor, T. M.; Haggarty, S. J., et al., Small molecule inhibitor of mitotic spindle bipolarity identified in a phenotype-based screen. *Science* **1999**, *286*, 971-974.

[12] Wang, S. L.; Sim, T. B.; Chang, Y. T., Tools for target identification and validation. *Curr. Opin. Chem. Biol.* **2004**, *8*, 371-377.

[13] Huisgen, R., 1,3-Dipolar cycloaddition-introduction, survey, mechanism. **1984**, *Vol 1*, 1-176.

[14] Scriven, E. F. V.; Turnbull, K., Azides - Their Preparation and Synthetic Uses. *Chem. Rev.* **1988**, *88*, 297-368.

[15] Rostovtsev, V. V.; Green, L. G.; Fokin, V. V., et al., A stepwise Huisgen cycloaddition process: Copper(I)-catalyzed regioselective "ligation" of azides and terminal alkynes. *Angew. Chem., Int. Ed.* **2002**, *41*, 2596-+.

[16] Tornoe, C. W.; Christensen, C.; Meldal, M., Peptidotriazoles on solid phase: 1,2,3 - triazoles by regiospecific copper(I)-catalyzed 1,3-dipolar cycloadditions of terminal alkynes to azides. *J. Org. Chem.* **2002**, *67*, 3057-3064.

[17] Breinbauer, R.; Kohn, M., Azide-alkyne coupling: A powerful reaction for bioconjugate chemistry. *Chembiochem* **2003**, *4*, 1147-1149.

[18] Anderson, S. P.; Dunn, C.; Laughter, A., et al., Overlapping transcriptional programs regulated by the nuclear receptors peroxisome proliferator-activated receptor alpha, retinoid X receptor, and liver X receptor in mouse liver. *Mol. Pharmacol.* **2004**, *66*, 1440-1452.

[19] Lewis, W. G.; Green, L. G.; Grynszpan, F., et al., Click chemistry in situ: Acetylcholinesterase as a reaction vessel for the selective assembly of a femtomolar inhibitor from an array of building blocks. *Angew. Chem., Int. Ed.* **2002**, *41*, 1053-+.

[20] Wang, Q.; Chan, T. R.; Hilgraf, R., et al., Bioconjugation by copper(I)-catalyzed azide-alkyne 3+2 cycloaddition. *J. Am. Chem. Soc.* **2003**, *125*, 3192-3193.

[21] Jessani, N.; Young, J. A.; Diaz, S. L., et al., Class assignment of sequence-unrelated members of enzyme superfamilies by activity-based protein profiling. *Angew. Chem., Int. Ed.* **2005**, *44*, 2400-2403.

[22] Adam, G. C.; Sorensen, E. J.; Cravatt, B. F., Chemical strategies for functional proteomics. *Mol. Cell. Proteomics* **2002**, *1*, 781-790.

[23] Speers, A. E.; Adam, G. C.; Cravatt, B. F., Activity-based protein profiling in vivo using a copper(I)-catalyzed azide-alkyne 3+2 cycloaddition. *J. Am. Chem. Soc.* **2003**, *125*, 4686-4687.

[24] Saghatelian, A.; Cravatt, B. F., Assignment of protein function in the postgenomic era. *Nat. Chem. Biol.* **2005**, *1*, 130-142.

[25] Bogyo, M.; McMaster, J. S.; Gaczynska, M., et al., Covalent modification of the active site threonine of proteasomal beta subunits and the Escherichia coli homolog HslV by a new class of inhibitors. *Proc. Natl. Acad. Sci. U. S. A.* **1997**, *94*, 6629-6634.

[26] Dick, L. R.; Cruikshank, A. A.; Grenier, L., et al., Mechanistic studies on the inactivation of the proteasome by lactacystin A central role for clasto-lactacystin beta-lactone. *J. Biol. Chem.* **1996**, *271*, 7273-7276.

[27] Fenteany, G.; Standaert, R. F.; Lane, W. S., et al., Inhibition of Proteasome Activities and Subunit-Specific Amino-Terminal Threonine Modification by Lactacystin. *Science* **1995**, *268*, 726-731.

[28] Kalgutkar, A. S.; Gardner, I.; Obach, R. S., et al., A comprehensive listing of bioactivation pathways of organic functional groups. *Curr. Drug Metab.* **2005**, *6*, 161-225.

[29] Koen, Y. M.; Hanzlik, R. P., Identification of seven proteins in the endoplasmic reticulum as targets for reactive metabolites of bromobenzene. *Chem. Res. Toxicol.* **2002**, *15*, 699-706.

[30] Monks, T. J.; Lau, S. S., Reactive Intermediates and Their Toxicological Significance. *Toxicology* **1988**, *52*, 1-53.

[31] Barbouche, R.; Miquelis, R.; Jones, I. M., et al., Protein-disulfide isomerase-mediated reduction of two disulfide bonds of HIV envelope glycoprotein 120 occurs post-CXCR4 binding and is required for fusion. *J. Biol. Chem.* **2003**, *278*, 3131-3136.

[32] Fenouillet, E.; Barbouche, R.; Courageot, J., et al., The catalytic activity of protein disulfide isomerase is involved in human immunodeficiency virus envelope- mediated membrane fusion after CD4 cell binding. *J. Infect. Dis.* **2001**, *183*, 744-752.

[33] Gallina, A.; Hanley, T. M.; Mandel, R., et al., Inhibitors of protein-disulfide isomerase prevent cleavage of disulfide bonds in receptor-bound glycoprotein 120 and prevent HIV-1 entry. *J. Biol. Chem.* **2002**, *277*, 50579-50588.

[34] Mandel, R.; Ryser, H. J. P.; Ghani, F., et al., Inhibition of a Reductive Function of the Plasma-Membrane by Bacitracin and Antibodies against Protein Disulfide-Isomerase. *Proc. Natl. Acad. Sci. U. S. A.* **1993**, *90*, 4112-4116.

[35] Ryser, H. J. P.; Levy, E. M.; Mandel, R., et al., Inhibition of Human-Immunodeficiency-Virus Infection by Agents That Interfere with Thiol-Disulfide Interchange Upon Virus-Receptor Interaction. *Proc. Natl. Acad. Sci. U. S. A.* **1994**, *91*, 4559-4563.

[36] Callens, N.; Ciczora, Y.; Bartosch, B., et al., Basic residues in hyervariable region 1 of hepatitis C virus envelope glycoprotein E2 contribute to virus entry. *J. Virol.* **2005**, *79*, 15331-15341.

[37] Dhaenens, L.; Szczebara, F.; Husson, M. O., Identification, characterization, and immunogenicity of the lactoferrin-binding protein from Helicobacter pylori. *Infect. Immun.* **1997**, *65*, 514-518.

[38] Speers, A. E.; Cravatt, B. F., Profiling enzyme activities in vivo using click chemistry methods. *Chem. Biol.* **2004**, *11*, 535-546.

[39] Chan, T. R.; Hilgraf, R.; Sharpless, K. B., et al., Polytriazoles as copper(I)-stabilizing ligands in catalysis. *Org. Lett.* **2004**, *6*, 2853-2855.

[40] Alvarez, S. G.; Alvarez, M. T., A practical procedure for the synthesis of alkyl azides at ambient temperature in dimethyl sulfoxide in high purity and yield. *Synthesis-Stuttgart* **1997**, 413-414.

5

Effect of Bleomycin on Hepatitis C Virus Replication

Introduction

The bleomycins (BLM) (Figure 5.1) are a family of antitumor antibiotics isolated from *Streptomyces verticillus,* in 1966 [1]. BLM is a glycopeptide with four well distinguished functional domains [2-4], which are highlighted in Figure 5.1. BLM contains a metal binding domain at the N-terminus, which is required for metal chelation, oxygen binding, and DNA binding. This domain includes pyrimidine, β-aminoalanine amide side chain, and β-hydroxy-L-histidine. The carbohydrate moiety (gulose and mannose) makes the second domain which enhances cellular uptake and is also involved in metal binding. The third domain is a DNA binding domain and is located at the C-terminus of BLM. This domain contains the aromatic bithiazole moiety, and a cationic substituent. Bleomycins differ from each other only at their substituent (R) at the C-terminus. Bleomycin A2, which contains the dimethyl sulfide functionality, is the major component of the commonly used anticancer drug blenoxane.

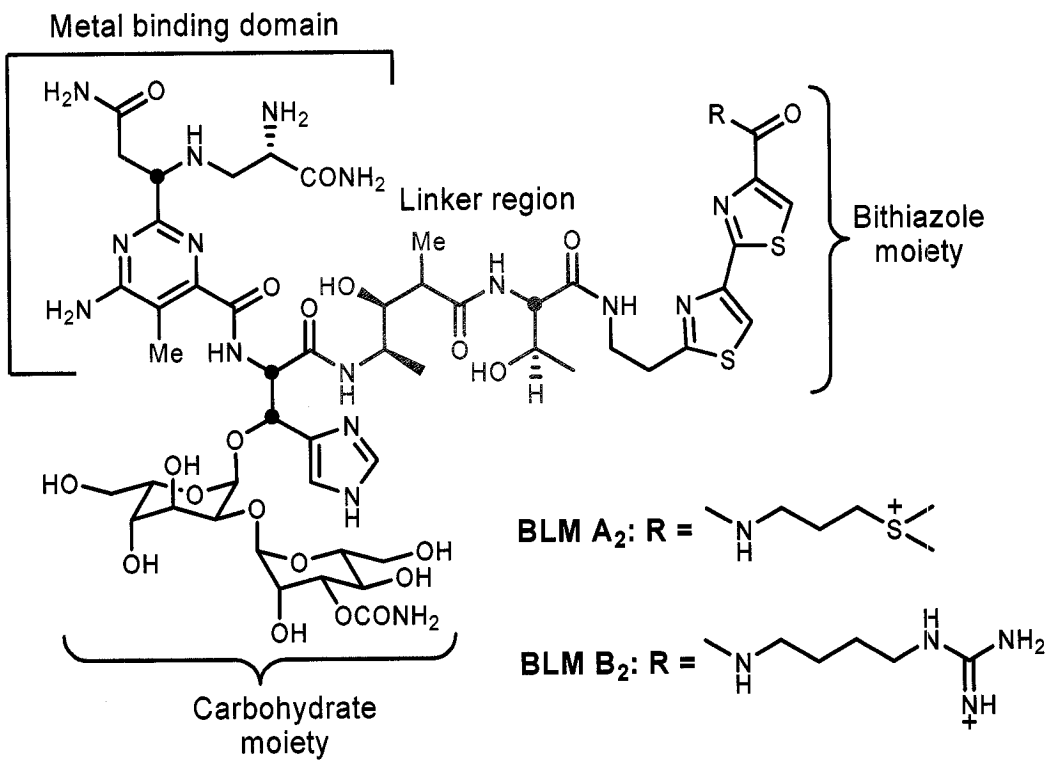

Figure 5.1: Structure of bleomycin (BLM) isomers A2 and B2. Highlighted are the four BLM functional domains (metal binding domain, linker region, bithiazole moiety and carbohydrate domain).

Bleomycins are known to bind to and degrade double-stranded (ds) DNA in a sequence-selective manner [5, 6]. BLM-mediated DNA degradation occurs at 5'-guanine-thymine-3', (5'-GT-3') and 5'-guanine-cytosine-3', (5'-GC-3') sequences in cell-free and cellular systems, including mammalian cells. In order to cleave the DNA, BLM requires activation with Fe(II) and oxygen [7]. This leads to formation of a ternary ferric superoxide complex of bleomycin, $^{\cdot}O_2^{-}$Fe(III)-BLM. The ternary complex has two fates: it can react with another ferric superoxide complex and upon disproportionation form activated bleomycin; or it can get reduced to activated bleomycin by cellular reductants. The proposed structure of the activated BLM-Fe(III)-O-OH complex is shown in Figure 5.2 [2, 3]. Electron paramagnetic resonance (EPR) study have shown that Fe in the Fe-(II)-BLM complex possesses a square-pyramidal geometry with the possibility of chelating one axial ligand [8]. This allows Fe(II) coordination to five nitrogens in bleomycin (nitrogens are shown in black, Figure 5.1). These are the α-amine and the secondary amine from β-amino alanine, the pyrimidine ring nitrogen, the deprotonated nitrogen in the peptide, and the nitrogen in imidazole. The sixth coordination is with the oxygen ligand (Figure 5.2).

Recent studies have shown that the metallobleomycin binding site envelopes two or three base pairs within the DNA minor groove, possibly through hydrogen bond formation [2, 3]. The bithiazole moiety enhances bleomycin DNA binding affinity, however, it is still not clear whether this occurs by intercalation, partial intercalation, or electrostatic interactions with the DNA minor groove. There are two proposed mechanisms of bleomycin-induced DNA degradation, depending on the oxygen concentration present in the system. These are presented in Scheme 5.1 and Scheme 5.2. In both mechanisms DNA

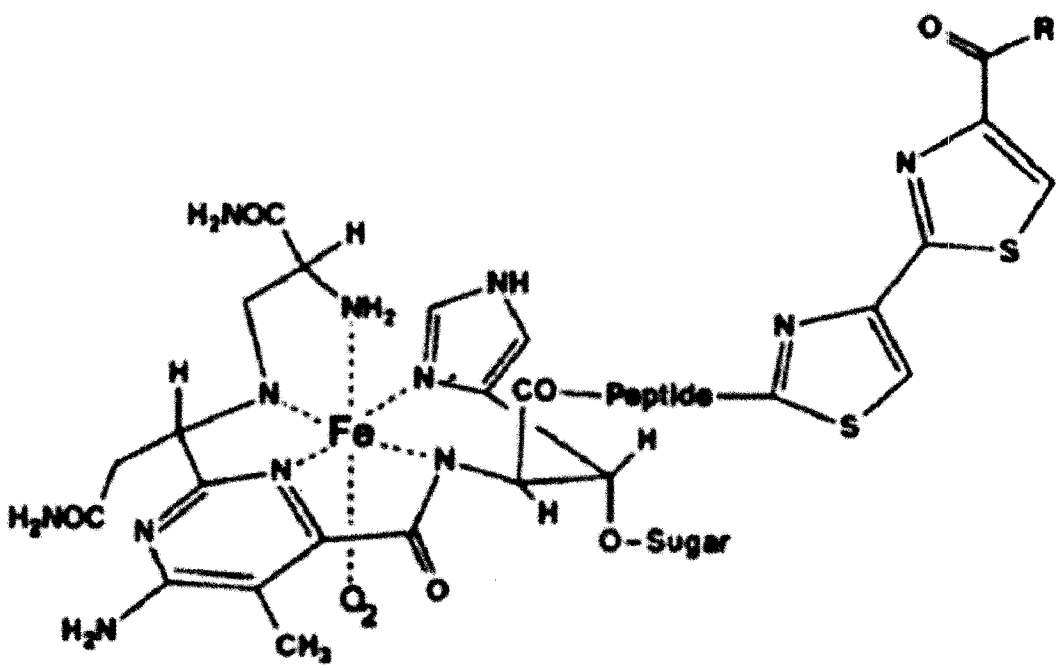

Figure 5.2: Proposed structure of bleomycin-iron, BLM-Fe(II) activated complex. Fe(II) is octahedrally coordinated with 5 coordination sites occupied by nitrogens of BLM and sixth site occupied by oxygen. This figure is copied from: Stubbe, J.; Kozarich, J. W., Mechanisms of bleomycin-Induced DNA-Degradation. *Chem. Rev.* **1987**, *87*, 1107-1136.

degradation is initiated by abstraction of the hydrogen atom from the C-4' atom of deoxyribose and formation of a C-4' deoxyribose radical (5.1.1 and 5.2.1). In the presence of oxygen, a 4'-peroxy radical is formed. The resulting 4'-peroxy radical is reduced to 4'-hydroperoxide 5.1.2. This is followed by a Criegee rearrangement to obtain intermediate 5.1.3, which upon phosphate elimination and cleavage of the C-3'-C-4' bond of the sugar, yields the formation of a nucleic base propenal 5.1.5 and oligonucleotide 3'-phosphoroglycolate 5.1.6 (Scheme 5.1). In the lack of oxygen, a 4'-radical intermediate is oxidized to a 4'-carbocation to which H_2O adds, generating the hydroxy intermediate 5.2.2. 5.2.2 undergoes immediate nucleic base release from the DNA strand forming alkali-labile 5.2.3. This strand is further cleaved by β-elimination of the 3'-phosphate forming the 5.2.4 DNA strand (Scheme 5.2).

More recently, BLMs have been shown to also cleave RNA, however in a site-selective manner. Examples include tRNA, mRNA, rRNA, and RNA-DNA duplexes [9-13]. Interestingly, BLM-mediated cleavage of RNA appears to be controlled by RNA tertiary structure rather than primary sequence and, with tRNA, cleavage occurs at sites containing both single-stranded and dsRNA [10]. The specific targeting of tertiary RNA structure implies that BLM may act selectively against other exogenous RNAs such as RNA viruses.

In this study we wanted to examine if bleomycin can be used as a chemical probe for targeting HCV RNA elements in sub-genomic HCV replicon cells without affecting cellular DNA. We postulated this because cytoplasmic RNAs are more easily targeted by BLM compared to genomic DNA that is localized in the nucleus [12]. HCV is a positive strand RNA virus of the Flaviviridae family with an ~9.6 kb genome (Figure 5.3a). HCV genomic

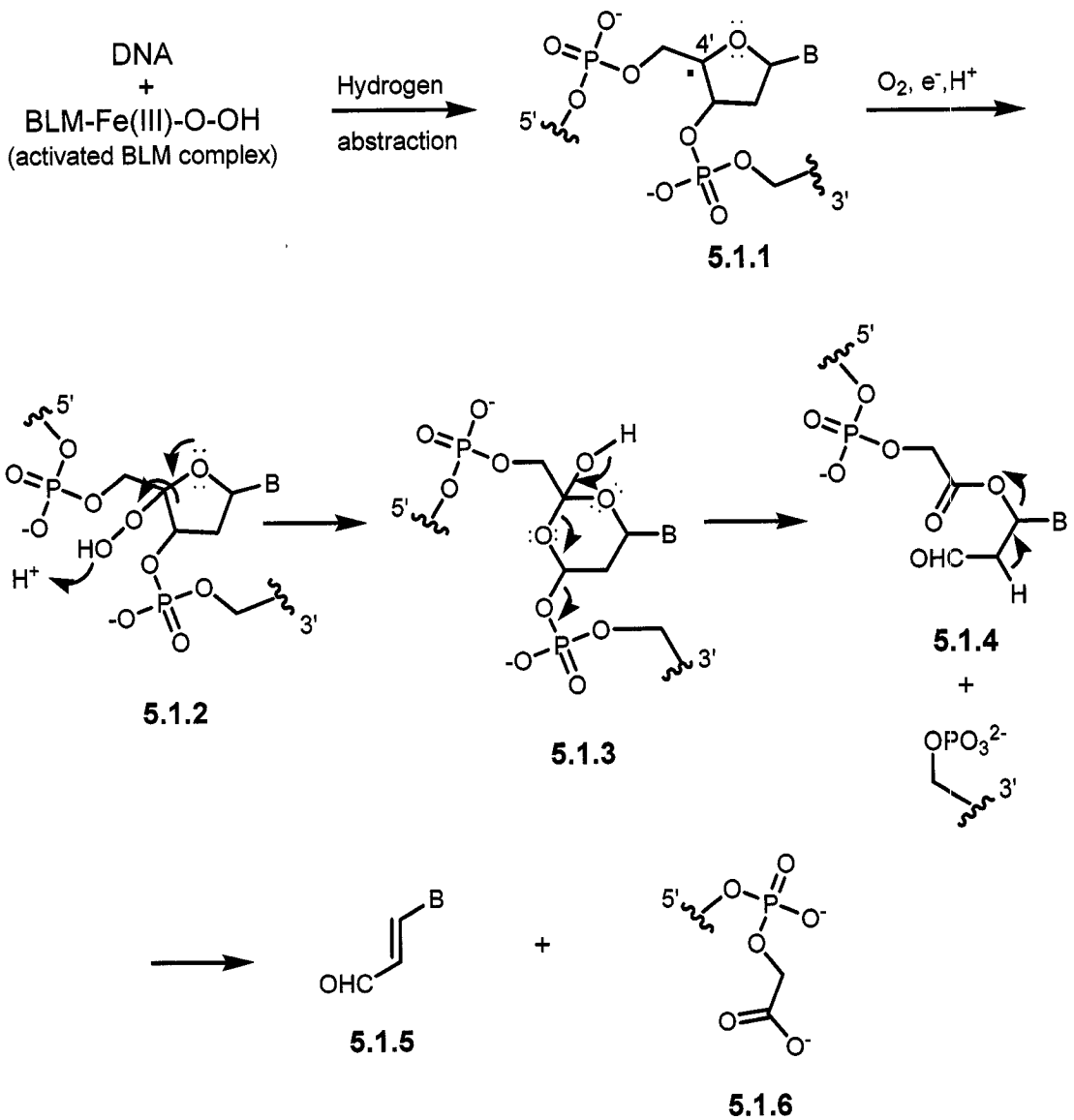

Scheme 5.1: Mechanism of DNA cleavage with activated bleomycin, BLM-Fe(II)-O_2 complex, in the presence of oxygen. Immediate DNA cleavage and Criegee rearrangement leads to formation of nucleic base propenal 5.1.5. This figure is copied from: Boger, D. L.; Cai, H., Bleomycin: Synthetic and mechanistic studies. *Angew. Chem.-Int. Edit.* **1999**, *38*, 448-476.

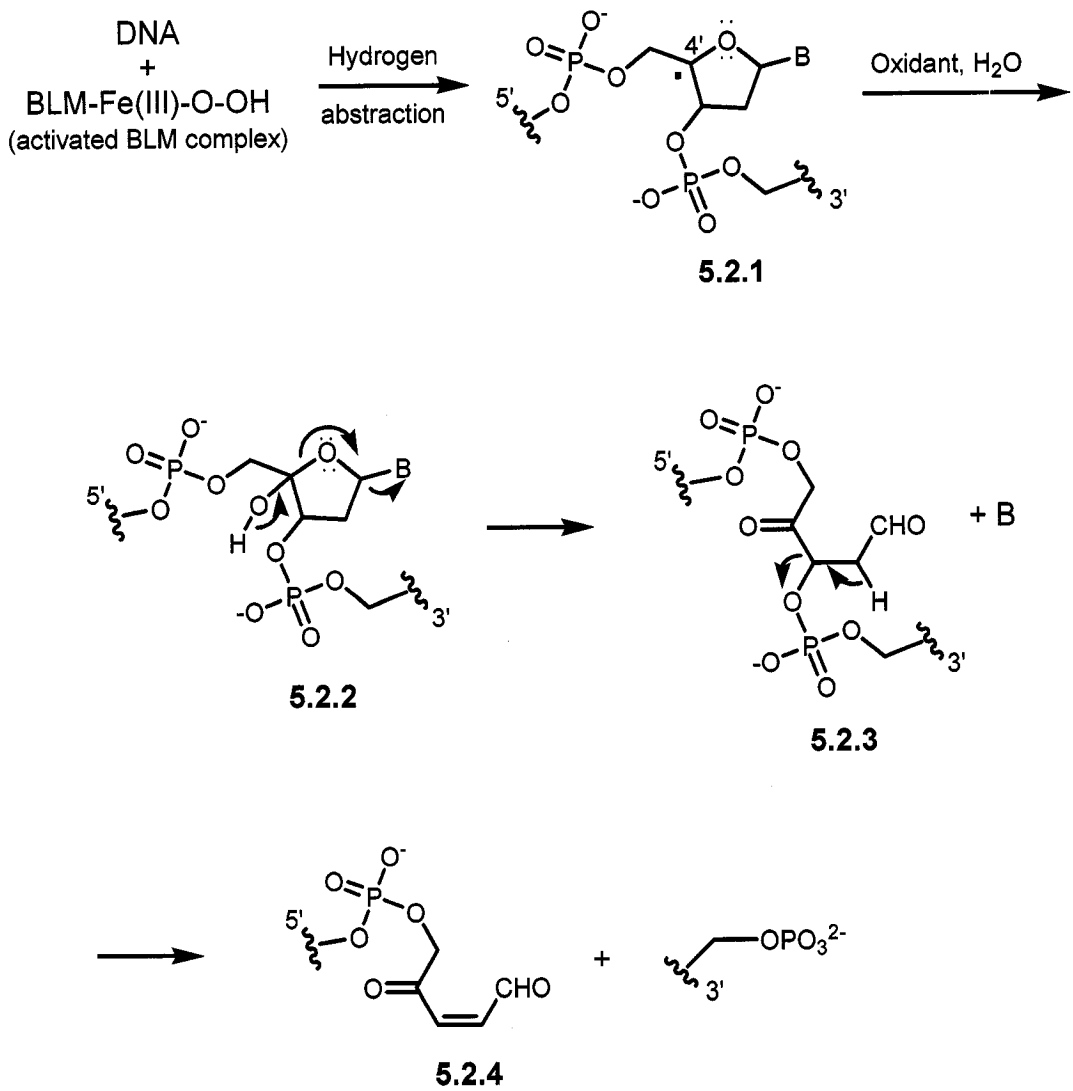

Scheme 5.2: Mechanism of DNA cleavage with activated bleomycin, BLM-Fe(II)-O_2 in the absence of oxygen. Formation of 4'-deoxyribose leads to immediate nucleic base release forming base-labile compound 5.2.3 that undergoes β-elimination of a 3' phosphate. This figure is copied from: Boger, D. L.; Cai, H., Bleomycin: Synthetic and mechanistic studies. *Angew. Chem.-Int. Edit.* **1999**, *38*, 448-476.

RNA contains many unique structural elements such as stem loops (SL), hairpins and bulges, which are formed from short stretches of complementary sequences. SL exist in the 3'-UTR and in the 5'-untranslated region (5'-UTR), which contains a structurally unique internal ribosomal entry site (IRES). There are also 2 SL in the core part of the genome and 6 that dominate the NS5B region [14-16]. In addition, NS5B protein mediates replication of HCV's genomic RNA and produces negative strand and dsRNA intermediates which resemble A-DNA helices. Therefore BLM may target the tertiary structure of single-stranded genomic viral RNA or dsRNA intermediates during replication [17]. The dsRNA intermediates represent potential targets for BLM because it may intercalate among unique structural elements in replicating, pathogenic dsRNA and initiate its destruction.

Results and Discussion

In order to determine BLM activity against HCV RNA, we first examined the effects of blenoxane, which is mixture of 75% BLM A2 and 25% BLM B2 towards subgenomic HCV replicons. We utilized Huh-7 cells harboring a tricistronic subgenomic HCV replicon, previously characterized in Chapter 2 (Figure 5.3c) [18]. We evaluated BLM activity using the genetic reporter firefly luciferase. After 24h and 48h exposures, the BLM concentration dependence of the luciferase signal was measured. After 24h treatment BLM, normalized to total protein content, showed a dose dependent inhibition of firefly luciferase activity and thus HCV inhibition. This effect was greater after 48h treatment (Figure 5.4). Using the results of the 48h treatment, we determined the IC_{50} against the HCV replicon to be 1.5 μM (Figure 5.5). BLM causes cytotoxicity by affecting the cellular DNA. To assess this, we performed a standard cytotoxic assay, by measuring the amount of lactate dehydrogenase

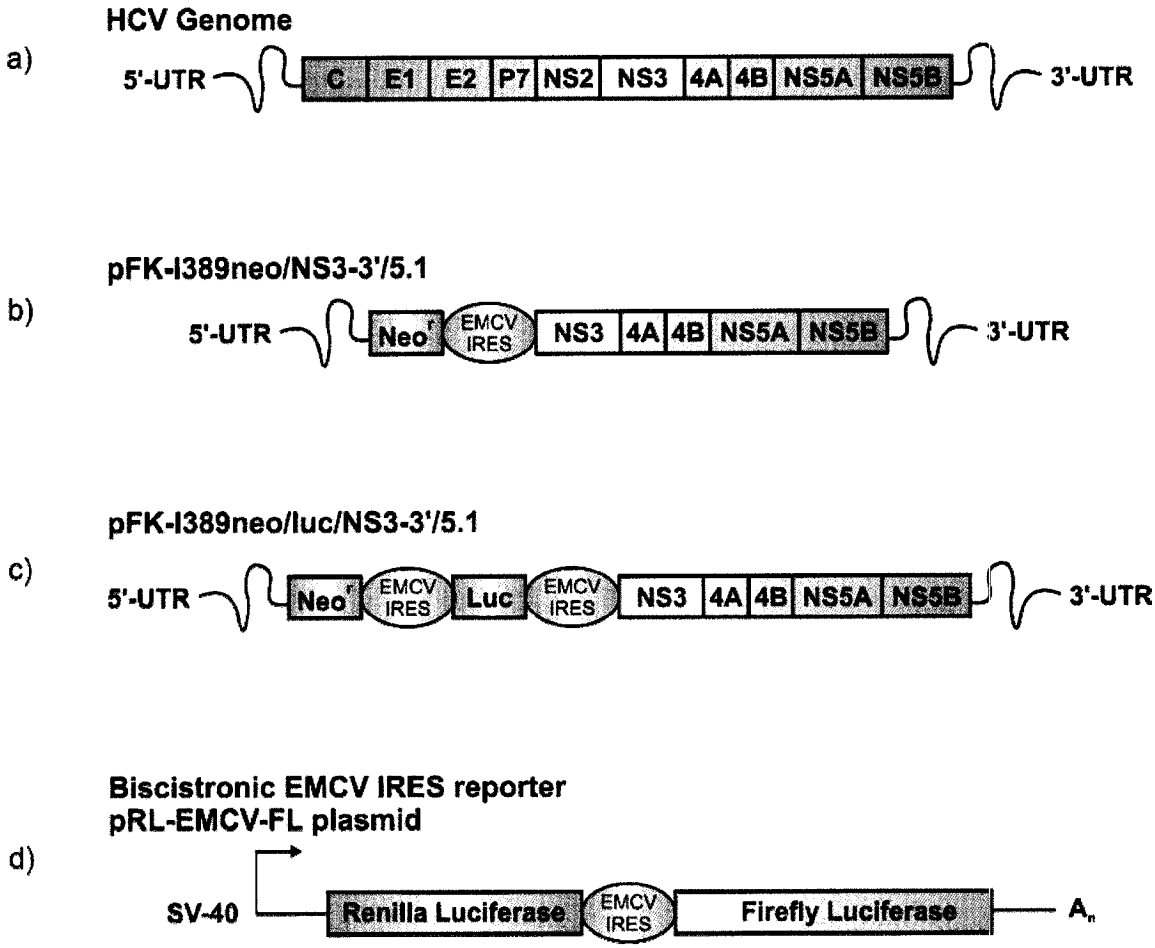

Figure 5.3: HCV replicons used in bleomycin study. a) Schematic representation of the HCV genome. b) HCV bicistronic sub-genomic replicon. c) HCV tricistronic sub-genomic replicon. d) The bicistronic plasmid encoding Renilla and firefly luciferase, which act as an internal control, and reporter of EMCV IRES activity, respectively.

released following lysis of cells after 48h treatment. The cell viability assay, shown in Figure 5.6, showed toxic effects of BLM on cellular DNA only at concentrations ≥10 μM and after prolonged exposure. This suggests a poor uptake of BLM through the nuclear membrane in Huh-7 cells, which is in agreement with literature [12]. Therefore, it is possible that due to diffusion rates BLM acts faster on HCV RNA located in the cytoplasm than on DNA located in the nucleus. Furthermore, unlike DNA, there is no mechanism by which RNA can repair itself. Thus, BLM-mediated damage to viral HCV RNA is irreversible, leading to immediate HCV inhibition.

To assess if BLM affected cellular RNA, total protein levels were quantified following cell lysis. No effects on cellular protein levels (Figure 5.4 in gray) were observed at concentrations of BLM sufficient to eliminate HCV replicon replication, suggesting host cell tRNAs and rRNAs are not affected. Taken together, these data support our hypothesis that BLM selectively targets HCV replicon RNA over cellular DNA located in the nucleus and cellular RNA in Huh-7 cells.

Although the subgenomic replicon used in our studies lacks the RNA coding for the structural HCV proteins, it contains the 5'-UTR, the NS3-NS5B region of the genome, and the 3'-UTR region. It also possesses a great deal of secondary and tertiary RNA structure as is found within the full-length genomic RNA. Therefore, it is not unexpected that BLM targets subgenomic HCV RNA. We postulated a couple of mechanisms by which BLM could inhibit viral replication (Scheme 5.3). One possibility is that BLM intercalates into dsRNA that is formed during viral replication. Another possibility is that BLM cleaves RNA by strand scission in the shallow minor groove of the NS5B region, most likely at the

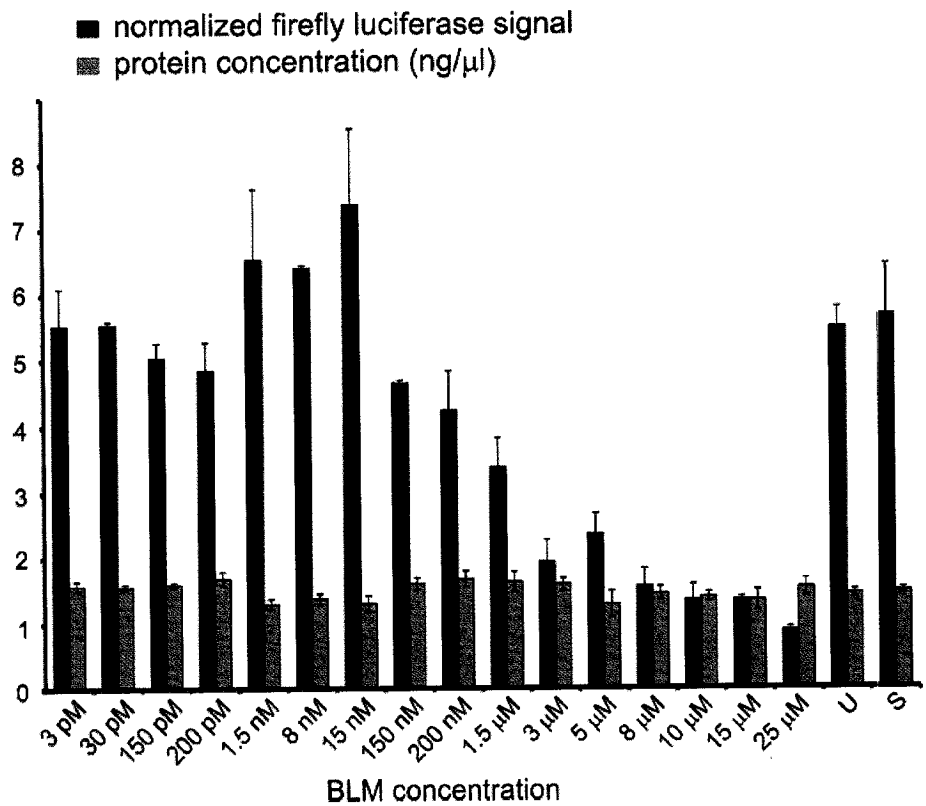

Figure 5.4: Normalized firefly luciferase data for Huh-7 replicon cells treated with bleomycin. Corresponding protein levels are shown in gray. Activity was determined following 48h treatment in concentrations ranging from 1 pM to 20 µM. S is the BLM solvent control and U is untreated cells. Error bars represent the mean ± SD.

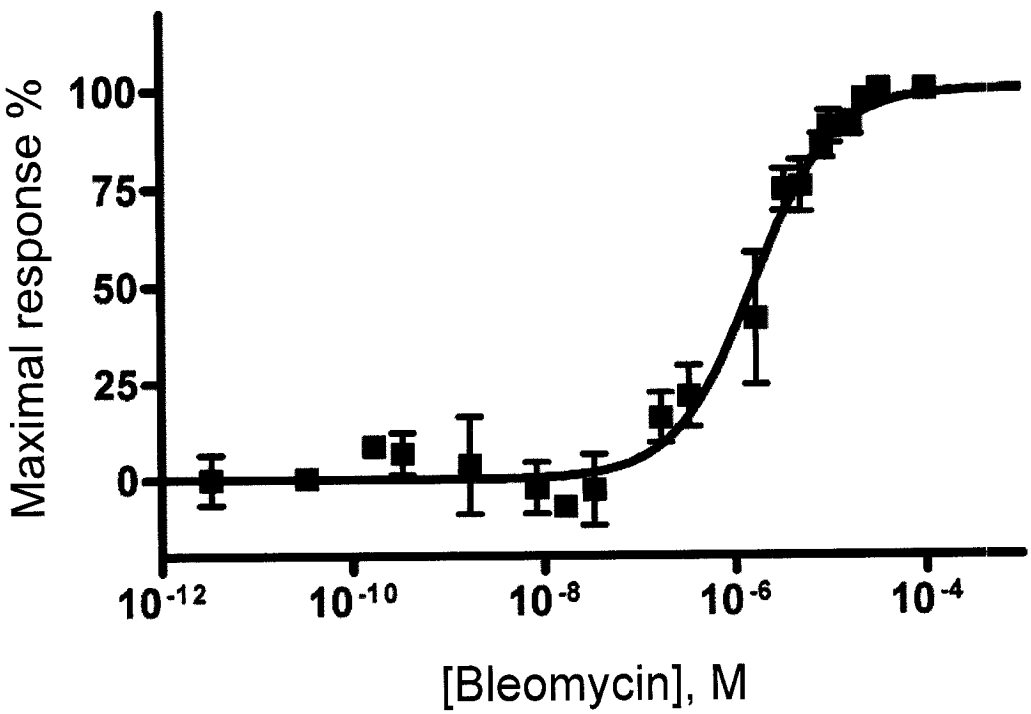

Figure 5.5: Bleomycin activity data expressed as IC_{50}. Data show the concentration-dependent inhibition of HCV replication by BLM in the subgenomic replicon system after 48h as measured by firefly luciferase assay. The IC_{50} value of BLM is determined to be 1.5 μM. Error bars represent the mean ± SD.

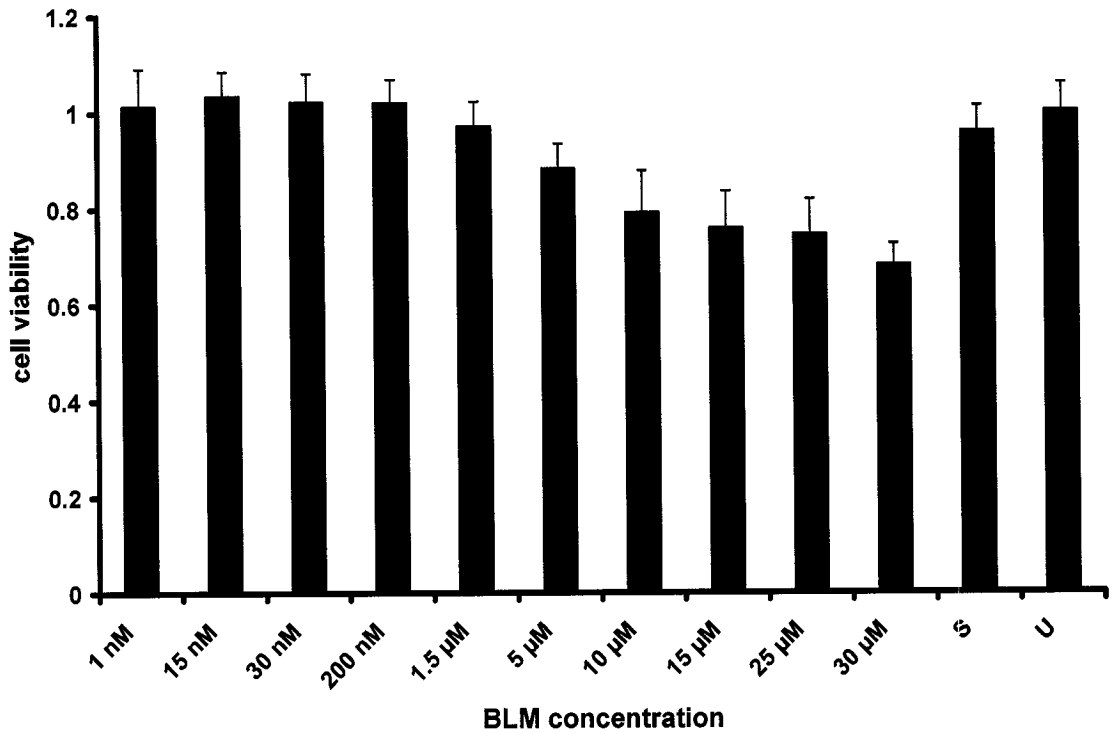

Figure 5.6: Cytotoxicity data for Huh-7 replicon cells treated with bleomycin (BLM). Cytotoxicity was determined by LDH assay following 48h cell treatment with BLM concentrations ranging from 30 µM to 1 nM. S is the BLM solvent control, and U is untreated cells. BLM showed significant toxicity at concentrations above 10 µM. Error bars represent the mean ± SD.

junction of the single- and double-stranded regions [12]. However, similar HCV inhibition would be observed if cleavage were to occur in the EMCV IRES of the replicon. Although EMCV IRES regulates translation of the HCV proteins it is non-HCV moiety. To assess if BLM could affect the EMCV IRES, we tested the activity of BLM in Huh-7 cells transfected with a bicistronic pRL-EMCV-FL plasmid that expresses firefly luciferese via EMCV IRES-dependent translation and *Renilla* luciferase via a cap-dependent mechanism [19-21]. Treatment with BLM for 24h and 48h resulted in no significant change in the firefly luciferase signals among replicas. Expression of *Renilla* luciferase was also not significantly affected by BLM. Results presented in Table 5.1 demonstrate that the EMCV IRES did not undergo BLM-mediated cleavage. Furthermore, transfected cells that were treated with IFNγ, a known inhibitor of HCV replication in cell culture, also did not affect the EMCV IRES [22]. This demonstrates that BLM cleavage of HCV replicon RNA is due to the HCV components of the replicon.

Immunoblotting was performed to confirm the specificity of BLM activity in HCV replicon-bearing cells. We found that BLM was effective at reducing HCV NS3 and NS5A protein levels at 1.5 μM (Figure 5.7). Observed decreases were similar to those seen with known inhibitors of HCV in cell culture, 25-hydroxycholesterol and interferon gamma, that were used as positive controls at their reported inhibitory concentrations of 5 μM and 50 U/ml, respectively [19, 22]. A larger decrease in HCV NS5A protein levels compared with NS3 levels with BLM treatment suggest different kinetics of protein degradation. Although the actual half-lives of proteins in replicon-containing cells is unknown and likely to vary, the phenomenon associated with the more rapid degradation of NS5A compared to NS3

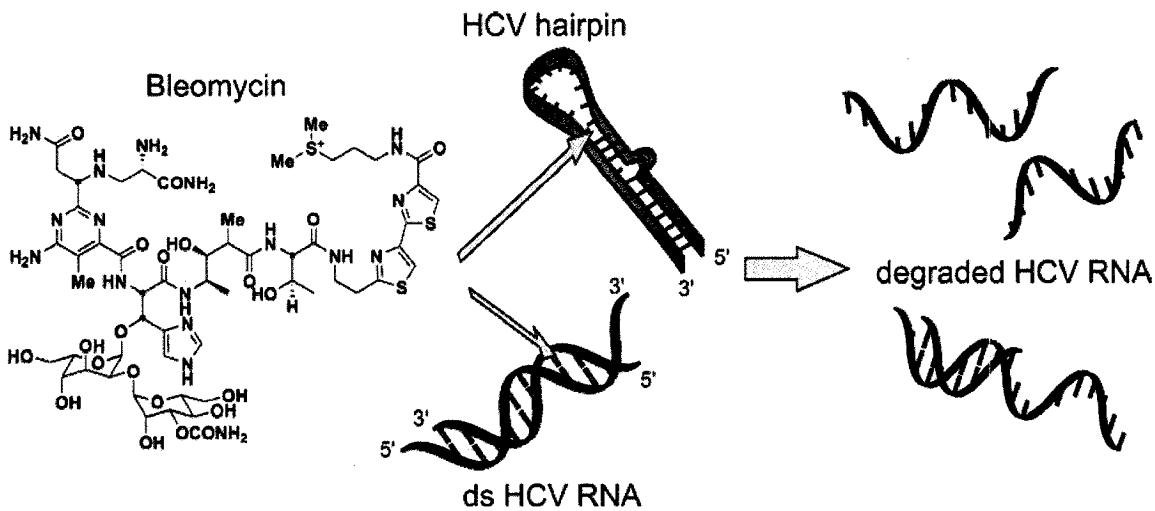

Scheme 5.3: Possible mechanism of HCV RNA degradation by bleomycin. BLM can intercalate into dsRNA that is formed during replication or cleave the tertiary structure of replicon HCV RNA.

Treatment	24h endpoint		48h endpoint	
	firefly	*Renilla*	firefly	*Renilla*
none	12.4±3.1	141.8±25.6	4.5±0.2	56.5±23.2
BLM solvent	11.4±4.9	96.9±54.6	7.4±3.9	57.4±32.5
1.5 μM BLM	14.3±2.3	97.3±29.0	9.5±0.5	79.6±13.4
3.0 μM BLM	9.3±1.5	72.2±11.3	6.7±3.0	64.9±40.6
10.0 μM BLM	12.0±1.8	98.1±15.2	6.5±0.8	61.3±14.4
IFNγ	12.9±1.0	128.6±27.4	6.9±1.6	53.0±7.3

Table 5.1: Firefly and *Renilla* luciferase activities of cells transfected with pRL-EMCV-FL and treated with bleomycin (BLM) or interferon gamma (IFNγ). Firefly luciferase and *Renilla* luciferase signals do not show significant changes suggesting that BLM treatment does not affect the EMCV IRES.

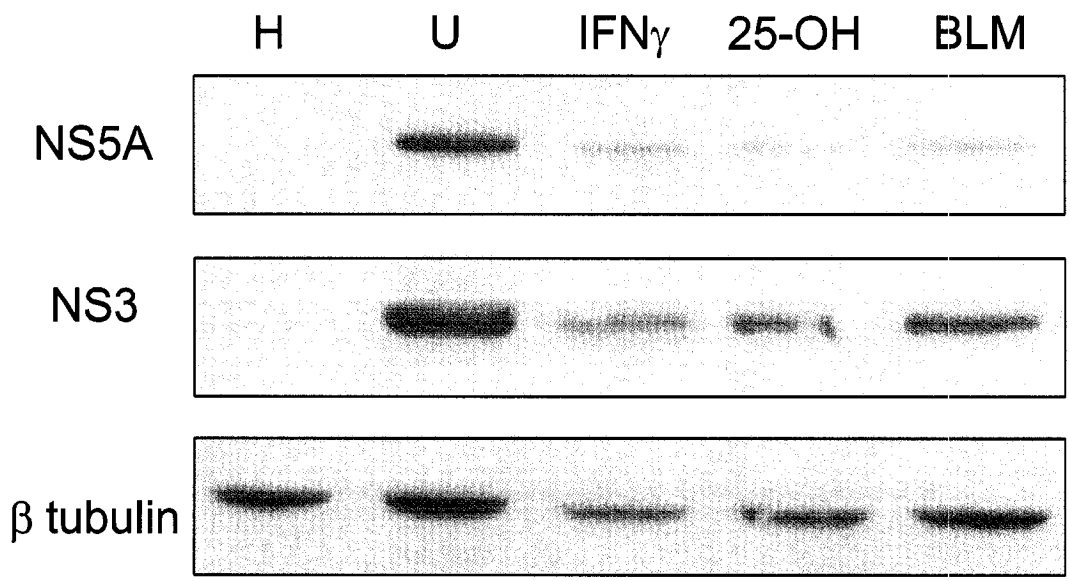

Figure 5.7: A western blot showing that levels of the HCV proteins NS3 and NS5A in HCV replicon cells were significantly lowered in the presence of 1.5 μM BLM. H is Huh-7 human hepatoma cells, U is the untreated HCV replicon cells, IFNγ is interferon gamma at 50 U/ml, and 25-OH is 25-hydroxycholesterol at 5 μM. β tubulin was used as a loading control.

protein was observed in all our studies. This also has been observed previously by others [23].

Previous studies have demonstrated that oligonucleotide strand scission by BLM requires the presence of both a redox-active metal and molecular oxygen, and involves the site-selective generation of reactive oxygen species including the hydroxyl radical [13, 24, 25]. We investigated whether the same held true for BLM cleavage of HCV replicon RNA. An *in vitro* cleavage experiment was performed under standard cleavage conditions where we incubated HCV replicon RNA with BLM Fe(II)-activated complex. Electrophoresis was performed using Agilent nano RNA chips. Electrophoretic mobility shift assays presented in Figure 5.8 confirmed that, in the absence of Fe(II), RNA stays intact for the incubation period of 2h. To discount ionic interference, we performed control experiments that showed that Fe(II) does not degrade the RNA.

We analyzed the electrophoretic mobility shift assay by looking at HCV RNA integrity via the reconstructed gel and by looking at the retention time of the intact and degraded RNA molecules (Figure 5.8). We found that HCV replicon RNA cleavage by BLM was both Fe(II) and concentration dependent. BLM activity led to the complete degradation of HCV RNA at concentrations ≥100 μM and much less degradation at 25 μM during 2h incubations *in vitro* as presented in Figure 5.8b. We observed that HCV replicon RNA cleavage by BLM also resulted in the formation of many cleavage products. This may be attributed to multiple binding and cleavage sites, or due to site-specific binding of BLM to HCV replicon RNA but occurring at sites of tertiary structure. The latter would result in the formation of cascade radicals that can attack a wide range of nucleotides within the primary

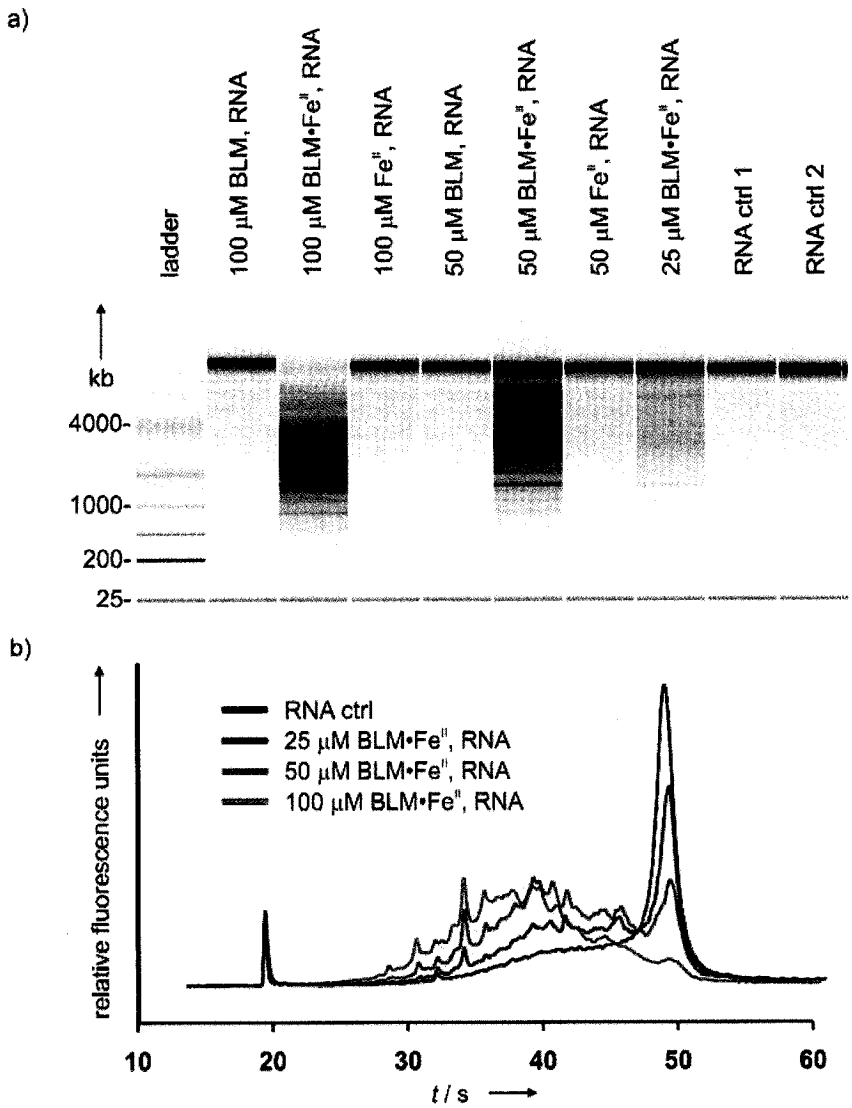

Figure 5.8: Electrophoretic mobility shift assay of BLM with IVT HCV RNA. a) Reconstructed gel showing the size of RNA cleavage products b) Electropherogram showing retention time of the intact and degraded RNA. Early times correspond to smaller RNA fragments.

sequence due to the folded structure. Detected RNA fragments ranged between 1.3 kb and 6.1 kb. The molecular weights of the smaller fragments suggested that cleavage of the SL in the NS5B region of the HCV RNA may be occurring. The details of BLM binding to elements of the HCV genomic RNA are to be further investigated. One possibility is by performing foot printing studies [26], however, the length of the subgenomic HCV RNA (~8Kb) precludes it.

We successfully showed in this study that BLM selectively cleaves genomic HCV RNA over cellular DNA and other cellular RNAs. This allows BLM to be used as a small molecule inhibitor for HCV replication. The fact that BLM appears to block HCV RNA replication directly by degrading the RNA indicates that it can be used to model the effects of the dsRNA response in cell culture without inducing the associated changes in gene expression. Although here we demonstrated that BLM can be used as an inhibitor of HCV replication in cellular models, it may also be useful for treating analogous viruses with large RNA genomes with complex tertiary structure.

Materials and Methods

Cell culture

Cell monolayers of the human hepatoma cell line Huh-7 and Huh-7 cells stably expressing HCV replicons were grown in complete Dulbecco's modified minimal essential medium (DMEM) supplemented with G418. For further details please refer to Chapter 2.

Replicon treatment with bleomycin

Bleomycin sulfate (Blenoxane) was bought from Alexis Biochemicals (San Diego, CA, USA). Bleomycin sulfate (BLM) consists of bleomycin A2, 65% and bleomycin B2, 30%. BLM was dissolved in normal saline (0.15 M NaCl) at a concentration of 2 mg/ml and stored at 4°C. Huh-7 cells harboring the HCV sub- genomic replicon were seeded at $1x10^4$ cells/well concentration in complete DMEM medium (without G418) in 96-well plates. After 24h, at a confluency of 70-80%, the cells were treated with BLM (serial dilution 40 μM to 5 pM), for 24h or 48h. The effect on HCV replicon was analyzed using firefly luciferase and toxicity assays.

Firefly luciferase reporter assay and total protein quantification

Huh-7 cells harboring subgenomic replicon were transfected with BLM as described above. At the assay time point, cells were washed once with 1X PBS and lysed with cell culture lysis buffer (Promega) for 10 min at room temperature (RT). For detailed information on the experimental protocol please refer to Materials and Methods in Chapter 2. Values were normalized against total protein content that was determined using the Bio-Rad DC protein assay (Bio-Rad) according to the manufacturer's protocol. Normalized values of each sample are shown as the mean ± SD. IC_{50} curve was obtained using GraphPadPrism 4 software.

Cytotoxicity assay

Huh-7 cells expressing HCV subgenomic replicon were treated with BLM as described above. After 24h or 48h, the cells were processed for the CytoTox 96 Non-Radioactive Cytotoxicity Assay (Promega) according to the manufacturer's protocol. The absorbance was read at 490/650 nm using the SPECTRAmax M2 plate reader and SOFTmax Pro

software. Values of each experiment are shown as the mean ± SD. For more details please refer to Materials and Methods in Chapter 2.

Immunoblot analysis

Huh-7 cells harboring subgenomic replicon derived from the clone pFK-I389neo/NS3-3'/5.1 ($5x10^5$cells) were seeded in 60 mm dishes for preparation of western blot lysates. After 24h, the cells were treated with 25 hydroxycholesterol (25-OH), 5 μM concentration, interferon γ (IFNγ), 50 U/ml, and BLM 1.5 μM. 48h later cells were washed and lysed using an SDS lysis buffer consisted of 50 mM Tris-HCl (pH 6.8), 2% SDS and 10% glycerol. Page gel and blotting were then conducted as described previously in Chapter 2. The membrane was probed for HCV NS5A and HCV NS3 protein using a mouse anti-NS5A primary antibody and a mouse anti-NS3 primary antibody (1:500 dilution, Virostat). Mouse anti-β-tubulin primary antibody (1:1000 dilution in 3% milk, BD Transduction Laboratories) was used a loading control. (HRP)-conjugated goat anti-mouse IgG antibody (1:1000 dilution) obtained from Jackson ImmunoResearch Laboratories Inc. was used as a secondary antibody.

EMCV IRES screen

Huh-7 cells were seeded at $5x10^4$ cells/well in complete DMEM in a 24-well plate. At 90% confluency, the cells were washed twice with 1X PBS, followed by addition of 0.5 ml of serum- and antibiotic-free DMEM containing only NEAA. Transfection complexes were prepared by mixing 0.25 μg of pRL-EMCV-FL plasmid DNA and 0.75 μl of lipofectamine 2000 (Invitrogen) in 100 μl total volume according to the manufacturer's protocol. Mock-transfected cells received only the transfection reagent. After 4h of culture, the media was

removed and replaced by complete DMEM. 24h post-transfection, cells were treated with bleomycin at 1.5 μM, 3 μM, and 10 μM concentrations and IFNγ at 50 U/ml. 24h and 48h later, the cells were washed once with 1X PBS and then lysed with 1X Passive Lysis Buffer (Promega Corp., Madison, WI) for 10 min at RT. Forty microliters per condition was transferred to a 96-well plate to perform the Dual Luciferase Reporter Assay (Promega) according to the manufacturer's protocol. Briefly, 50 μl of LAR II and Stop & Glo® reagents were sequentially added to each well and both firefly and Renilla luciferase activities were measured after a 2 s delay using the Lmax luminometer.

Fe(II)•bleomycin- mediated HCV RNA cleavage

In vitro transcripts of HCV RNA were generated using a MEGAscript™ (Ambion, Austin, TX, USA) according to the manufacturer's protocol. In brief, the template DNA was linearized with the restriction enzyme *Sca*I (New England BioLabs, Pickering, ON, Canada), precipitated for less than 30 min, and resuspended in RNase-free water to a concentration of 0.5μg/μl. The *in vitro* reaction was set up and incubated at 37°C for 2h. To degrade the DNA template, 1μl of DNaseI was added and incubated for another 15min at 37°C. The *in vitro* transcripts were then cleaned using the MEGAclear kit (Ambion) according to the manufacturer's protocol. A 20 μl-reaction usually produced 100 μg of RNA. The concentration was determined by measuring the absorbance at 260 nm with a ND-1000 Spectrophotometer (NanoDrop Technologies, Rockland, DE, USA) and RNA integrity was verified by electrophoresis using the Agilent 2100 bioanalyzer with the RNALabChip® kit according to the manufacturer's protocol.

All reaction mixtures (10 µl total volume) contained 0.5 µM IVT HCV RNA (final concentration) in nuclease free water. BLM solutions were prepared by diluting 1.3 mM BLM stock solution in 0.5 M NaCl, in nuclease free water. Fe(II) solutions were prepared by diluting 1.3 mM $Fe(NH_4)_2(SO_4)_2$ stock solution in 0.1 M phosphate buffer pH 7.5, in nuclease free water. The reactions were initiated by simultaneous addition of equimolar amounts of freshly prepared BLM and $Fe(NH_4)_2(SO_4)_2$ to final concentrations of 100 µM, 50 µM, and 25 µM. As controls, IVT HCV RNA was reacted with BLM alone (100 µM and 50 µM final BLM concentrations) and with Fe(II) alone (100 µM and 50 µM final Fe(II) concentrations). Reaction mixtures were incubated at 22°C for 2h. All samples were then diluted by adding 10 µl of nuclease free water and heat denaturing for 2 min at 75°C. In addition two HCV RNA controls were used. RNA ctrl1 was incubated at the same conditions but without BLM or Fe(II), while RNA ctrl2 was kept at -80°C prior to denaturing. 1 µl of reaction sample was then loaded onto the RNA nano chip and reactions were analyzed by doing RNA 6000 nano assay (Agilent Technologies, Palo Alto, CA, USA) according to the manufacturer's protocol. RNA integrity was verified by electrophoresis using the Agilent 2100 bioanalyzer.

References:

[1] Umezawa, H.; Maeda, K.; Takeuchi, T., et al., New antibiotics, bleomycin A and B. *J. Antibiot. (Tokyo)* **1966**, *19*, 200-209.

[2] Chen, J. Y.; Stubbe, J., Bleomycins: Towards better therapeutics. *Nat. Rev. Cancer* **2005**, *5*, 102-112.

[3] Claussen, C. A.; Long, E. C., Nucleic acid recognition by metal complexes of bleomycin. *Chem. Rev.* **1999**, *99*, 2797-2816.

[4] Hecht, S. M., The Chemistry of Activated Bleomycin. *Accounts Chem. Res.* **1986**, *19*, 383-391.

[5] Quada, J. C.; Boturyn, D.; Hecht, S. M., Photoactivated DNA cleavage by compounds structurally related to the bithiazole moiety of bleomycin. *Bioorg. Med. Chem.* **2001**, *9*, 2303-2314.

[6] Burger, R. M., Cleavage of nucleic acids by bleomycin. *Chem. Rev.* **1998**, *98*, 1153-1169.

[7] Burger, R.; Peisach, J.; Horwitz, S., Activated bleomycin. A transient complex of drug, iron, and oxygen that degrades DNA. *J. Biol. Chem.* **1981**, *256*, 11636-11644.

[8] Sugiura, Y., Bleomycin-Iron Complexes - Electron-Spin Resonance Study, Ligand Effect, and Implication for Action Mechanism. *J. Am. Chem. Soc.* **1980**, *102*, 5208-5215.

[9] Holmes, C. E.; Duff, R. J.; vanderMarel, G. A., et al., On the chemistry of RNA degradation by Fe-bleomycin. *Bioorg. Med. Chem.* **1997**, *5*, 1235-1248.

[10] Carter, B. J.; Devroom, E.; Long, E. C., et al., Site-Specific Cleavage of Rna By Fe(Ii).Bleomycin. *Proc. Natl. Acad. Sci. U. S. A.* **1990**, *87*, 9373-9377.

[11] Abraham, A. T.; Lin, J. J.; Newton, D. L., et al., RNA cleavage and inhibition of protein synthesis by bleomycin. *Chem. Biol.* **2003**, *10*, 45-52.

[12] Hecht, S. M., Rna Degradation by Bleomycin, a Naturally-Occurring Bioconjugate. **1994**, *5*, 513-526.

[13] Holmes, C. E.; Carter, B. J.; Hecht, S. M., Characterization of Iron(Ii).Bleomycin-Mediated Rna Strand Scission. *Biochemistry* **1993**, *32*, 4293-4307.

[14] Brown, E. A.; Zajac, A. J.; Lemon, S. M., In-Vitro Characterization of an Internal Ribosomal Entry Site (Ires) Present within the 5' Nontranslated Region of Hepatitis a Virus-Rna - Comparison with the Ires of Encephalomyocarditis Virus. **1994**, *68*, 1066-1074.

[15] Hofacker, I. L.; Fekete, M.; Flamm, C., et al., Automatic detection of conserved RNA structure elements in complete RNA virus genomes. **1998**, *26*, 3825-3836.

[16] Friebe, P.; Boudet, J.; Simorre, J. P., et al., Kissing-loop interaction in the 3 ' end of the hepatitis C virus genome essential for RNA replication. **2005**, *79*, 380-392.

[17] Lindenbach, B. D.; Rice, C. M., Unravelling hepatitis C virus replication from genome to function. **2005**, *436*, 933-938.

[18] Sagan, S. M.; Rouleau, Y.; Leggiadro, C., et al., The influence of cholesterol and lipid metabolism on host cell structure and hepatitis C virus replication. *Biochem. Cell Biol.* **2006**, *84*, 67-79.

[19] Su, A. I.; Pezacki, J. P.; Wodicka, L., et al., Genomic analysis of the host response to hepatitis C virus infection. *Proc. Natl. Acad. Sci. U. S. A.* **2002**, *99*, 15669-15674.

[20] Kruger, M.; Beger, C.; Welch, P. J., et al., Involvement of proteasome alpha-subunit PSMA7 in hepatitis C virus internal ribosome entry site-mediated translation. **2001**, *21*, 8357-8364.

[21] Tonary, A. M.; Pezacki, J. P., Simultaneous quantitative measurement of luciferase reporter activity and cell number in two- and three-dimensional cultures of hepatitis C virus replicons. *Anal. Biochem.* **2006**, *350*, 239-248.

[22] Feld, J. J.; Hoofnagle, J. H., Mechanism of action of interferon and ribavirin in treatment of hepatitis C. **2005**, *436*, 967-972.

[23] Kapadia, S. B.; Chisari, F. V., Hepatitis C virus RNA replication is regulated by host geranylgeranylation and fatty acids. *Proc. Natl. Acad. Sci. U. S. A.* **2005**, *102*, 2561-2566.

[24] Pogozelski, W. K.; Tullius, T. D., Oxidative strand scission of nucleic acids: Routes initiated by hydrogen abstraction from the sugar moiety. *Chem. Rev.* **1998**, *98*, 1089-1107.

[25] Boger, D. L.; Cai, H., Bleomycin: Synthetic and mechanistic studies. *Angew. Chem.-Int. Edit.* **1999**, *38*, 448-476.

[26] Kieft, J. S.; Zhou, K. H.; Jubin, R., et al., Mechanism of ribosome recruitment by hepatitis CIRES RNA. *RNA-Publ. RNA Soc.* **2001**, *7*, 194-206.

Appendix

Spot #	Identified Protein	Accession no. [a]	Theoretical MW/pI [b]	Score/ coverage % [c]
1	chaperonin (heat shock protein 60)	NCBI-41399285	61.016/5.7	1125
	prolyl 4-hydroxylase, beta subunit	NCBI-20070125	57.081/4.76	258
	(PDI, thyroid hormone binding precursor)			
	Pyruvate kinase 3, isoform 1	NCBI- 31416989	57.942/7.96	214
	Chain B, Ige Fv Spe7 Complexed With A	NCBI-42543181	13.444/4.5	125
	Recombinant Thioredoxin			
	ATP synthase beta subunit	NCBI-179279	56.861/5.39	119
	transformation upregulated nuclear protein	NCBI-460789	51.040/5.13	49
	chaperonin containing TCP1, subunit 6A isoform b	NCBI-58331171	53.255/6.85	43
	Na+,K+ ATPase	NCBI-1359715	111.91/5.22	34
	ZNF496 protein	NCBI-19387885	58.085/5.57	23
	KIAA1212 protein	NCBI-20521794	90.242/7.8	23
	sarcoma antigen NY-SAR-41 (NY-SAR-41)	NCBI-56204569	122.188/5.61	21
	KIAA1712 protein	NCBI-12697969	44.24/5.13	20
2	chaperonin (heat shock protein 60)	NCBI-306890	60.986/5.7	437
	eukaryotic translation elongation factor 1 alpha 1	NCBI-4503471	50.109/9.1	177
	collagen binding protein 2	NCBI-1199487	46.506/8.89	169
	calumenin	NCBI-2809324	37.050/4.47	162
	alpha-actin	NCBI-178027	42.081/5.23	120
	phosphogluconate dehydrogenase	NCBI-40068518	53.106/6.8	112
	DNA-binding protein B	NCBI-181486	39.954/9.82	67
	Chain B, Ige Fv Spe7 Complexed With A	NCBI-42543181	13.444/4.5	55
	NADP-dependent isocitrate dehydrogenase	NCBI-3641398	46.659/6.34	34
	fumarate hydratase precursor	NCBI-19743875	54.602/8.85	28
	HC6	NCBI-10799024	14.705/9.18	16
3	alpha-actin	NCBI-178027	42.081/5.23	574
	isocitrate dehydrogenase 1 (NADP+), soluble	NCBI-28178825	46.63/6.53	179
	elongation factor Tu	NCBI-704416	49.509/7.7	78
	S-adenosylhomocysteine hydrolase	NCBI-178277	47.684/6.03	75
	acyl-Coenzyme A dehydrogenase, C-4 to C-12 straight chain	NCBI-4557231	46.559/8.61	17

4	glyceraldehyde-3-phosphate dehydrogenase	NCBI-31645	36.031/8.26	334
	Glyceraldehyde-3-phosphate dehydrogenase,	NCBI-120643	35.853/6.6	224
	muscle (GAPDH)			
	mutant beta-actin (beta-actin)	NCBI-28336	41.786/5.22	209
	heterogeneous nuclear ribonucleoprotein	NCBI-14043072	37.407/8.97	159
	A2/B1 isoform B1			
	mitochondrial malate dehydrogenase precursor	NCBI-21735621	35.481/8.92	150
	eukaryotic translation elongation factor 1 delta isoform 2	NCBI-25453472	31.103/4.9	132
	Chain B, Ige Fv Spe7 Complexed With A	NCBI-42543181	13.444/4.5	120
	Recombinant Thioredoxin			
	APEX nuclease	NCBI-17939646	35.546/8.33	100
	eukaryotic translation elongation factor 1 alpha 1	NCBI-4503471	50.109/9.1	42
	Coproporphyrinogen oxidase	NCBI-16877987	50.143/8.59	40
	pyrophosphatase	NCBI-727225	13.037/4.8	26
	crystallin, zeta variant	NCBI-62089008	35.385/8.57	25
	capping protein alpha	NCBI-433308	32.727/5.58	22
	lactate dehydrogenase A	NCBI-5031857	36.665/8.44	19
	SFRP4	NCBI-SFRP4	39.832/9.12	18
	hnRNP-E2	NCBI-460773	38.556/6.33	17

Claims to Original Research

1. Studied the effects of modulation of peroxisome proliferators activated receptor α on Hepatitis C Viral replication in a cellular model system.
2. Investigated the effects of abscisic acid analogs on inhibiting HCV life cycle.
3. Discovered novel host proteins necessary for HCV proliferation.
4. Studied the effect of the antitumor antibiotic bleomycin on HCV RNA.

Publications from This Work

1) Rakic, B., Clarke, J., Tremblay, T., Taylor, J., Schreiber, K., Nelson, K.,Nelson, K., Abrams, S. R.; Pezacki, J. P. A Small Molecule Probe for Hepatitis C Virus Replication That Blocks Protein Folding. *Chemistry & Biology* (2006) **13**, 1051-1060.

2) Rakic, B., Brulotte, M., Rouleau, Y., Belanger, S., Pezacki, J. P. Bleomycin is a Potent Small Molecule Inhibitor of Hepatitis C Virus Replication. *ChemBioChem* (2006) **7**, 1330-1333.

3) Rakic, B., Sagan, M S., Noestheden, M., Belanger, S., Nan, X., Evans, L. C., Xie, X. S., Pezacki, J. P. Peroxisome Proliferator-Activated Receptor α Antagonism Inhibits Hepatitis C Virus Replication. *Chemistry & Biology* (2006) **13**, 23-30.